System Equivalent for

Real Time Digital Simulator

By

Xi Lin

A Thesis

Submitted to the Faculty of Graduate Studies in Partial Fulfillment

of the Requirements for the Degree of

Doctor of Philosophy

Department of Electrical and Computer Engineering

University of Manitoba

Winnipeg, Manitoba

Dedicated to My Parents

Acknowledgements

It is a pleasure to thank all people who have helped and inspired me during my Ph.D. study.

I especially want to thank my advisor, Prof. Aniruddha M. Gole, for his guidance during my research and study at the University of Manitoba. With his enthusiasm, his wisdom, and his inspiration, he helped to make me a better researcher and engineer. Throughout my thesis-writing period, he provided encouragement, sound advice, good teaching, good company, and lots of good ideas.

I spent a significant part of my Ph.D. period in RTDS Technologies Inc. I thank Ming Yu, Trevor Maguire, Yi Zhang, and Park In-Kwon for many insightful conversations during the development of the ideas in this thesis. I thank the whole team in RTDS, especially Rick Kuffel, for their help during my research at RTDS.

I was delighted to interact with Prof. Udaya D. Annakkage and Prof. Robert W. Menzies, by attending their classes, and with Prof. Athnla Rajapakse by serving as TA for him. I learnt a lot from them.

I am indebted to my many fellow students for providing a stimulating and fun environment in which to learn and grow. I am especially grateful to Ali B. Dehkordi, Gregory Jackson, Jeewantha De Silva, Bathiya Jayasekara, Shaahin Filizadeh, Behzad Qahraman, Ebrahim Rahimi, and Yuefeng Liang.

Throughout of my Ph.D. student life in Winnipeg, my wife Dongyun Wu accompanied me. Some parts of the four years were quite tough. Without her supports, this thesis would not have been possible.

Lastly, and most importantly, I wish to thank my parents, Xiaobing Liang and Ronghua Lin. They bore me, raised me, supported me, taught me, and loved me. To them I dedicate this thesis.

Abstract

The purpose of this research is to develop a method of making system equivalents for the Real Time Digital Simulator (RTDS), which should enhance its capability of simulating large power systems.

How to make an appropriate external system equivalent is a basic problem in power system time domain simulation area. As a real time application of Electromagnetic Transient (EMT) simulation, RTDS is a wide frequency band simulation tool, so the equivalent made for it also needs to be a wide band equivalent, by which both the high frequency and low frequency behaviors of the external system should be preserved.

This report describes a method of developing wide-band multi-port system equivalents for use with RTDS. The proposed equivalent combines a Frequency Dependent Network Equivalent (FDNE) for the high frequency electromagnetic transients and a Transient Stability Analysis (TSA) type simulation block for the electromechanical transients.

The frequency dependent characteristic for FDNE is obtained by curve-fitting frequency domain admittance characteristics using the Vector Fitting method. An approach for approximating the frequency dependent characteristic of large power networks from readily available typical power-flow data is also introduced.

The differences between EMT simulation and TSA simulation are investigated. A new scheme of incorporating TSA solution in RTDS is proposed. This report shows how the TSA algorithm can be adapted to a real time platform.

The validity of this method is confirmed with examples, including the study of a multi in-feed HVDC system based network.

Table of Contents

List of Figures

List of Tables

1 Introduction

1.1 Digital Time Domain Simulation in Power System Studies

This thesis deals with the techniques of making system equivalents for Real Time Digital Simulator, a digital time domain simulation tool being increasingly used in the power industry [1][2]. The purpose of making such an equivalent is to enhance the capability of RTDS of handling large size power systems.

Power system networks are generally regarded as the most complex structures ever built by humanity. There are tens of thousands of buses, transmission lines, transformers, generators etc., and they work together in one large network to supply the necessary power to human society.

From the 1960's, digital time domain simulation tools have been extensively used in power system studies. In many areas, such as transient stability analysis, switching over-voltage analysis, power electronic studies etc., digital time domain simulations have become the industry standard tools. There are many factors that lead to the popularity of digital time domain simulations, some of them are:

(1) Modern power systems are very large dynamic systems. Dynamic interactions between equipments are critical to the power system. Steady state analysis methods like power-flow are not sufficient for studying the power system.

(2) Many components of the power system have nonlinear characteristics, as well as non-continuous characteristics.

(3) A single component of the power system such as a synchronous generator can be very complex and often requires very detailed time domain modeling to represent the full range of phenomena.

(4) The time frames of the important behaviors of the power system range from microseconds to hours. For example, a voltage collapse may involve induction machine stalling, which happens in a couple of seconds; transformer tap change, whose time frame is tens of seconds; Automatic Generation Control (AGC) actions, whose time frame is minutes; and many other actions with time frames ranging from second to tens of minutes. There are very complex interactions between these behaviors. The time domain simulation is the only accurate way to study these behaviors.

(5) The scales of power system networks are so large and the structures and components are so complicated, that to build and maintain a scaled down physical model of a power system with appropriate accuracy are difficult and expensive, in many cases also impractical.

In digital time domain simulations, the nonlinear differential equations are solved by using step-by-step numerical integration techniques. By appropriately choosing the models, algorithms and time-step sizes, power system behaviors can be well emulated, predicted and studied.

There are two major types of digital time domain simulation tools in power system studies. They have been developed separately since the 1960s. One is the electromechanical transient simulation, which is also well known as Transient Stability Analysis (TSA). This type of simulation tools is mainly used for predicting whether a

large power system can regain an acceptable equilibrium point (stable and secure) after being subjected to big disturbances (short circuit fault, disconnection of lines, transformers, generators, malfunction of controls etc. , or so called ‘contingencies’) [3]. In such studies, the dynamic behaviors of large inertia power system components and the dynamic interactions between them which cause large energy flow variations are of main concern. In such methods, the major part of the electrical network can be represented as a quasi-steady state phasor model, with the large inertia components being represented with time domain differential equations.

The other type is the electromagnetic transient simulation referred to as EMT simulation. It focuses on emulating the detailed behaviors of the components of the power system, such as voltage spikes, current surges, voltage and current waveform distortions, harmonics etc. As power electronic devices are widely applied in modern power systems, simulating the very detailed semiconductor switching transients has become one of the major applications of EMT simulation tools [4].

These two types of simulations will be further discussed in the next chapter.

1.2 Real Time Digital Simulator

Real Time Digital Simulator (RTDS) is a real time implementation of EMT simulation. To achieve real-time simulation speeds, the power system to be simulated is divided into parts by utilizing the traveling wave characteristic of transmission lines. The relativistic speed limit allows complete separation of the systems if simulation time step is smaller than the travelling time of light over the distance of the transmission line. Hence the two systems can be simulated in parallel on different processors. A custom powerful parallel computation platform is used to solve the nonlinear differential equations. In this way,

the size of the system to be simulated is not limited by one processor or one computer, and systems of hundreds of buses have been simulated in real time [1]. The relativistic speed limit also automatically ensured manageable scalability. The larger the system, the more is the number of interconnected subsystems, each connected to the others by isolating transmission lines. However, the size of each subsystem does not grow, and hence nor does the processing power required to solve it. Hence, the larger problem can be solved simply by adding a larger number of processors. Had the subsystem size increased, it would have expanded beyond the processing power of a single processor.

Simulations of the power system in real time is not just for saving the computation time; more important, actual protective relays and control equipments can be connected to the RTDS in a closed loop and be tested as if they are in a real power system [2]. Thus RTDS has been widely used by manufacturers, research institutes and utilities.

It should be noted that though RTDS is an EMT type simulation tool, the technique requirements for it are significantly different from those for a non-real-time EMT program or those for a TSA type program.

In conventional non-real-time EMT simulations, it is common engineering practice that only a small part of a large power system is modeled. There are a few reasons for such a simplification:

(1) Detailed EMT type simulations require large amount of computation, even with a state of the art computer, simulating a large power system model would be either impractically slow or impossible.

(2) Making a detailed EMT type large power system model is very difficult. Huge amount of data needs to be collected, verified and properly included in the

model. Due to the details that need to be considered, building an EMT type model needs much more work than building a TSA type model for the same power system.

(3) The electromagnetic transient behaviors that the EMT type simulation focuses on are in the time frame of 10^{-7} second ~ 10^{-1} second. This type of transient is normally damped out very quickly and hence the duration of an EMT type simulation is normally only 1~2 seconds (system time), and the electromagnetic transients normally are damped out in a very short electrical distance, thus any power system equipment which is far away from the location where the fast transients occur is considered not to be affected by such transients and will not respond to them in the short duration, and hence need not to be modeled.

On the other hand, in the TSA type simulation, a large amount of power system equipments located over a large geographical area is modeled in order to catch the power system transient behavior in the time frame of 0.1 second ~ 20 second range. Simplified models are used to represent the equipment. Basically, any dynamic behavior in the time frame less than 0.02 second can be ignored. Another simplification normally implemented in TSA simulation is that the three phase AC system is approximated as a single phase system (positive sequence)[21].

However, all of these simplifications in the EMT and TSA modeling approaches have their limitations. For example, how will a large power system behave after being subjected to a serious unbalanced fault which is close to an important HVDC inverter? Neither an EMT simulation nor a TSA simulation can easily give a convincing answer.

On the EMT side, without a major part of the AC system being modeled, the AC system behaviors cannot be correctly simulated. These include the AC voltage magnitude and frequency variations at the inverter bus, which will interact with the HVDC system significantly. It will be hard to tell from the simulation whether the system will lose its stability after being subjected to the fault.

On the TSA side, how the HVDC system will react to a close fault (especially an unbalanced fault) cannot be correctly represented. The commutation failure and the recovery process of the HVDC system cannot be properly simulated in the TSA simulation, and these behaviors will largely affect the energy flow of the AC/DC system and hence affect the stability of the system.

Thus a lot of engineer's judgments are required when using either the EMT or the TSA simulation tools. The engineer needs to determine if the tool is suitable for a certain scenario, what modeling approaches need to be used and what models need to be included. The engineer also needs to estimate how reliable the simulation results are.

The major advantage of RTDS is that a real physical controller can be connected to it. In addition to the simulation running at real-world speed, it is also required to run on a continuous basis, i.e. minutes, hours, or even days. In such a time frame, in a real power system, almost all dynamic behaviors can occur. For a real controller, it is not possible to separate its "slow" and "fast" behaviors and characteristics, its response is a full range response, and hence the RTDS which is to be connected to the real controller is also expected to represent a full range of characteristics and behaviors of a real power system. To do this, in a RTDS simulation, not only does each of the power system components need to be modeled in full detail, but also a large number of components need to be

modeled. Technically such a modeling approach can be applied in RTDS, since its distributed computation platform is scalable. However, to model a practical power system in full RTDS detail needs large amount of RTDS hardware and hence the hardware cost can be practically prohibitive. This is the major motive of this research.

1.3 System Equivalent for RTDS

The question of how to make the system equivalent for the digital time domain simulation has been an important issue since the beginning of the technique itself. The demand for accurate and detailed simulation is usually compromised by the limited computation capability and time. The scale of a modern interconnected power system can be so large that it is often not practical for any digital time domain simulation tool to run a large power system model in which all the components are modeled with the full modeling capability.

The basic concept of system equivalent can be illustrated by Figure 1-1. The "Internal System" is the system that we need to study in detail, so all the generators, controls, HVDC devices etc. in this area have to be modeled in detail. But the behaviors of the internal system are influenced by the interactions between the internal system and the external system. The external system is not required to be studied in detail, but in order to simulate the interactions with high accuracy it is also modeled in detail with the corresponding demand for a large amount of computation resources. To save the resources, a simplified model is used to replace the detailed model of the external system. This simplified model should be able to replicate the responses of the external system to the changes of internal system with a reasonable accuracy, but demand much less computation resources.

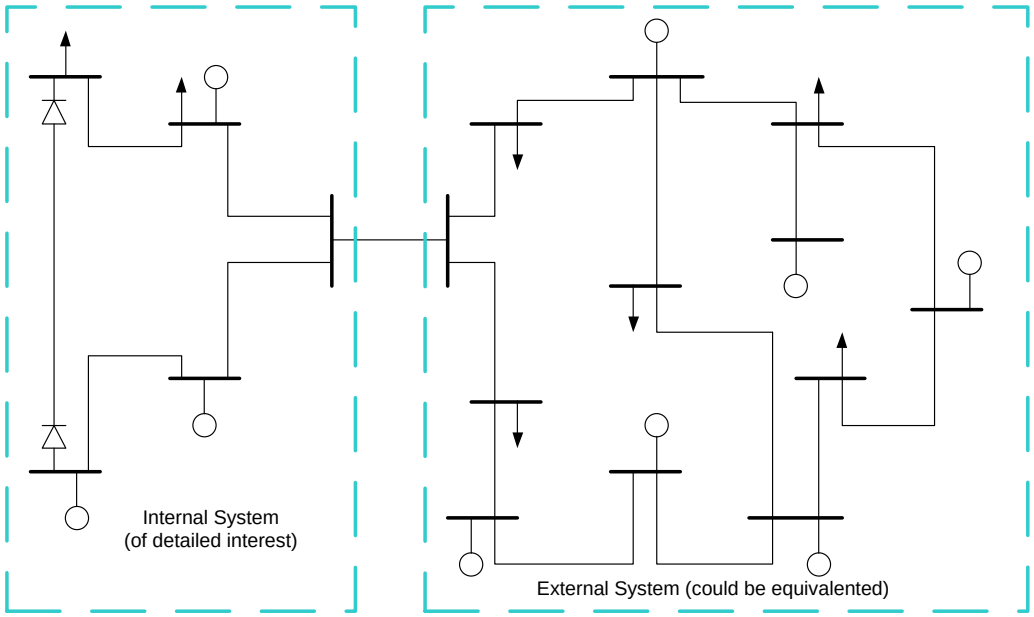

Figure 1-1 Internal System and External System

As the TSA and EMT simulation tools themselves, the equivalencing techniques for these two types of tools have also been developed separately.

1.3.1 Equivalencing Techniques for TSA Simulation Programs

In the early years of TSA simulation programs, the capability of the tool was seriously limited by the computer capability. Many equivalencing techniques were developed simultaneously with the developments of the TSA simulation techniques. These equivalencing techniques focused on emulating the large real and reactive power flow variations of the tie lines using a simplified system model which requires less computation resources than the original full system model.

The most widely used techniques in the industry can be categorized as “coherency” based techniques [5][6][7][8][9]. They are based on the observations that after a large disturbance, a group of generators which are electrically (and geographically) close to

each other and have similar machine and control parameters, tend to swing together. If a group of such coherent generator models in the external system are replaced with a single equivalent generator model, the response sensed by the internal system might be similar to those of the original full system model. In this way, the size of the external system model can be significantly reduced.

These techniques normally include three steps:

(1) Coherency group identification.

(2) Network reduction. The coherency generator buses are replaced by a new generator bus. The network is reduced in the way that the tie line power flows are maintained.

(3) Equivalent generator model parameter tuning. A single generator model is inserted into the network at the new generator bus. The model parameters (including control parameters) are tuned to achieve the best fit of the behaviors of the models of the original generators.

With the developments of computer techniques, the capabilities of TSA type simulation programs have been improved a lot. Today's TSA programs can easily simulate a power system of thousands of buses and hundreds of generators in an average speed equal or faster than real-time. However, when simulating a super large power system, which has very complicated interconnections, the equivalencing is often required. There are many such huge interconnected power systems in North America, Europe and Asia.

The equivalencing techniques of TSA simulation is not in the scope of this research, and hence will not be further discussed in this thesis.

1.3.2 Equivalencing Techniques for EMT Simulations

EMT type simulations need much more computation resources compared to TSA simulations. Due to this limitation, in most EMT applications, the study of system wide phenomenon is not generally possible. In many EMT simulations, the power system area of main interest is modeled in full EMT detail; and the remainder of the system is normally modeled as a simple Thevenin impedance and a voltage source.

Using such a simplified equivalencing approach doesn't guarantee a good re-production of the high frequency range responses of the external system. Also the slow electromechanical response of the external system is simply ignored. The popularity of this approach is rather due to the practical limitations of the computation resources. The application of such an approach involves a lot of engineering judgements. And when the system configuration is complicated, it is difficult to achieve viable simulation results.

It was found that in some simulation studies, the electromagnetic responses of the external system are critical, and a simple Thevenin impedance which only matched the external system short circuit impedance at the fundamental frequency is not adequate for re-producing the critical responses. Many previous researchers were focusing on improving this area [10][11][12][13]. Their approach is referred to as Frequency Dependent Network Equivalents (FDNE). The basic idea is to consider the external system as a linear network, and use a more complex Thevenin impedance to represent the network instead of using a first order L-R circuit. The improved Thevenin impedance not only matches the external system at the fundamental frequency, but also in a defined frequency range. A FDNE method can normally be classified based on the following features:

- it is a single-port or multi-port equivalent;
- the form of the circuit or the mathematical function chosen to represent the external system;
- the way that the coefficients of the circuit/function are determined (tuning/fitting);
- the way that the frequency domain characteristic of the external system is estimated; and
- the way that the circuit/function is modeled in the EMT simulation.

Previous research work in the FDNE area mainly focused on the following problems:

(1) How to fit the complex frequency domain characteristic of a power system.

(2) How to model the equivalencing circuit/function in the EMT simulation.

(3) How to make a stable EMT simulation model with the FDNE. This problem is related to the first two problems. It was found that making a stable EMT simulation model with FDNE can be very difficult, especially in the multi-port FDNE case. A numerically unstable simulation model (in many cases due to impassivity) can cause the time-domain simulation to fail (blow-up).

There is another practical problem in the process of making a FDNE: it is very difficult to obtain the frequency domain characteristic of a large power system.

In this thesis, a special frequency domain fitting technique called Vector Fitting [13] is implemented. A practical method of obtaining frequency domain characteristics of large power systems is introduced. FDNE is an important topic of this research, and it will be further discussed in Chapter 3 and Chapter 4.

1.3.3 Hybrid Simulation

Compared to simplified equivalent model which matches the fundamental frequency short circuit impedance of the external system, FDNE, especially multi-port FDNE is a big advance. However, this field is still a new one and requires significant more work. It should be noticed that FDNE only deals with the high frequency responses which are caused by the R-L-C oscillations of the external system. The low frequency responses of the external system, which are mainly caused by the oscillations of the generators and generation control actions, are not considered. The capability of reproducing the slow (low frequency) behaviors together with the fast (high frequency) behaviors of the power system is critical for some EMT simulation studies (for example, studies of tightly interconnected HVDC/AC system). Such capability is particularly important for RTDS, because in a RTDS simulation with real physical equipment in closed loop, it is difficult to decouple the fast and slow behaviors of the system as discussed in section 1.2.

Since TSA type simulation has been shown to be more efficient to reproduce the slow transients of the power system, many researchers have proposed the idea of combining EMT and TSA type simulation together. Such schemes are called Hybrid Simulation. In one group of such schemes, a part of the power system is modeled in EMT, and the other part is modeled in TSA. The EMT simulation algorithm and the TSA simulation algorithm are applied to the two parts respectively and there is an interface between the EMT and TSA simulations. These Hybrid Simulation schemes can also be regarded as one in which a suitable equivalent is created for EMT, because the TSA part (i.e. the equivalent) is modeled in less detail and requires less computation resources.

The efforts in this area date back to early 1980's. Heffernan et al. used a detailed HVDC model inside a TSA type AC system model [14]; the information of the

simulations of the two models is exchanged at the interface bus periodically, but the fast transient response of the external system is neglected in their configuration. Reeve et al. pointed out that one way to preserve such response is to extend the interface further into the external system, and to model more components in detail in this in-between area [15]. This is based on the experience that the fast transient responses are mainly dominated by the components which are close to the interface bus. But in a dense network, such an extension greatly increases the number of the components to be modeled in detail as well as increases the number of the interface ports of the equivalent. To resolve such difficulty, Anderson et al. further included the FDNE to represent the fast transient response of the network of the external system [16]; where the FDNE method of [10] is applied. Su et al. made the attempt to implement hybrid simulation on a real time digital simulation platform [17]; where the same FDNE technique as [16] was applied. In the above research, only a single port (three phase) interface has been considered, the more complicated mutual coupling between multiple ports have not been examined. Wang et al. gave a multi ports application example of EMTDC-TSA hybrid simulation, though the network is only represented by a fundamental frequency model [18].

The Hybrid Simulation is not yet a mature technique. There are a few significant difficulties in its industrial implementation:

(1) Coordinating and interfacing the EMT and TSA simulations is not straight forward because of the theoretical differences in the nature of the EMT and TSA algorithms. The two algorithms will be further discussed in Chapter 2.

(2) The TSA part is used to represent the low frequency characteristics of the external system. To make a fundamental frequency, multi-port network equivalent can be

difficult in many cases. There are still difficulties in representing the high frequency characteristics (as discussed in the last subsection).

(3) Both the traditional EMT techniques and the traditional TSA techniques are generally variable speed (not to be confused with variable time-step) simulation techniques, because the time required for computation can vary at different steps of the simulation. This makes the implementation difficult for a hard real-time platform like RTDS and there needs to be special considerations for the implementation of the TSA algorithm.

1.4 Proposed Wide-band Two Parts Equivalent for RTDS

In this research, a wide-band two parts equivalencing technique is developed. The basic structure of the equivalent is illustrated in Figure 1-2. The technique is an extension of that reported in [16][17].

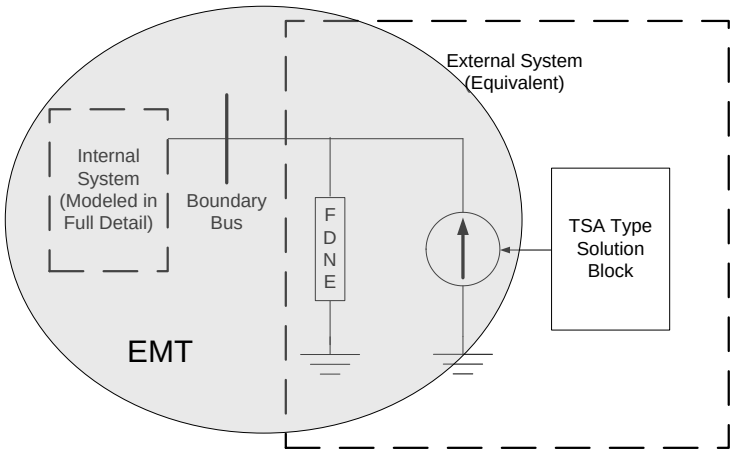

Figure 1-2 Wide Band Two Parts Equivalents

A multi-port FDNE is connected to the internal system. The FDNE represents the high frequency characteristics of the external system. It matches the frequency dependent self-admittances (between boundary nodes and the ground) and the frequency dependent

mutual-admittances (between different boundary nodes) of the external system in the frequency range of interest (not only at the fundamental frequency). In this way, the linear R-L-C characteristics of the external system are preserved.

Sinusoidal fundamental frequency Norton current sources are connected between each boundary node and ground. The phase angles and magnitudes of the Norton current sources are determined by the phase angles and magnitudes of the internal voltages (say E_q'') of the generators in the external system. (Note that this is a simplified statement. Other equipments such as motors, nonlinear loads, FACTS etc. also have similar effects on the phase angles of magnitudes of the Norton current sources at the boundary). During the simulation, the phase angle and the magnitude of the internal voltage of each generator in the external system is calculated by a TSA simulation block, which includes the dynamic models of the external system and an interface to the EMT simulation.

This research is a further development of the previous research work in the FDNE area [10][11][12][13][19] and Hybrid Simulation area [14][15][16][17][18]. The new developments reported in this thesis include:

(1) a modified TSA simulation algorithm which is suitable for a hard real-time platform (RTDS);

(2) a simple and accurate interface scheme between the TSA simulation and the EMT simulation;

(3) a practical way of obtaining the frequency dependent characteristics of large AC power systems; and

(4) Vector Fitting algorithm [13] is implemented for determining the coefficients of the multi-port FDNE. A heuristic method of handling the passivity issue of the FDNE is introduced.

1.5 Organization of the Thesis

In this chapter, the background information of the digital time domain simulation in power system studies, the RTDS and the equivalencing techniques for EMT and TSA simulations are introduced. A wide-band two-part equivalencing technique is proposed.

In Chapter 2, the basic theories and structures of the EMT simulation and the TSA simulation are reviewed and compared. The combination of these two simulation methodologies is one of the essential parts of this research.

Chapter 3 reviews the equivalencing techniques for the EMT simulation.

In Chapter 4 the process of the derivation of the frequency dependant admittance matrix of the external network from readily available power flow data, the conversion of the admittance matrix to equivalent rational functions and the modeling of the rational functions in the RTDS simulation are presented. Frequency domain and time domain simulation examples are given in this chapter. The passivity issue of the FDNE is also discussed in this chapter, and a heuristic method of mitigating the passivity violation is introduced.

Chapter 5 focuses on another major part of this research. In this chapter, a new scheme of incorporating TSA type solution with RTDS is presented. The interfacing between EMT and TSA is another major topic of this chapter. The TSA type network solution and the TSA type modeling of power system equipments are also discussed.

In Chapter 6, the synthesis of the entire equivalent is explained. Some practical issues of implementing the proposed equivalent are discussed.

Several examples are presented in Chapter 7. These examples show the capability of the proposed equivalencing method. The comparisons between RTDS full model simulation, TSA simulation and RTDS simulation using the proposed equivalent are discussed.

Chapter 8 summaries the conclusion and presents suggestions for future works.

2 Digital Time Domain Simulation Approaches

Two different types of digital time domain simulation approaches are introduced and compared in this chapter.

2.1 The Dynamic Behaviors of Power Systems, from a Simulation Point of View

Power system dynamic behaviors are combinations of various transient phenomena. A rough classification of these phenomena is given in Figure 2-1. This classification is made from a power system time domain simulation point of view, and illustrates the major characteristics only. Power system behaviors are complicated and precise classification is difficult.

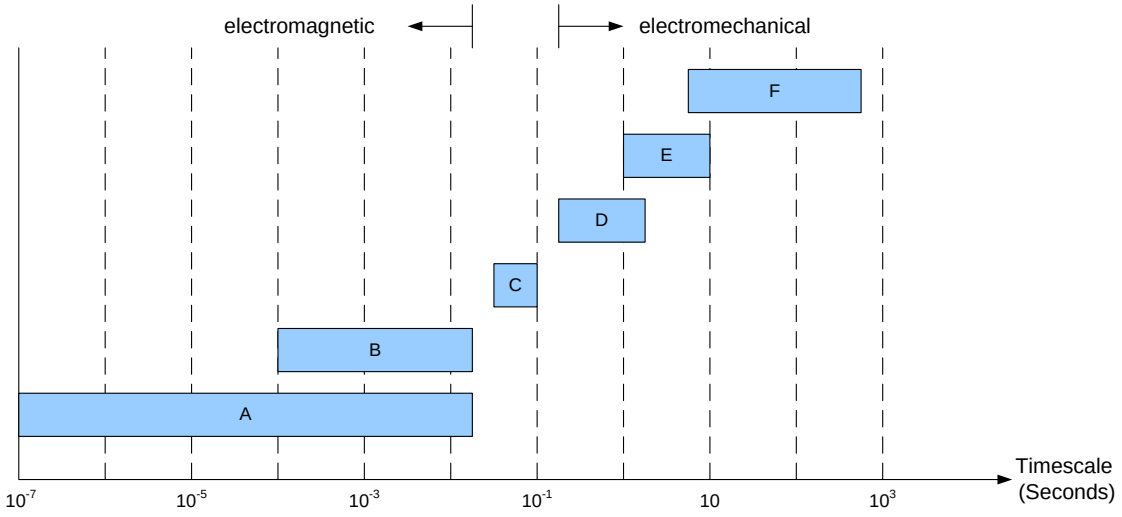

Figure 2-1 Time Frames of Various Power System Transient Phenomena

A: To simulate R, L, C oscillations, the network components, such as transmission lines, cables, transformers, shunt capacitors, shunt reactors, filters etc. need to be represented by partial and ordinary differential equations. Both the linear and nonlinear characteristics should be modeled. Depending on the phenomena to be studied, some components might need to be modeled in very great detail. For example, in lightening studies, the transformer might be modeled as a distributed component instead of a lumped component.

B: To simulate power electronic switching transients, the converters need to be modeled in detail, in which semiconductor switches are explicitly modeled [20]. Traditionally phenomena A and B fall under the category of electromagnetic transient.

C: Sub-synchronous Resonance is the result of the interactions between the mechanical torsional oscillations of the generator rotor and the oscillations of the network (or the controller) [21]. So the mechanical characteristic of the rotor as a set of several mass parts has to be modeled using differential equations, also the network has to be modeled using differential equations.

D & E: There is no clear distinction between the local mode rotor angle oscillation and the inter-area mode rotor angle oscillation. However, local mode rotor angle oscillations mainly involve generators in a small area, usually associated with the rotor angle oscillation of a single power plant against the rest of the power system. The oscillation frequencies of such oscillations are higher than the inter-area mode [21]. To study local mode rotor angle oscillations, there might be a couple of generators and the corresponding exciters and stabilizers that need to be modeled in detail. To study inter-area mode rotor angle oscillations, a larger number of generators that are located in large

area need to be modeled in detail; generator governors as well as loads and the supplementary controls of HVDC and FACTS play important roles in these phenomena. In both of these phenomena, electromagnetic transient plays a lesser role and can usually be neglected.

F: Voltage collapses of power systems are normally slow processes. Load characteristics play critical roles in these phenomena; auto transformer tap changers, excitation protective controls, load shedding relays are the important factors that need to be considered and they must be modeled in appropriate detail.

2.2 EMT Simulation

For several decades, EMT simulation tools have been the industry standard for studying the detailed transient behaviors of power system equipments, especially power electronic equipments, and small power networks. EMTP and PSCAD/EMTDC are well known EMT simulation tools. RTDS is a real time implementation of the EMT simulation algorithm.

Traditionally, the typical applications of EMT simulation tools include insulation coordination, study of over-voltages due to switching surges, power electronic transient performances, sub-synchronous resonances and ferroresonance phenomena etc., i.e., those phenomena from A to C in Figure 2-1.

There are some basic features of EMT simulation tools [22][23][24] as stated below:

The trapezoidal integration rule is applied for solving the differential equations. It is stability-preserving for linear systems. That means a large time-step will not cause numerical instability (blow out) during the integration, though the results might lose accuracy.

Applying the trapezoidal integration rule, the differential equation of a linear component (reactor, capacitor etc.) is represented by a constant conductance in parallel with a history current term. The value of the history current term is determined only by past (history) information. For example, an inductor is represented in the EMT simulation as shown in Figure 2-2.

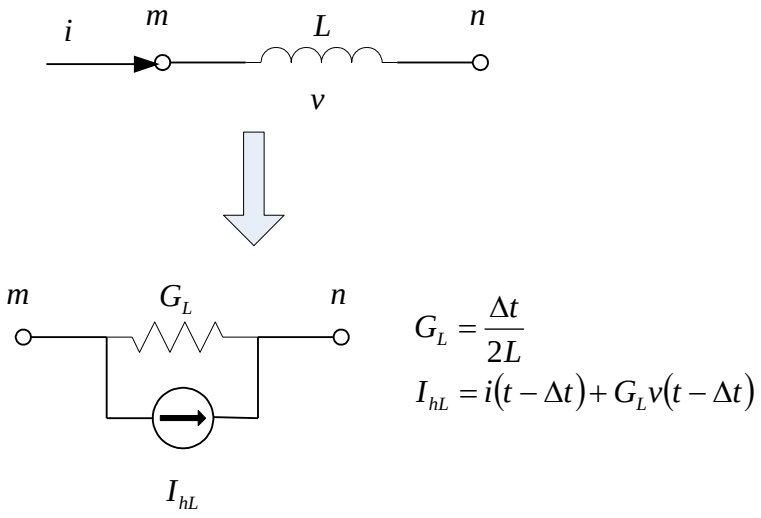

Figure 2-2 Modeling of a Inductor in EMT Simulation

The system equations are built by using the standard nodal approach [25].

The traveling wave theory is applied to distributed components (overhead transmission line and cable) [26]. For the transmission line or cable, any effect from one end can only be 'sensed' by the other end after a time delay (for a 100km line, the time delay is more than 333μs). So, the power network can be divided into several sub-networks by transmission lines and cables. The equations of different sub-networks need not to be solved together; the interactions between different sub-networks are represented as

history current terms. This feature is utilized in RTDS and parallel computation hardware is employed to solve the equations of different sub-networks simultaneously.

Switches (breaker, power electronic) are modeled as variable conductances.

The synchronous machine is modeled in a state equation formula with a current source interface to the network [27].

A simplified structure of the power system model for EMT simulation is shown in Figure 2-3. A simplified typical flowchart of EMT simulation is shown in Figure 2-4.

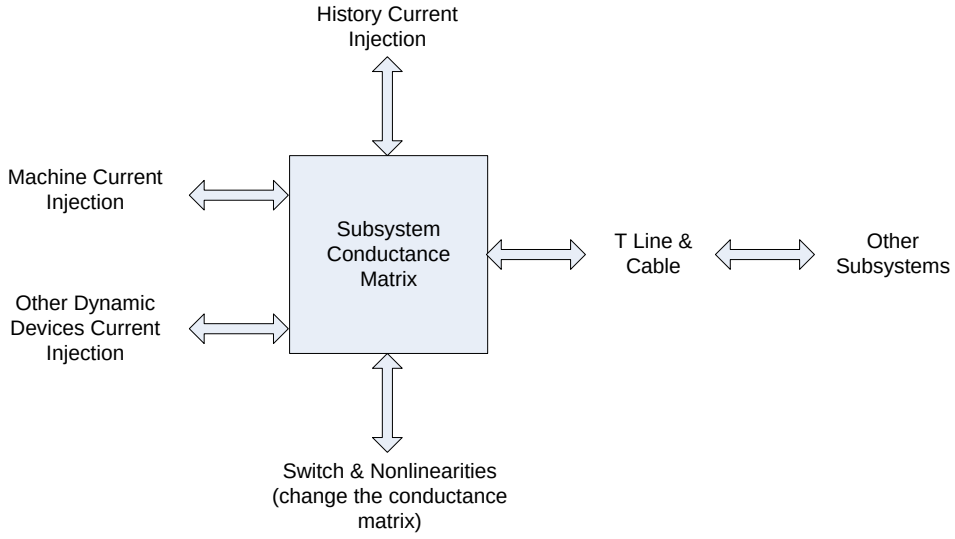

Figure 2-3 Structure of the Power System Model for EMT Simulation

In EMT simulation, every phase of the power system network is modeled. Hence unbalanced phenomena and after transient behaviors can be simulated.

What transient behavior can be simulated in EMT simulation is determined by the model details and the time-step. The common time-step is 50μs, with which most electromagnetic switches and power electronic related transients of the power system can

be captured. For lightning studies and high speed power electronics (for example, PWM based power electronic converter) simulation, much smaller time-steps must be used.

Because a small time-step has to be used, and a lot of details must be included, EMT simulation is very computationally intensive and time consuming. For example, to simulate using PSCAD/EMTDC a 5 seconds transient on a power system model with 130 AC bus-bars, 11 generators and two bi-pole HVDC links, it takes about 33 minutes on a 2.53 GHz Pentium4 computer with 1G RAM.

RTDS runs in real time, which means that the simulation keeps in synchronism with a real world clock, i.e., each 50μs time-step (say) simulation is completed within 50μs. The largest reported power system model ever been simulated on a RTDS (as of 2008) is made for the South Korean power system [1]. It contains 326 AC bus-bars and 110 generators. 26 RTDS racks, or 338 3PC cards, were employed to run this model in real time.

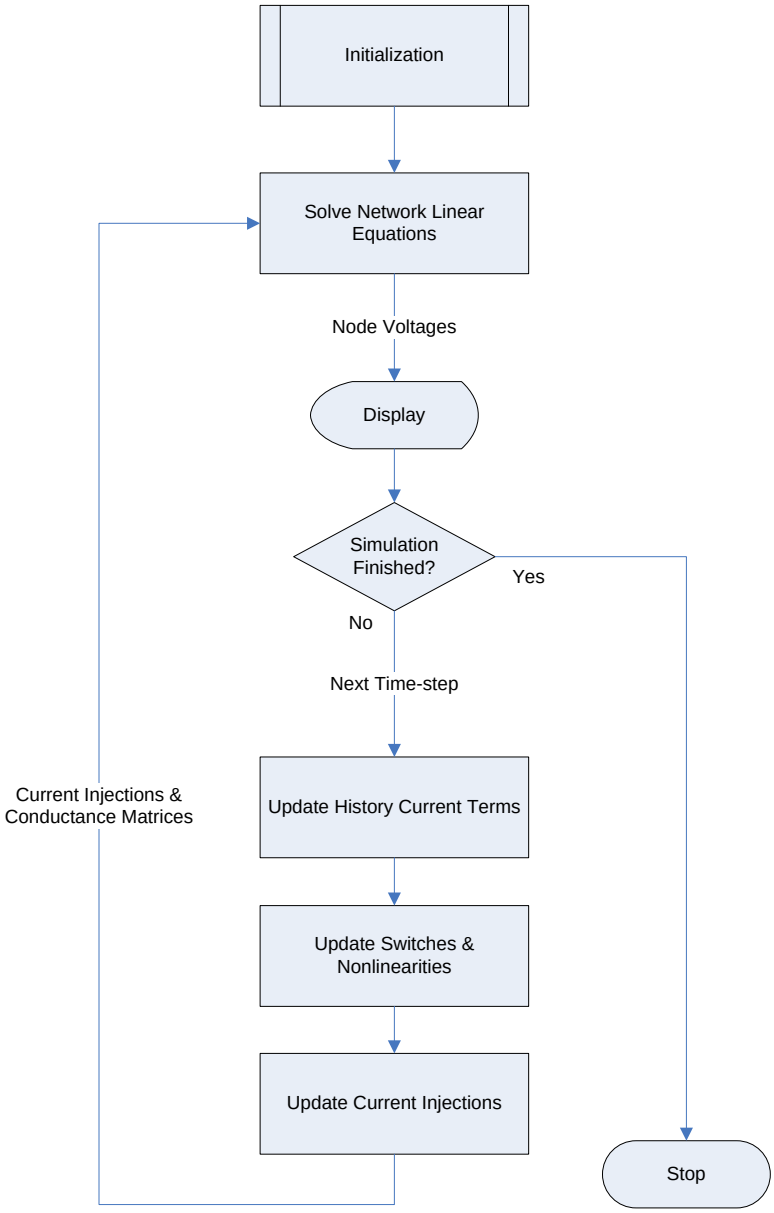

Figure 2-4 Simplified Typical Flowchart of EMT Simulation

2.3 TSA Simulation

Modern TSA simulation tools like PSS/E, TSAT and BPA are widely used in the power industry, especially by power system operators and planners. These tools are the industry standard tools for studying power system transient stability problems; they are also employed for voltage stability studies, small signal stability studies and frequency stability studies. That is they are used for studying the phenomena from D to F in Figure 2-1, especially phenomena D and E.

Practical power systems with tens of thousands bus-bars and hundreds of generators are readily handled by such tools. For example, one of the largest power system models ever simulated is made for the NERC eastern North America interconnection system. This model contains more than 40000 AC bus-bars, more than 5000 generators and 15 HVDC links, and it keeps growing. Fifteen seconds simulation of this extremely large model on TSAT can be finished in around 10 minutes, using a 2 GHz PENTIUM 4 PC.

With TSA simulation, there are some widely accepted engineering practices [21].

The electrical transients of the network are neglected, assuming that the voltage and current transients of the network decay in a period smaller than the simulation time-step. So the network can be represented by algebraic equations of phasor quantities instead of differential equations. The frequency of the system is assumed to be close to the fundamental frequency and the network is represented by a complex admittance matrix.

The synchronous machine stator transient is neglected. The differential equations of the stator are simplified as algebraic equations.

Like stator transients, the switching transients of power electronics are neglected, algebraic equations are used to represent the converter.

All components in the TSA simulation have fundamental frequency phasor domain representations. No instantaneous AC voltage and current waveforms are calculated in the simulation.

The three phase AC system is assumed to be balanced. The positive sequence single line network is used for representing it. The unbalance of the network itself is ignored. The effect of unbalanced faults is modeled by an effective impedance in the positive sequence network.

The commonly used time-step ranges from one-eighth cycle to half cycle (for a 60Hz system, it is 2.083ms~8.333ms), which is 2 orders of magnitude larger than for EMT simulations.

Other fast transients whose time frames are shorter than the simulation time-step are neglected.

A simplified structure of the power system model for TSA simulation is shown in Figure 2-5. A simplified typical flowchart of TSA simulation is shown in Figure 2-6, in which the integration method is assumed to be the second order Runge-Kutta method (RK2) [28].

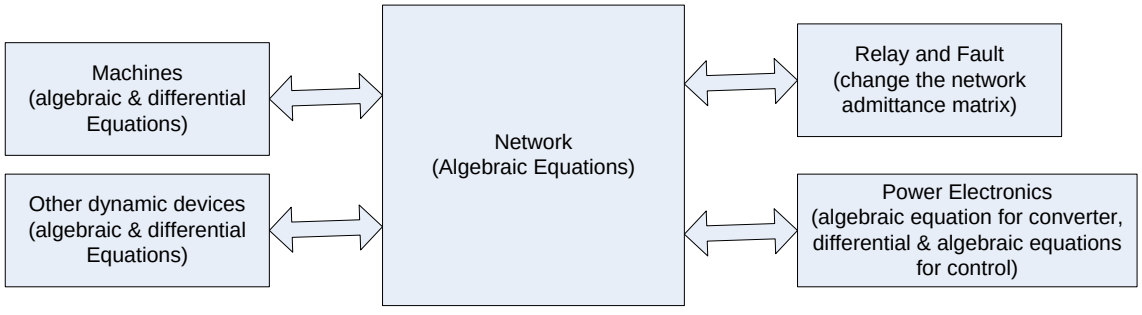

Figure 2-5 Structure of the Power System Model for TSA Simulation

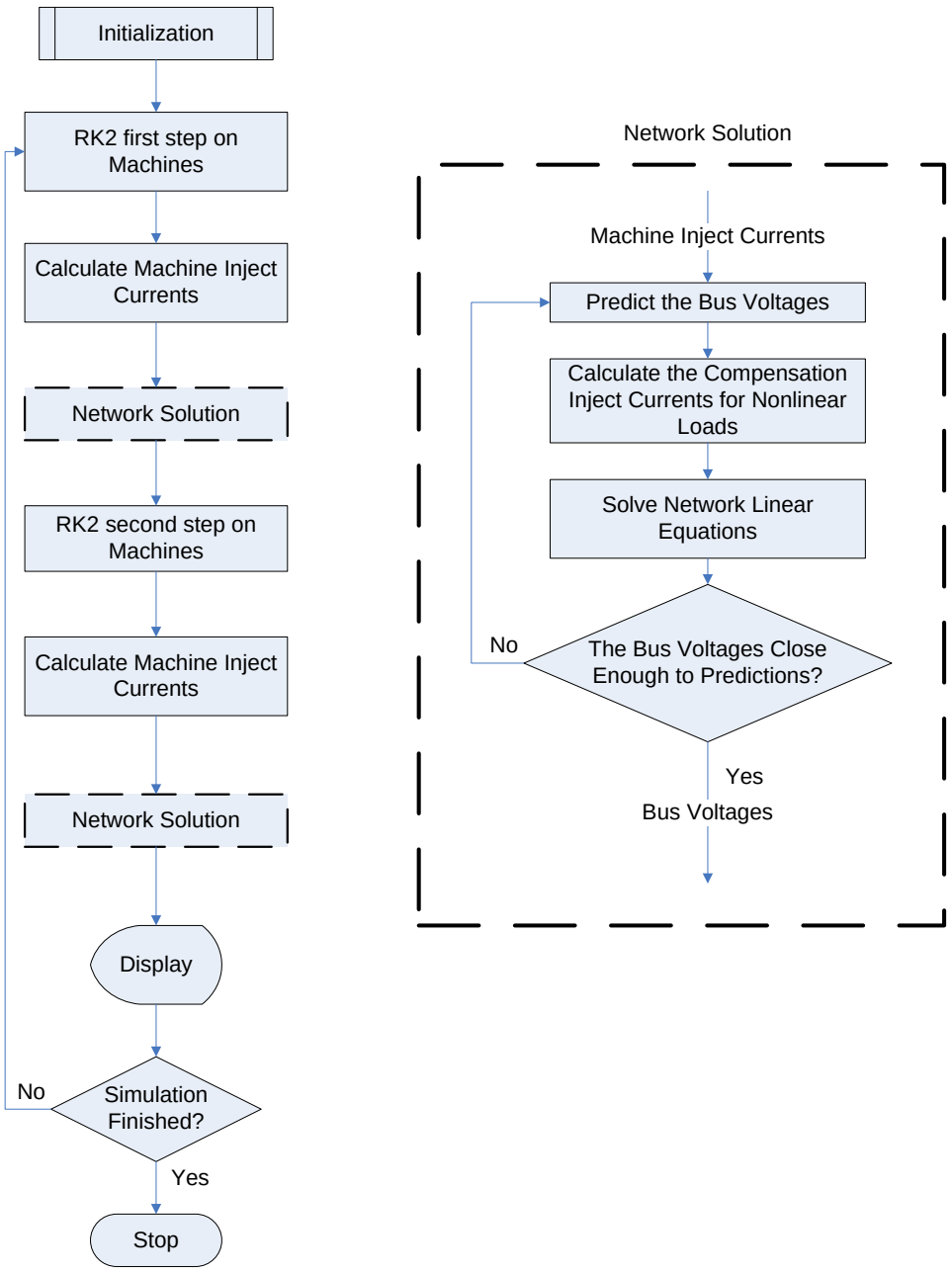

Figure 2-6 Simplified Typical Flowchart of TSA Simulation

2.4 The Differences between the Two Types of Simulation Approaches

The principle differences between the TSA and the EMT simulations are summarized in this section.

The TSA simulation is built in the fundamental frequency, positive sequence, phasor domain. On the other hand, in EMT simulation, real physical values such as instantaneous voltage and current are directly computed. No matter how small the time-step is, TSA simulation cannot simulate the phenomena from A to C in Figure 2-1. By its nature, TSA simulation cannot represent waveform distortions, harmonics and accurate switch behaviors etc.

Theoretically, all the behaviors that can be simulated by the TSA tools can also be simulated by the EMT tools. EMT simulation is able to cover all the phenomena from A to F in Figure 2-1. But due to the large computation needed by EMT simulation, the length of EMT simulation is usually limited to one to two seconds. In such short periods the phenomena from D to F are not revealed or are only partly revealed. The real time digital simulation is running at the speed of real time and can run as long as the user wants. But it is not possible to use such tools to simulate an AC system which has hundreds of buses and tens of generators without building a super large scale simulator whose price can be prohibitive. The oscillation behaviors of a complicated interconnected system are affected by a large number of dynamic and nonlinear devices spread in a large area. Unless such devices and the main part of the network are modeled in appropriate detail, it is not possible to study the complex dynamic behaviors of large practical power systems. Thus, the EMT simulation tools, including RTDS are not being widely used in large power system dynamic studies as they could.

3 Equivalencing Methods for EMT Simulation

This chapter discusses the equivalencing methods for EMT simulations.

3.1 Simplified Equivalent for EMT Simulation

Typically very simplified equivalents are used with EMT simulation. The most commonly used equivalent consists of a Thevenin impedance, which is derived from the fundamental frequency short circuit impedance at the terminal bus and a Thevenin voltage source behind the impedance as shown in Figure 3-1.

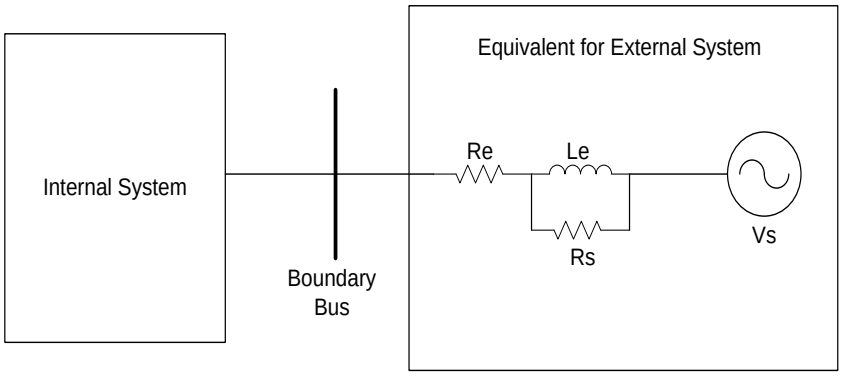

Figure 3-1 Simplified Equivalent in EMT Simulation

The R-L||R circuit represents the fundamental frequency short circuit impedance of the external system seen from the boundary bus. Surge resistor Rs provides a route for the current at high frequencies when the inductor Le is virtually open circuited, preventing an open circuit [29].

Vs is a constant sinusoidal voltage source whose frequency, phase and magnitude are fixed. Since the oscillations of the generators are normally slow (typically in 0.1~1Hz range), for most EMT simulations which end in about 1 second, they are assumed to have no significant impact on the internal system. Thus the generators can be seen as constant sources. This is one of the reasons why the constant sinusoidal source (voltage or current) is widely used to represent the dynamic sources, mainly generators, of the external system. More important is that the constant source is the simplest model and requires minimum computation. Thus such practice is widely accepted.

This equivalent only represents the external system at the fundamental frequency and steady state. Neither the fast response (electromagnetic) nor the slow response (electromechanical) of the external system can be properly re-produced by such a simplified equivalent. It is recommended that the devices close to the internal system (typically in the range of two to three buses/layers) should be modeled in detail [29]. In many cases such an expansion is not practical, especially when the network is dense. Also the reproduction of the fast response is not guaranteed, and the slow response is even not considered.

So there are two questions which need to be answered when making system equivalents for EMT simulation tools. One is how to represent the fast transient response of the external system; the other is how to represent the slow nonlinear dynamic response of the external system.

3.2 Frequency Dependant Network Equivalent

The research trying to answer the first question can be generally categorized as Frequency Dependant Network Equivalent (FDNE).

With approximations and simplifications, the external AC system can be seen as a linear network with some dynamic sources connected to it. The FDNE aims on making a model which can be simulated in the time domain and has similar frequency response as the linear external network and hence has similar time domain response as the external network. This model should be computationally more efficient than the original external network model.

Seen from the boundary buses, the external linear network can be represented as a frequency dependant admittance matrix. It can also be seen as a small network tgat

consists of some frequency dependant branches as shown in Figure 3-2, which shows a three phase boundary bus.

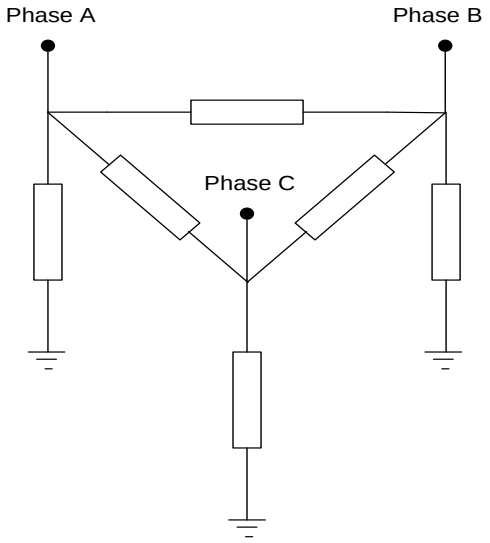

Figure 3-2 External Network as Seen From the Boundary

The individual branches in Figure 3-2 are derived from the self and mutual impedances observed at the boundary. Each of them is a frequency dependant admittance:

$$Y(\omega) = \frac{I(\omega)}{V(\omega)} \tag{3.1}$$

The early attempts in this area considered replacing each branch with a equivalent network consisting of lumped R, L, C components. The values of these components were determined and hence the equivalent network had approximately the same frequency response as the branch [10][11]. In many cases, the external network consists of distributed parameter components such as transmission lines. Using lumped physical R, L, C components to capture its behaviors is often inadequate.

Presently, efforts have been concentrated on finding a good rational function approximation for the frequency dependant branch. Two forms of transfer functions can

be used: the power series polynomial function and the orthogonal polynomial function. Mathematically these two are equivalent, but the numerical methods used for deriving the coefficients of these two forms of transfer functions (the fitting processes) are totally different.

3.2.1 Power Series Polynomial Function

In principal, a given frequency response of a linear system can be fitted by optimizing the coefficients of the following power series polynomial function:

$$f(s) = \frac{a_0 + a_1 s + a_s s^2 + \cdots + a_N s^N}{1 + b_1 s + b_s s^2 + \cdots + b_N s^N} \tag{3.2}$$

The fitting of this transfer function in the frequency domain is fairly straight forward. Suppose the impedances/admittances at various frequency points are known:

$$Z(j\omega_i) = R_i + jX_i \qquad (i = 1 \cdots M) \tag{3.3}$$

M is the number of the frequency points, which normally is much larger than N, the order of the transfer function f.

We can write the equation for all these frequency points:

$$f(j\omega_i) = \frac{a_0 + a_1 j\omega_i + a_2 (j\omega_i)^2 + \cdots + a_N (j\omega_i)^N}{1 + b_1 j\omega_i + b_2 (j\omega_i)^2 + \cdots + b_N (j\omega_i)^N} \approx R_i + jX_i \qquad (i = 1 \cdots M) \tag{3.4}$$

After rewriting:

$$\begin{aligned} &\left(a_0 + a_1 j\omega_i + a_2 (j\omega_i)^2 + \cdots + a_N (j\omega_i)^N\right) \\ &\approx \left(1 + b_1 j\omega_i + b_2 (j\omega_i)^2 + \cdots + b_N (j\omega_i)^N\right)\left(R_i + jX_i\right) \quad (i = 1 \cdots M) \end{aligned}$$

$$\begin{aligned} &a_0 + a_1 j\omega_i + a_2 (j\omega_i)^2 + \cdots + a_N (j\omega_i)^N - \\ &\left(R_i + jX_i\right) b_1 j\omega_i - \left(R_i + jX_i\right) b_2 (j\omega_i)^2 - \cdots - \left(R_i + jX_i\right) b_N (j\omega_i)^N \\ &\approx R_i + jX_i \qquad (i = 1 \cdots M) \end{aligned} \tag{3.5}$$

Now there are M complex linear equations, and $2\times N+1$ variables (R_i, X_i and ω_i are given. $a_0 \cdots a_N$, $b_1 \cdots b_N$ are unknowns which are to be determined). They can be written into a $(2\times M, 2\times N+1)$ real linear equation set. Because M is much larger than N, this is an over-determined linear equation set, and it can be solved as a linear least square problem by standard least square algorithms [31].

The difficulty of solving such a problem is that these equations are badly scaled and ill conditioned due to the powers of ω in the equations. Especially when a high order approximation needs to be used, or a wide range frequency response needs to be fitted. Some attempts in this direction [19] showed the drawbacks of this form of transfer functions.

3.2.2 Time Domain Fitting

In spite of the problems identified in the previous subsection, the power series polynomial function is still very attractive, because its optimization is a linear problem; even though it is very ill conditioned by nature. Abur and Singh [12] have presented an alternative method. Instead of fitting the power series polynomial function in the frequency domain, they showed that this problem can be solved in the time domain.

Suppose the voltage-current relationship is:

$$I(s) = V(s)\, f(s) = V(s)\frac{a_0 + a_1 s + a_s s^2 + \cdots + a_N s^N}{1 + b_1 s + b_s s^2 + \cdots + b_N s^N} \tag{3.6}$$

This can be written as:

$$I(s)\left(1 + b_1 s + b_s s^2 + \cdots + b_N s^N\right) = V(s)\left(a_0 + a_1 s + a_s s^2 + \cdots + a_N s^N\right) \tag{3.7}$$

Which can be written in a operator form as:

$$\left(1+b_1\frac{d}{dt}+b_s\frac{d}{dt^2}+\cdots+b_N\frac{d}{dt^N}\right)I(t)=\left(a_0+a_1\frac{d}{dt}+a_s\frac{d}{dt^2}+\cdots+a_N\frac{d}{dt^N}\right)V(t) \qquad (3.8)$$

Define a series of internal variables as:

$$\begin{aligned} i_1&=\frac{di}{dt}, \quad i_2=\frac{d^2i}{dt^2}, \quad \cdots \quad i_N=\frac{d^Ni}{dt^N} \\ v_1&=\frac{dv}{dt}, \quad v_2=\frac{d^2v}{dt^2}, \quad \cdots \quad v_N=\frac{d^Nv}{dt^N} \end{aligned} \qquad (3.9)$$

Applying the Backward Euler method to obtain the difference equations:

$$\begin{aligned} i_{j+1}(t)&=\frac{1}{\Delta t}\left[i_j(t)-i_j(t-\Delta t)\right] \quad j=0,1,\cdots N \\ v_{j+1}(t)&=\frac{1}{\Delta t}\left[v_j(t)-v_j(t-\Delta t)\right] \quad j=0,1,\cdots N \end{aligned} \qquad (3.10)$$

Δt is the time-step in the time domain simulation. These equations can be applied recursively to convert equation (3.8) into a difference equation:

$$i(t)+h_1i(t-\Delta t)+\cdots h_Ni(t-N\Delta t)=g_0v(t)+g_1v(t-\Delta t)+\cdots g_Nv(t-N\Delta t) \qquad (3.11)$$

If a series of $i(t)$, $i(t-\Delta t)$, $i(t-2\Delta t)$ … $i(t-M\Delta t)$; and $v(t)$, $v(t-\Delta t)$, $v(t-2\Delta t)$ … $v(t-M\Delta t)$ are known; normally M is much larger than N; then (3.11) becomes another linear least square problem. A set of optimized $h_1,\cdots,h_N,g_0,g_1,\cdots,g_N$ can be obtained by solving this problem.

The time domain response $i(t)$, $i(t-\Delta t)$, $i(t-2\Delta t)$… $i(t-M\Delta t)$ and $v(t)$, $v(t-\Delta t)$, $v(t-2\Delta t)$ … $v(t-M\Delta t)$ can be obtained from a time domain simulation of the full external network where the excitation signal should be a sum of multiple sinusoidal signals of different frequencies, which can ensure that the response can cover a wide frequency range.

It is possible to derive the converting equations between $h_1,\cdots,h_N,g_0,g_1,\cdots,g_N$ of (3.11) and $b_1,\cdots,b_N,a_0,a_1,\cdots,a_N$ of (3.6), but this conversion is numerically impractical. Due to the powers of Δt in the converting matrix, the matrix is very ill conditioned (from this it can also be realized that the power series polynomial function is numerically ill conditioned). So, the fitted $h_1,\cdots,h_N,g_0,g_1,\cdots,g_N$ must be used in the time domain simulation directly. The equivalent of the external network is in the history current form as:

$$\begin{aligned} i(t) &= g_0 v(t) + ih(t) \\ ih(t) &= g_1 v(t-\Delta t) + \cdots + g_N v(t-N\Delta t) - h_1 i(t-\Delta t) - \cdots - h_N i(t-N\Delta t) \end{aligned} \tag{3.12}$$

This time domain fitting technique is simple and easy to implement, the main shortcomings of this method are:

(1) The coefficients $h_1,\cdots,h_N,g_0,g_1,\cdots,g_N$ in (3.12) are time-step dependant, and so the time-step used in the time domain simulation using the equivalent has to be the same as the time-step used for obtaining the equivalent. If the former one is to be changed, the equivalent process has to be done again.

(2) Many tests done in this research showed that the order of the fitted equivalent is much higher than necessary even when the time domain response is error-free. Also the stability of the equivalent cannot be guaranteed.

(3) It was also found in the tests that the noise in the time domain response can easily lead to an unsuccessful fitting.

(4) Most important, this method requires a time domain simulation of the full detailed model, which is not practical in many cases.

3.2.3 Orthogonal Polynomial Function

The application of the power series polynomial function in FDNE is challenging due to the large range of the coefficients, which is a result of the powers of ω, which has a range over several decades. In contrast, the coefficients of the orthogonal polynomial function have a much smaller range.

$$I(s) = \left[g_0 + sh_0 + \sum_k \frac{a_k}{s - c_k} \right] V(s) \tag{3.13}$$

The use of such an orthogonal polynomial function can be seen as an expansion of the lumped R, L, C network equivalent:

In (3.13), g_0 and h_0 are real numbers. a_k and c_k can be either real or complex, in the case of complex coefficient, the conjugate part must appear.

The g_0 can be seen as a resistor, sh_0 is a capacitor, $\frac{a_k}{s - c_k}$ can be either a RL branch for real a_k and c_k, or a more complicated R-L-C||R arrangement when a_k and c_k are complex. All these branches are parallel connected together to form a network.

In a physical network, R, L, C are required to be positive. In the equation form of (3.13), more flexibility is permitted because some of the coefficients can lead to negative R, L, C. Thus the rational function (3.13) has more freedom. However, the passivity of the entire equivalent must still be maintained.

The difficulty of fitting the orthogonal function arises from the fact that the unknowns c_k appear in the denominators, which makes the fitting a nonlinear problem.

The obvious approach of optimizing the coefficients is continuous linearization using, say, Newton type method [31].

Writing (3.13) for given frequency points:

$$g_0 + j\omega_i h_0 + \sum_k \frac{a_k}{j\omega_i - c_k} = G_i + jB_i \qquad (i = 1 \cdots M) \tag{3.14}$$

It can be seen that (3.14) is a set of nonlinear equations with unknowns g_0, h_0, a_k, c_k.

Given a set of initial values of g_0, h_0, a_k, c_k, the nonlinear equation (3.14) can be linearized at the initial point by using the first derivatives of g_0, h_0, a_k, c_k, and a set of linear equations can be constructed. The over-determined linear equations can be solved using standard linear least square techniques. The results can be used for updating g_0, h_0, a_k, c_k, and then the nonlinear equation (3.14) can be linearized at the new point. This can be done iteratively until convergence is obtained.

This method is quite straight forward, and it is a standard technique for solving nonlinear least square problems. But numerical tests showed that for this special problem, this technique has difficulty in converging to a good result. The main reason is that this problem is very nonlinear, especially when there are resonance peaks to be fitted.

3.2.4 Vector Fitting

Gustavsen and Semlyen [13] proposed the Vector Fitting algorithm. The basic concept of this algorithm can be described as follows:

Assuming actual transfer function to be $f(s)$, the purpose is to find a rational fitting function $f_{fit}(s)$ that can satisfy the following equation:

$$f(s) \approx f_{fit}(s) = g_0 + sh_0 + \sum_{k=1}^{N} \frac{a_k}{s - c_k} = h_0 \frac{\prod_{k=1}^{N+1}(s - z_k)}{\prod_{k=1}^{N}(s - c_k)} \tag{3.15}$$

Introduce a rational function $\sigma(s)$, which has arbitrary given poles d_1, $d_2 \ldots d_N$:

$$\sigma(s) = 1 + \sum_{k=1}^{N} \frac{b_k}{s - d_k} = \frac{\prod_{k=1}^{N}(s - y_k)}{\prod_{k=1}^{N}(s - d_k)} \tag{3.16}$$

Function $\sigma(s)$ is required to satisfy the condition:

$$f_{fit}(s) \cdot \sigma(s) = l_0 + m_0 s + \sum_{k=1}^{N} \frac{e_k}{s - d_k} = m_0 \frac{\prod_{k=1}^{N+1}(s - x_k)}{\prod_{k=1}^{N}(s - d_k)} \tag{3.17}$$

Which means $f_{fit}(s) \cdot \sigma(s)$ has the same poles as $\sigma(s)$. From (3.15) and (3.16), it can be noted that:

$$f_{fit}(s) \cdot \sigma(s) = h_0 \frac{\prod_{k=1}^{N+1}(s - z_k)}{\prod_{k=1}^{N}(s - c_k)} \cdot \frac{\prod_{k=1}^{N+1}(s - y_k)}{\prod_{k=1}^{N}(s - d_k)} \tag{3.18}$$

For arbitrary given poles d_1, $d_2 \ldots d_N$, the necessary condition for $f_{fit}(s) \cdot \sigma(s)$ and $\sigma(s)$ having the same poles is that:

$$\prod_{k=1}^{N+1}(s - y_k) = \prod_{k=1}^{N}(s - c_k) \tag{3.19}$$

Which means the zeros of $\sigma(s)$ should be equal to the poles of $f_{fit}(s)$.This is the key point of Vector Fitting.

The frequency characteristic of $f(s)$ is known as a frequency spectrum. At a typical frequency point ω_i, equation (3.15), (3.16) and (3.17) can be reorganized (with $s = j\omega_i$) as:

$$f_{fit}(j\omega_i) \approx f(j\omega_i) = v_i + jw_i \tag{3.20}$$

$$f(s)\cdot\sigma(s) \approx f_{fit}(s)\cdot\sigma(s) = l_0 + m_0 s + \sum_{k=1}^{N}\frac{e_k}{s-d_k} \tag{3.21}$$

Substitute $f(s)$ in (3.21) with $v_i + jw_i$ in (3.20):

$$(v_i + jw_i)\cdot\left(1+\sum_{k=1}^{N}\frac{b_k}{j\omega_i - d_k}\right) \approx l_0 + m_0 j\omega_i + \sum_{k=1}^{N}\frac{e_k}{j\omega_i - d_k} \tag{3.22}$$

With arbitrary given poles $d_1,\ d_2 \ldots d_N$, equation (3.22) is a linear equation with the unknowns b_k, l_0, m_0, e_k . Writing equation (3.22) at a series of given frequency point, an over-determined linear problem can be obtained (because the number of the frequency points is much larger than the number of the unknowns):

$$\begin{cases} (v_1 + jw_1)\cdot\left(1+\sum_{k=1}^{N}\frac{b_k}{j\omega_1 - d_k}\right) \approx l_0 + m_0 j\omega_1 + \sum_{k=1}^{N}\frac{e_k}{j\omega_1 - d_k} \\ (v_2 + jw_2)\cdot\left(1+\sum_{k=1}^{N}\frac{b_k}{j\omega_2 - d_k}\right) \approx l_0 + m_0 j\omega_2 + \sum_{k=1}^{N}\frac{e_k}{j\omega_2 - d_k} \\ \vdots \\ (v_M + jw_M)\cdot\left(1+\sum_{k=1}^{N}\frac{b_k}{j\omega_M - d_k}\right) \approx l_0 + m_0 j\omega_M + \sum_{k=1}^{N}\frac{e_k}{j\omega_M - d_k} \end{cases} \tag{3.23}$$

As all the unknowns b_k, l_0, m_0, e_k appear in the numerator, equation (3.23) can be solved by standard linear least square techniques. In this way, the original nonlinear problem of finding the poles of $f_{fit}(s)$ is converted to a linear problem of finding the residues of $f_{fit}(s)\cdot\sigma(s)$ and $\sigma(s)$.

The process of Vector Fitting is thus summarized below:

i. Select a set of poles $d_1, d_2 \ldots d_N$ as seed values for the procedure. Although in theory, their selection can be arbitrary, in practice the algorithm works better when the initial poles are selected close to the likely pole positions, for example, at peaks of the frequency response characteristic of the magnitude function.

ii. Construct equation (3.23) and use a standard linear least square technique to solve it, find the residues of $\sigma(s)$. Knowing the poles and residues of $\sigma(s)$ allows one to write the full transfer function for $\sigma(s)$. The zeros of $\sigma(s)$ can now be evaluated.

iii. Theoretically, this should end the search because the poles of $f_{fit}(s)$ are the zeros of $\sigma(s)$. However, it has been found [13] that using these newly calculated poles as seed values for step ii in an iterative manner improves the fitting accuracy. The procedure stops when the movement in the pole values from the previous interval is below a selected threshold.

iv. As we know that there cannot be unstable pole, if any are found, they are flipped to the left half plane during this process [13]. In most cases, the unstable poles occur in intermediate iterations of the vector fitting process. The final iteration usually yields stable poles as desired. If there is any left, they are flipped as well. From experiments, it has minor effect on the final fitting results.

v. With the converged poles of $f_{fit}(s)$, the residues of $f_{fit}(s)$ can be found by solving linear least square problem.

The Vector Fitting algorithm is a special technique for this special problem, and numerical tests showed that it is promising. It is employed in this research for calculating the coefficients of the FDNE.

4 Frequency Dependant Network Equivalent for a Large Power System

This chapter deals with the development of the high frequency part of the wide band two parts equivalent proposed in chapter 1.

4.1 Frequency Dependant Admittance Matrix of the External System as Seen From the Boundary

In section 3.2 the methods of finding a model to fit the frequency dependant admittance matrix of the external system as seen from the boundary have been reviewed. In the earlier description, it was assumed that the frequency response of the external network was available. However, this response must first be obtained. Hence the first step of making the FDNE is to derive the frequency dependant matrix which represents the frequency domain characteristics of the external system as seen from the boundary.

If the external system is connected to the internal system at a three phase bus boundary (one port), then the frequency dependant admittance matrix of the external system as seen from the boundary is a 3×3 complex matrix whose entries are functions of frequency. If there is a boundary of two three phase buses (two ports), it is a 6×6 frequency dependant complex matrix.

There are three ways to obtain the frequency domain characteristics of the external system: by on-site experiments on the actual network, by full detailed model time domain simulations using a multi-frequency excitation and by frequency scans.

The on-site experimental data of the frequency response of a power network is rarely available. Also the mutual interactions between two or more boundary buses on different locations are difficult to measure.

The full detailed model EMT time domain simulation is difficult to conduct for a system of more than one hundred buses, and multiple runs are needed in such applications. So this method is not practical for many FDNE applications.

The frequency scan or frequency domain identification includes three steps. The first is deriving the frequency dependant admittance matrix of each component in the external network. Then in the second step the whole frequency dependant admittance matrix of the external network can be derived. The procedure is based on the concept that the frequency dependant admittance matrix of a power network is the superposition of the frequency dependant admittance matrices of individual components of the power network. For a linear network, this is true. In the third step internal nodes are eliminated and the whole frequency dependant admittance matrix (N×N, where N is the number of the nodes of the external network) of the external network is directly reduced to a multi-port Thevenin impedance at the boundary. The Thevenin equivalent is represented by a frequency dependant admittance matrix of dimension 3×3 for a single 3-phase boundary or 3K×3K for a K port 3-phase boundary.

The second and third steps of this procedure directly follow the standard network theory and matrix algebra [25][32]. However many utilities do not maintain detailed parameter data suitable for frequency domain studies, hence there are practical difficulties when implementing this method.

4.2 Frequency Dependant Admittance Matrices of Power System Components

The complex admittance matrix of a network can be calculated as follows [25]:

$$Y = [y_{ij}]_{\substack{i=1,\dots N \\ j=1,\dots N}} \tag{4.1}$$

Where N is the number of the nodes in the network.

$$y_{ii} = \sum_{j=1}^{N} a_{ij} \tag{4.2}$$

$$y_{ij} = -a_{ij} \tag{4.3}$$

Where a_{ij} is the admittance connected between node i and node j. And a_{ii} is the admittance connected between node i and ground (reference).

For typical components like R (resistor), L (reactor), C (capacitor) connected between node i and node j, the admittance a_{ij} would be:

Resistor: $a_{ij} = 1/R$ (4.4)

Reactor: $a_{ij} = 1/j2\pi fL$ (4.5)

Capacitor: $a_{ij} = j2\pi fC$ (4.6)

Where f is the frequency at which the admittance matrix is being calculated.

The complexities of the frequency dependant admittance matrices of the power system components range from very simple (as shown by R, L, C components) to very complicated. For example, the transmission line and cable are commonly seen as the most complicated linear frequency dependant components in the power system. In the frequency domain, a transmission line can be defined by the per unit length impedance matrix, the per unit length admittance matrix and the line length.

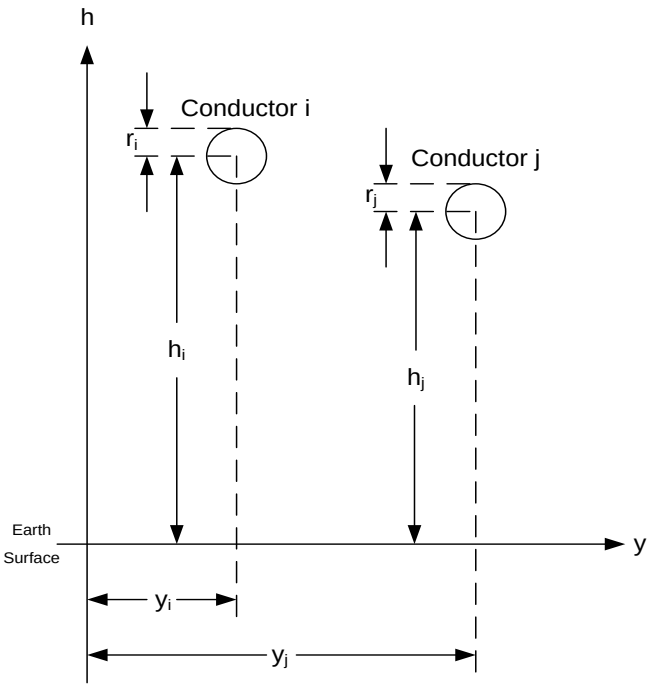

Figure 4-1 Transmission Line Geometry

For a two conductor transmission line shown in Figure 4-1, the two matrices can be calculated as [26][33]:

(1) per unit length impedance matrix

$$Z_{pu\_ii} = Z_{pu\_ii}\_Int + Z_{pu\_ii}\_Ext \tag{4.7}$$

$$Z_{pu\_ii}\_Int = \frac{\rho_i \cdot m(\omega)}{2\pi \cdot r_i}\coth[0.7777 m(\omega)\cdot r_i] + \frac{0.3565\rho_i}{\pi \cdot r_i^2} \qquad (\Omega/m) \tag{4.8}$$

$$Z_{pu\_ii}\_Ext = \frac{j\omega\mu_0}{2\pi}\ln\left(\frac{2(h_i + d_e)}{r_i}\right) \qquad (\Omega/m) \tag{4.9}$$

Where:

$$\mu_0 = 4\pi \times 10^{-7} (H/m)$$

$$m(\omega) = \sqrt{\frac{j\omega\mu_0}{\rho_i}} = \frac{1}{d_{conductor}(\omega)}$$

$$d_e(\omega) = \sqrt{\frac{\rho}{j\omega\mu_0}}$$

Here $\rho_i\ (\Omega/m)$ is the conductor resistivity, and $\rho\ (\Omega/m)$ is the earth resistivity. r_i is the conductor radius.

And,

$$Z_{pu\_ij} = \frac{j\omega\mu_0}{2\pi} \ln\left[\frac{\sqrt{(y_i - y_j)^2 + (h_i + h_j + 2d_e)^2}}{\sqrt{(y_i - y_j)^2 + (h_i - h_j)^2}}\right] \quad (\Omega/m) \tag{4.10}$$

(2) per unit length admittance matrix

Similarly:

$$\left[Y_{pu}(\omega)\right] = \left[P(\omega)\right]^{-1} \tag{4.11}$$

$$P_{ij} = \frac{\ln\left[\frac{\sqrt{(y_i - y_j)^2 + (h_i + h_j)^2}}{d_{ij}}\right]}{j2\pi\omega\varepsilon_0} \quad (\Omega/m) \tag{4.12}$$

$$d_{ij} = \begin{cases} \sqrt{(y_i - y_j)^2 + (h_i - h_j)^2} & (i \neq j) \\ r_i & (i = j) \end{cases} \tag{4.13}$$

Here $\varepsilon_0 = \frac{10^{-9}}{36\pi}$ (F/m)

The frequency dependant admittance matrix of the transmission line is:

$$Y(\omega) = \begin{bmatrix} Y_0 \coth(\Gamma l) & -Y_0 \cos ech(\Gamma l) \\ -Y_0 \cos ech(\Gamma l) & Y_0 \coth(\Gamma l) \end{bmatrix} \tag{4.14}$$

Where:

$$[Y_0] = \sqrt{\frac{[Y_{pu}]}{[Z_{pu}]}} \tag{4.15}$$

$$[\Gamma] = \sqrt{[Z_{pu}][Y_{pu}]} \tag{4.16}$$

And l is the length of the line.

For a two conductor transmission line, $Y(\omega)$ is a 4×4 matrix. For a three phase transmission line, it is a 6×6 matrix.

From the transmission line example, it can be seen that in order to derive the accurate frequency dependant admittance matrix of the power network, the detailed parameters of the components need to be known.

4.3 Derivation of the Frequency Dependant Admittance Matrices of Power System Components from Power Flow Data

For large scale power networks, the detailed parameters of components are difficult to obtain. The commonly available data of the network for the power system analysis is the power flow data which is valid for the fundamental frequency analysis [34]. For example, power flow data files in the PSS/E raw data format [35] are widely available. These kinds of data are simplified; they only contain the fundamental frequency parameters of the power system. However after making some assumptions and approximations, the frequency dependant admittances of common power system components can be derived from their fundamental frequency parameters. Here the transmission line is used as an example.

First a lossless transmission line is investigated.

For lossless line:

$$Z_{pu\_ii}\_Int = 0 \qquad (\Omega/m) \tag{4.17}$$

$$Z_{pu\_ii}\_Ext = \frac{j\omega\mu_0}{2\pi}\ln\left(\frac{2h_i}{r_i}\right) \qquad (\Omega/m) \tag{4.18}$$

$$Z_{pu\_ij} = \frac{j\omega\mu_0}{2\pi}\ln\left[\frac{\sqrt{(y_i-y_j)^2+(h_i+h_j)^2}}{\sqrt{(y_i-y_j)^2+(h_i-h_j)^2}}\right] \qquad (\Omega/m) \tag{4.19}$$

$$\left[Y_{pu}(\omega)\right] = \left[P(\omega)\right]^{-1} \tag{4.20}$$

$$P_{ij} = \frac{\ln\left[\dfrac{\sqrt{(y_i-y_j)^2+(h_i+h_j)^2}}{d_{ij}}\right]}{j2\pi\omega\varepsilon_0} \quad (\Omega/m) \tag{4.21}$$

Note that equations (4.18) and (4.19) have a common multiplier $j\omega$. And in equation (4.21) there is a multiplier $1/j\omega$. Hence:

$$\left[Z_{pu}(\omega)\right] = j\omega\cdot[\mathcal{Z}] \tag{4.22}$$

$$\left[P(\omega)\right] = \frac{1}{j\omega}[\mathcal{P}] \tag{4.23}$$

$$\left[Y_{pu}(\omega)\right] = j\omega\cdot[\mathcal{P}]^{-1} = j\omega\cdot[\mathcal{Y}] \tag{4.24}$$

$$[Y_0] = \sqrt{\frac{[Y]}{[Z]}} = \sqrt{\mathcal{Y}\,\mathcal{Z}^{-1}} = [\mathcal{Y}_0] \tag{4.25}$$

$$[\Gamma] = \sqrt{[Z][Y]} = j\omega\sqrt{\mathcal{Z}\mathcal{Y}} = j\omega\cdot[\mathcal{L}] \tag{4.26}$$

Here $\mathcal{Z}$, $\mathcal{P}$, $\mathcal{Y}$, $\mathcal{Y}_0$ and $\mathcal{L}$ are constant. Then:

$$Y(\omega)=\begin{bmatrix} Y_0\coth(\Gamma l) & -Y_0\cos ech(\Gamma l) \\ -Y_0\cos ech(\Gamma l) & Y_0\coth(\Gamma l) \end{bmatrix}$$

$$=\begin{bmatrix} [\Upsilon_0]\coth(j\omega\cdot[\mathcal{L}]\cdot l) & -[\Upsilon_0]\cos ech(j\omega\cdot[\mathcal{L}]\cdot l) \\ -[\Upsilon_0]\cos ech(j\omega\cdot[\mathcal{L}]\cdot l) & [\Upsilon_0]\coth(j\omega\cdot[\mathcal{L}]\cdot l) \end{bmatrix} \quad (4.27)$$

$$=\begin{bmatrix} [\Upsilon_0]\coth(j\omega\cdot[\mathcal{L}_l]) & -[\Upsilon_0]\cos ech(j\omega\cdot[\mathcal{L}_l]) \\ -[\Upsilon_0]\cos ech(j\omega\cdot[\mathcal{L}_l]) & [\Upsilon_0]\coth(j\omega\cdot[\mathcal{L}_l]) \end{bmatrix}$$

Since the line length l is constant, $\mathcal{L}_l$ is constant.

At the fundamental frequency (60Hz or 50Hz), the admittance matrix entries $y(\omega)$ are known. Hence we can get the values of $[\Upsilon_0]$ and $[\mathcal{L}_l]$ (for multi phase line, they are matrices). As they are constant, once the values calculated at one frequency, they are known at all other frequencies. Hence the admittance matrices at other frequencies can be **accurately** derived from the admittance matrix at the fundamental frequency, which can be found in the power flow data.

Lossy line

For a lossy line, $[\Upsilon_0]$ and $[\mathcal{L}_l]$ are not constant anymore. In this case, the frequency dependant admittance matrix cannot be derived with only the information of the electrical parameters at the fundamental frequency. Other parameters such as the tower geometry and the ground resistance etc. need to be known.

In order to represent the distributed nature of the line resistance, the line is represented as a two section Bergeron model as shown in Figure 4-2d. The resistance is distributed in four locations, one at each terminal of the two Bergeron line sections. For more accuracy, the line could be divided into larger number of line sections, but this makes very marginal improvement in accuracy [23].

Figure 4-2 demonstrates the process of deriving the distributed parameter transmission line model from power flow data. At each stage, the model matches the model of previous stage at the fundamental frequency, except for the marginally small shunt conductance.

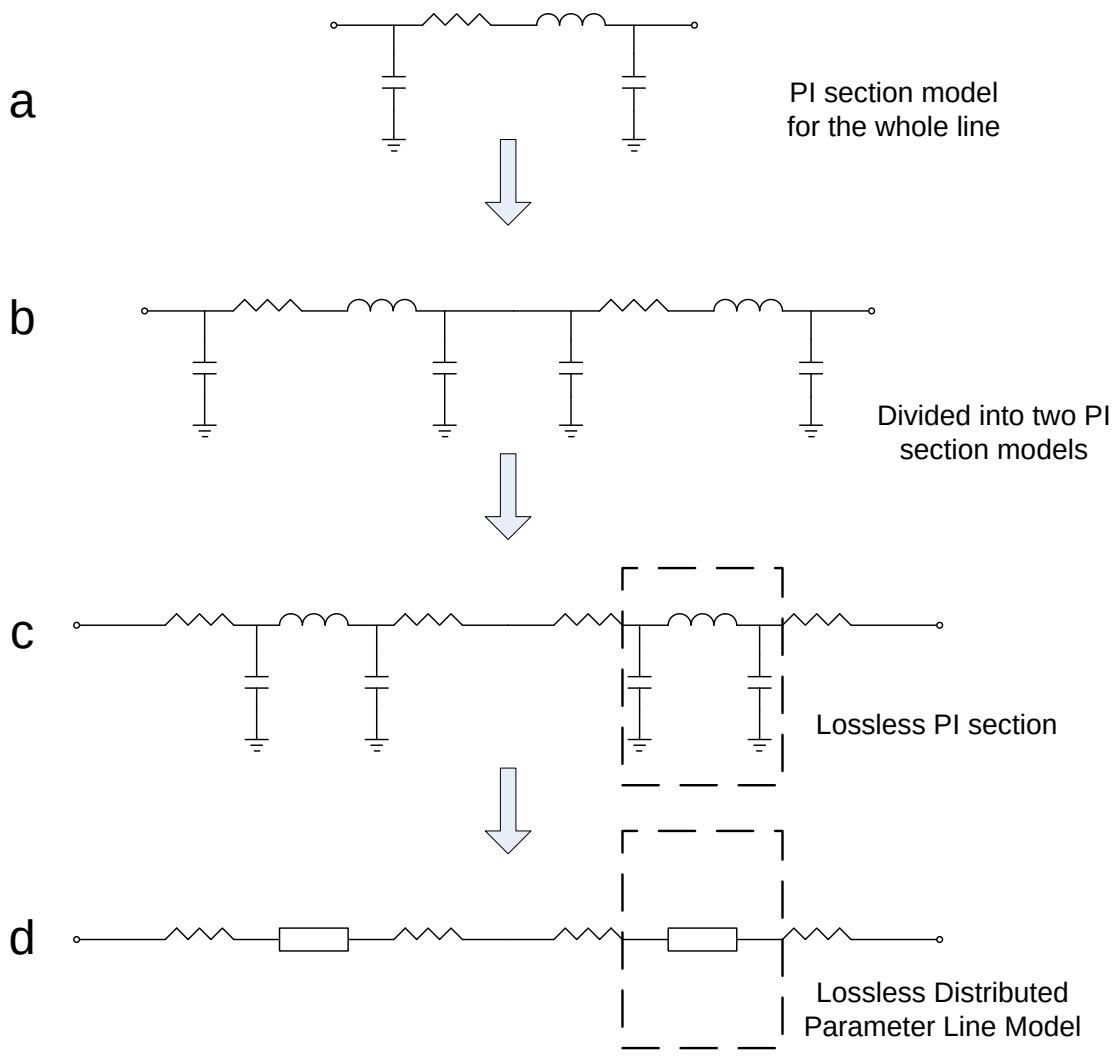

Figure 4-2 Derivation of the Simplified Distributed Parameter Transmission Line Model

The frequency response of the Bergeron model at high frequencies (for instance above 1 kHz) is approximate (since the skin effect is not included) and the imbalance of the network is ignored. It should be pointed out that this approximation is not inherent in the above method. The approximation arises only when the user is forced to estimate line characteristics (using the method discussed in this section) when he or she does not have recourse to detailed line geometrical information as is the case with many utility users.

By following a similar procedure with the other network elements, the admittance matrix $Y(\omega)$ can be assembled using the nodal analysis formulation [11]. For many network elements, some simplifications and assumptions have to be made due to the lack of detailed information. However, the generator is a special case. Adequately detailed parameters of the generators are widely available in the dynamic data used in the TSA type studies. But the frequency dependent characteristic of the generator is very complicated, and such a characteristic is neither linear nor passive, hence cannot be reproduced by a linear equivalent. As an approximation, the sub-transient impedance $R_a + jX_d''$ is used to represent the generator, and the impedance is modeled as a resistor in series with a inductor.

In the proposed method, any imbalance in the network is ignored. It should also be noticed that in the above procedure, the fundamental frequency zero sequence parameters of the network are also used for estimating the mutual coupling between the three phases. This information can be gathered from the sequence network data for the short circuit current calculations. If such data is not available, the zero sequence parameters are approximated from the positive sequence parameters using experimental equations.

The advantages of the above proposed method are:

- $Y(\omega)$ can be rapidly obtained by processing of the standard power-flow data file.
- When more detailed information is available, it can be incorporated to improve the accuracy of the model. For example if detailed geometrical and physical data is available for an important line or element close to the boundary with the internal network, the element can be represented by a more accurate frequency dependent two-port admittance which can replace the simplified admittance calculated from the fundamental frequency data.
- The method provides an opportunity to be selective. Some components have nonlinear characteristics, for example, synchronous generators. Such characteristics can be intentionally simplified to linear form in order to avoid numerical difficulties in the curve fitting process. The non-linear model of the generator is important for the low frequency electromechanical transient and is fully included therein, thereby negating the need for it to be also included in the FDNE.

4.4 Vector Fitting Example

After the frequency dependant admittance matrix of the external system as seen from the boundary is known, the frequency dependant admittance of each branch can be derived and the Vector Fitting algorithm can be applied for finding the rational function approximations of these branches. This algorithm was introduced in section 3.2.4.

A small three phase passive network is used here as an example. There are seven transmission lines and four loads in this network.

Seen from the boundary, this small network can be equivalenced to a one port three phase FDNE. The FDNE consists of six frequency dependant branches, as shown in Figure 4-3. Assuming the original network to be balanced, the branches aa, bb and cc become identical to each other, as branches ab, bc and ca.

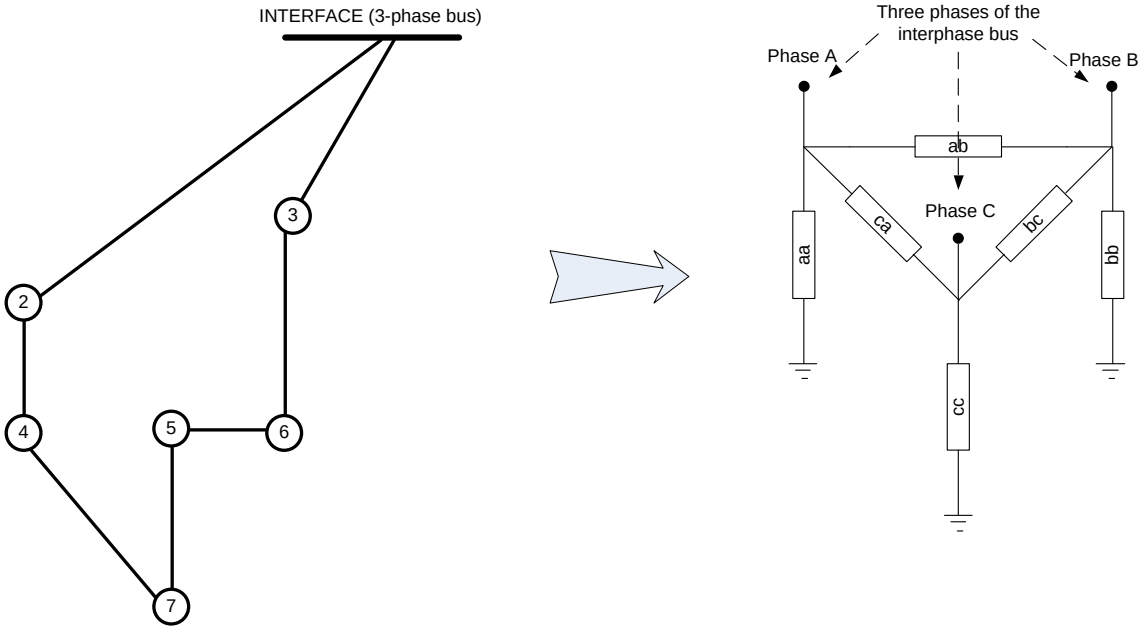

Figure 4-3 FDNE Example

The frequency domain identification and fitting results of branches aa and ab are shown in Figure 4-4 and Figure 4-5 respectively. They show both the conductance (real part), and the susceptance (imaginary part). It can be seen that the frequency spectra of this small network are still complicated, but can be accurately fitted.

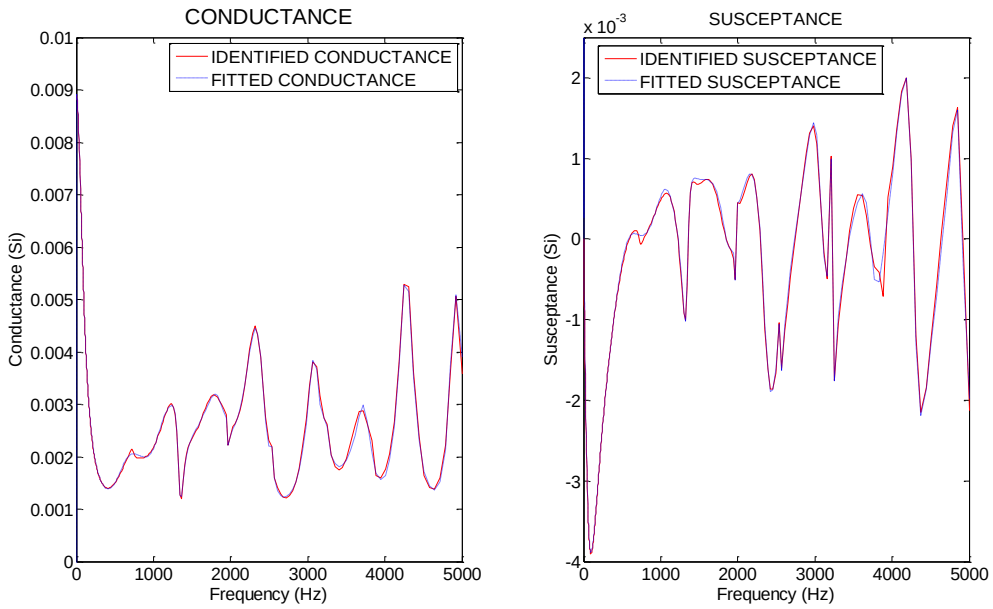

Figure 4-4 Vector Fitting Example of Self Admittance

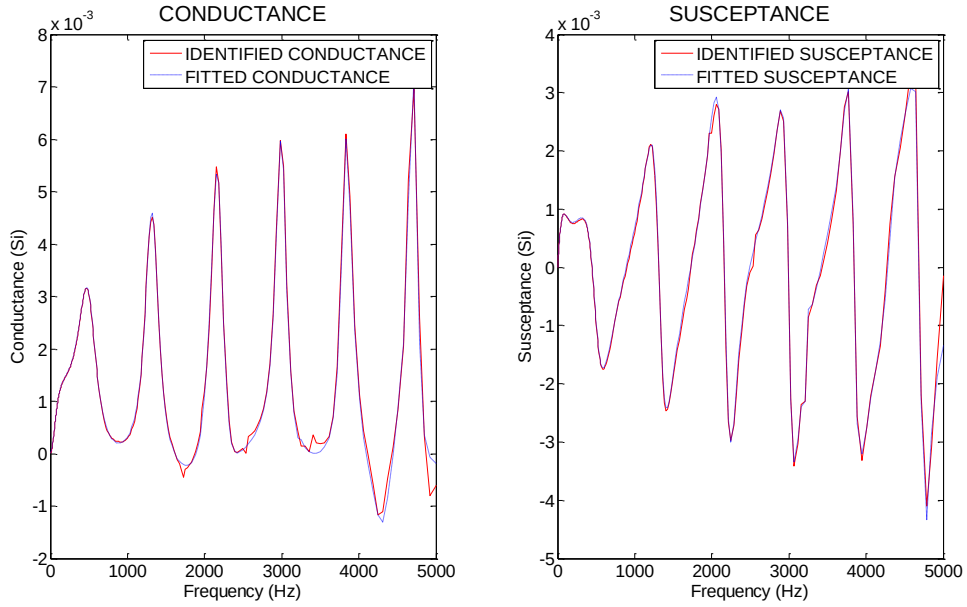

Figure 4-5 Vector Fitting Example of Inter-phase Admittance

4.5 Modeling of Rational Functions

Once the frequency dependant admittance of a branch is fitted with a rational function, the branch can be modeled in an EMT time domain simulation program.

4.5.1 Basic Modeling Technique of the EMT Time Domain Simulation

The foundation of the EMT time domain simulation is the trapezoidal integration rule, which converts power system components into Norton equivalents [22][23][24]. Each Norton equivalent consists of a Norton conductance which is a function of the component parameters, and a Norton current source which is a function of the past history (i.e. voltage/current from previous time-steps). Once all components are converted to such Norton equivalent form, a conductance matrix for the whole network can be constructed easily with standard network theory and matrix algebra [25][32]. This can be implemented to obtain the voltage magnitudes of all network nodes in a given time-step.

The modeling of typical components like R (resistor), L (reactor), C (capacitor) in an EMT program is introduced as follows:

(1) A resistor R connected between node m and node n is simply modeled as a conductance $G_R = 1/R$.

(2) For a reactor L, the relationship between the voltage and current is:

$$v = L\frac{di}{dt} \tag{4.28}$$

Or:

$$\frac{di}{dt} = \frac{1}{L}v \tag{4.29}$$

Applying the trapezoidal integration rule:

$$\begin{aligned} i(t) &\approx i(t-\Delta t) + \frac{1}{2}\left(\frac{di}{dt}_{(t)} + \frac{di}{dt}_{(t-\Delta t)}\right)\Delta t \\ &= i(t-\Delta t) + \frac{1}{2}\left(\frac{1}{L}v(t) + \frac{1}{L}v(t-\Delta t)\right)\Delta t \\ &= \frac{\Delta t}{2L}v(t) + \left(i(t-\Delta t) + \frac{\Delta t}{2L}v(t-\Delta t)\right) \\ &= G_L v(t) + I_{hL} \end{aligned} \tag{4.30}$$

Where Δt is the time-step of the integration. Equation (4.30) means a reactor can be modeled as a Norton conductance and a Norton current source. The value of the Norton current source is determined by the values of the voltage and current of the previous time-step, hence is known. That is why this current source is called the "history" current term.

(3) Similarly a capacitor can also be modeled as a Norton conductance and a Norton history current term.

$$\begin{aligned} i(t) &\approx \frac{2C}{\Delta t}v(t) + \left(-i(t-\Delta t) - \frac{2C}{\Delta t}v(t-\Delta t)\right) \\ &= G_C v(t) + I_{hC} \end{aligned} \tag{4.31}$$

The modeling of R, L, C components in an EMT program is illustrated in Figure 4-6.

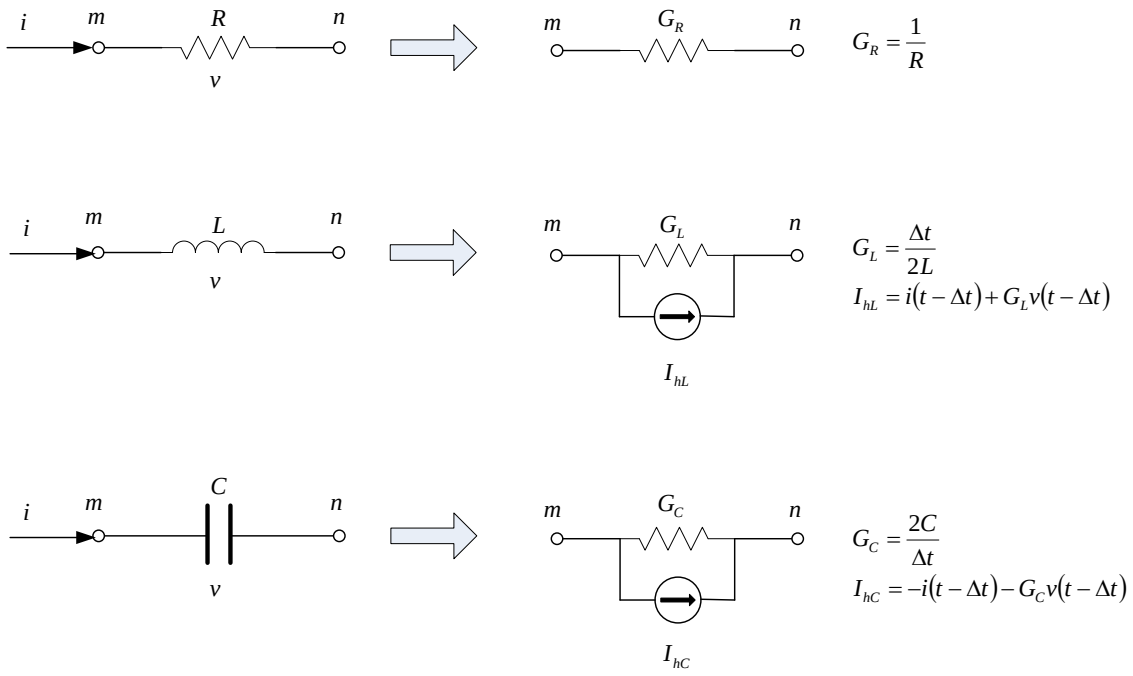

Figure 4-6 Modeling of R, L, C in EMT Program

4.5.2 Modeling Admittance with Rational Function Representation in EMT Time Domain Simulation Program

In order to include a fitted FDNE rational function as a component of an EMT program, it is necessary to be able to represent it as a Norton equivalent as was done in the previous sub-section for R, L and C elements. This is discussed in this sub-section. As discussed in section 4.4, the rational function is given in the following form:

$$I(s) = \left(g_0 + sh_0 + \sum_k \frac{a_k}{s - c_k} \right) V(s) \tag{4.32}$$

In (4.32), a_k and c_k can be either real or complex number. In the complex number case, they will appear in conjugate pairs. That is:

$$\frac{a_k}{s - c_k} + \frac{a_{k+1}}{s - c_{k+1}} \quad , \quad a_{k+1} = a_k' \quad , c_{k+1} = c_k' \tag{4.33}$$

Rational function (4.32) can be seen as:

$$I(s) = I_C(s) + I_R(s) + \sum_{kr} I_{kr}(s) + \sum_{kc} I_{kc}(s) \tag{4.34}$$

Where:

$$\begin{cases} I_C(s) = sh_0 V(s) \\ I_R(s) = g_0 V(s) \\ I_{kr}(s) = \dfrac{a_{kr}}{s - c_{kr}} V(s) \\ I_{kc}(s) = \left(\dfrac{a_{kc}}{s - c_{kc}} + \dfrac{a'_{kc}}{s - c'_{kc}} \right) V(s) \end{cases} \tag{4.35}$$

For a real pole in (4.34):

$$I_{kr}(s) = \frac{a_{kr}}{s - c_{kr}} V(s)$$

or in the time domain form:

$$\dot{I}_{kr}(t) = c_{kr} I_{kr}(t) + a_{kr} V(t) \tag{4.36}$$

Using Trapezoidal Rule:

$$\begin{aligned} I_{kr}(t) = {} & I_{kr}(t - \Delta t) + hc_{kr} I_{kr}(t - \Delta t) + ha_{kr} V(t - \Delta t) \\ & + hc_{kr} I_{kr}(t) + ha_{kr} V(t) \end{aligned} \tag{4.37}$$

Here h is half time-step.

$h = \Delta t / 2$.

$$\begin{aligned} I_{kr}(t) &= \frac{I_{kr}(t - \Delta t) + hc_{kr} I_{kr}(t - \Delta t) + ha_{kr} V(t - \Delta t)}{1 - hc_{kr}} + \frac{ha_{kr}}{1 - hc_{kr}} V(t) \\ &= I_{Hkr} + G_{kr} V(t) \end{aligned} \tag{4.38}$$

As in the case of a reactor or a capacitor in section 4.5.1, equation (4.38) is also in a constant conductance plus history current term format.

For a complex pole in (4.34):

Assuming $a_{kc} = m + jn$ and $c_{kc} = p + jq$:

$$\begin{aligned} I_k(s) &= \left(\frac{a_{kc}}{s - c_{kc}} + \frac{a'_{kc}}{s - c'_{kc}} \right) V(s) \\ &= \left(\frac{m + jn}{s - p - jq} + \frac{m - jn}{s - p + jq} \right) V(s) \\ &= \left(\frac{2ms - 2mp - 2nq}{s^2 - 2ps + p^2 + q^2} \right) V(s) \end{aligned} \tag{4.39}$$

Let

$$M = 2m$$

$$N = -2mp - 2nq$$

$$P = -2p$$

$$Q = p^2 + q^2$$

M, N, P, Q are all real numbers.

Hence the time domain equation is:

$$\ddot{I}_{kc}(t) + P\dot{I}_{kc}(t) + QI_{kc}(t) = M\dot{V}(t) + NV(t) \tag{4.40}$$

Use two state variables for (4.40):

I_{kc} and $X = \dot{I}_{kc} - MV$, we can get two first order differential equations:

$$\begin{cases} \dot{I}_{kc}(t) = X(t) + MV(t) \\ \dot{X}(t) = -QI_{kc}(t) - PX(t) + (N - MP)V(t) \end{cases} \tag{4.41}$$

Using trapezoidal rule on (4.41):

$$\begin{cases} I_{kc}(t) = I_{kc}(t-\Delta t) + hX(t-\Delta t) + hMV(t-\Delta t) + hX(t) + hMV(t) \\ X(t) = X(t-\Delta t) - hQI_{kc}(t-\Delta t) - hPX(t-\Delta t) + h(N-MP)V(t-\Delta t) \\ \qquad - hQI_{kc}(t) - hPX(t) + h(N-MP)V(t) \end{cases} \tag{4.42}$$

Let $\beta_1 = \dfrac{1-hP}{1+hp}$, $\beta_2 = \dfrac{-hQ}{1+hp}$ and $\beta_3 = \dfrac{h(N-MP)}{1+hp}$, then:

$$X(t) = \beta_1 X(t-\Delta t) + \beta_2 I_{kc}(t-\Delta t) + \beta_3 V(t-\Delta t) + \beta_2 I_{kc}(t) + \beta_3 V(t) \tag{4.43}$$

$$\begin{aligned} I_{kc}(t) &= I_{kc}(t-\Delta t) + hX(t-\Delta t) + hMV(t-\Delta t) + hX(t) + hMV(t) \\ &= (1+h\beta_2) I_{kc}(t-\Delta t) + (h+h\beta_1) X(t-\Delta t) + (hM + h\beta_3) V(t-\Delta t) \\ &\quad + (hM + h\beta_3) V(t) + h\beta_2 I_{kc}(t) \end{aligned} \tag{4.44}$$

$$\begin{cases} I_{kc}(t) = \dfrac{(1+h\beta_2) I_{kc}(t-\Delta t) + (h+h\beta_1) X(t-\Delta t) + (hM + h\beta_3) V(t-\Delta t)}{1-h\beta_2} \\ \qquad + \dfrac{hM + h\beta_3}{1-h\beta_2} V(t) \\ \qquad = I_{Hkc} + G_{kc} V(t) \\ \\ X(t) = \beta_1 X(t-\Delta t) + \beta_2 I_{kc}(t-\Delta t) + \beta_3 V(t-\Delta t) + \beta_2 I_{kc}(t) + \beta_3 V(t) \end{cases} \tag{4.45}$$

Repeat a similar procedure for the $I_C(s)$ term in (4.34):

$$I_C(s) = sh_0 V(s) \tag{4.46}$$

$$I_C(t) = h_0 \dot{V}(t) \tag{4.47}$$

Using trapezoidal rule:

$$\frac{hI_C(t-\Delta t)+hI_C(t)}{h_0}=V(t)-V(t-\Delta t) \tag{4.48}$$

$$\begin{aligned} I_C(t) &= \frac{h_0}{h}V(t)+\left[-\frac{h_0}{h}V(t-\Delta t)-I_C(t-\Delta t)\right] \\ &= I_{HC}+G_C V(t) \end{aligned} \tag{4.49}$$

Similarly for the I_R term in (4.34):

$$I_R(t)=g_0 V(t) \tag{4.50}$$

Combine the equations (4.38), (4.45), (4.49) and (4.50) together:

$$\begin{aligned} I(t) &= (g_0+G_C+\sum_{kr}G_{kr}+\sum_{kc}G_{kc})\cdot V(t)+(I_{HC}+\sum_{kr}I_{Hkr}+\sum_{kc}I_{Hkc}) \\ &= G_N\cdot V(t)+I_H \end{aligned} \tag{4.51}$$

Equation (4.51) is in a history current term (I_H) plus constant conductance (G_N) format. The value of the history current term (I_H) is determined only by the information of previous time-step and hence is in the standard Norton equivalent form requested in the EMT algorithm. This model is readily to be put into an EMT network model.

4.6 Time Domain Simulation Example

The small passive network and its one port FDNE are tested on RTDS. Voltage sources which have the same frequency, magnitude and phase are used for energizing the small passive network (in which all the transmission lines are modeled as Bergeron models) and the FDNE. The two models are excited at various frequencies ranging from 30 Hz to 1.8 kHz. The simulation results of the detailed network model and the FDNE are compared as shown in Figure 4-7 (6 cycles shown for each frequency). The simulation

results from the two models are practically identical to each other with non-significant difference shown only when the frequency of the excitation increases to about 1.8 kHz.

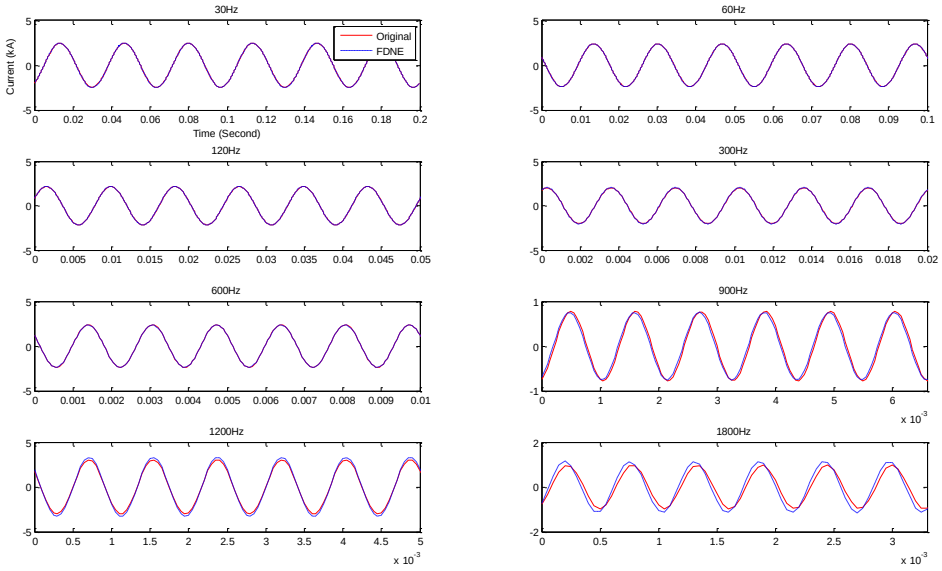

Figure 4-7 FDNE Simulation Results: Excitation at Different Frequencies

4.7 FDNE Passivity Considerations

It is found that occasionally the Frequency Dependant Network Equivalent (FDNE) model shows numerical instability in the time domain simulation even though the rational functions have left plane poles only. This section provides a simple explanation for this phenomenon.

4.7.1 Simple Circuit Example

Consider a simple circuit as shown in Figure 4-8. This circuit includes normal R, L and C components. The two port equivalent R-L-C circuit which matches the original R-L-C circuit at 60 Hz is also shown in Figure 4-8. Note that the series resistance in the equivalent circuit is negative, even though the original circuit doesn't contain any

negative resistance. A negative resistor doesn't exist in the physical world. However, it can be represented by mathematical equations and implemented in a digital time domain simulation.

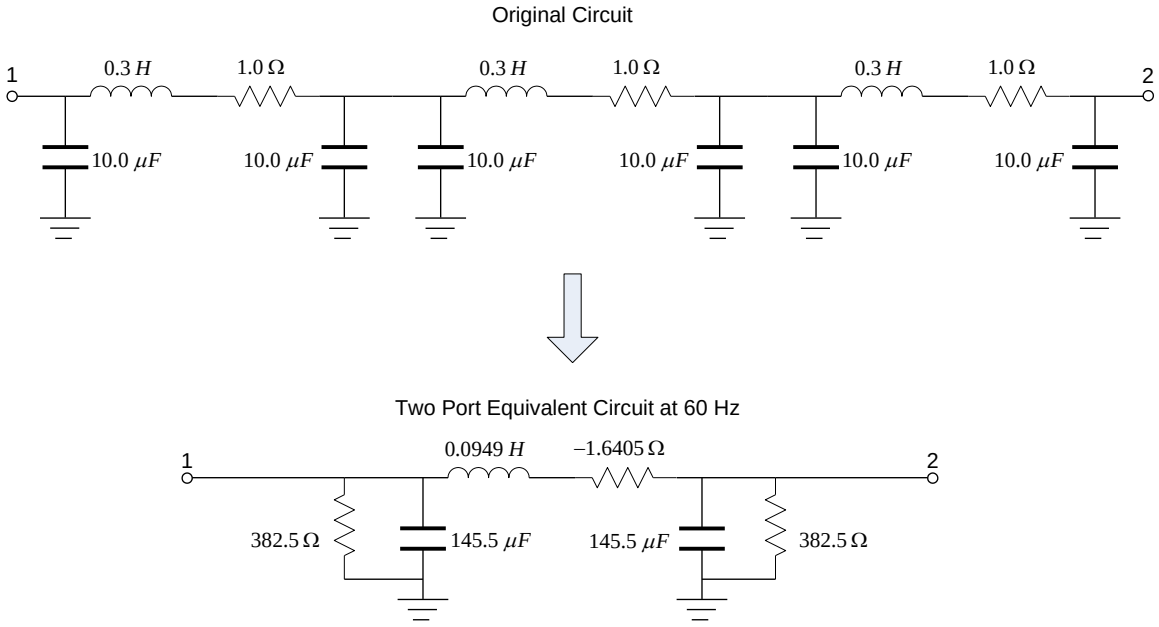

Figure 4-8 Simple R-L-C Circuit and its Two Port Equivalent at 60 Hz

If we energize the original circuit and the equivalent circuit with a pure 60 Hz sinusoidal voltage source from node 1, then both the original circuit and the equivalent circuit can be seen as the same Thevenin impedance as shown in Figure 4-9. The resistance of the Thevenin impedance is positive, which means both the original circuit and the two-port equivalent circuit are passive when energized by a 60 Hz source from node 1.

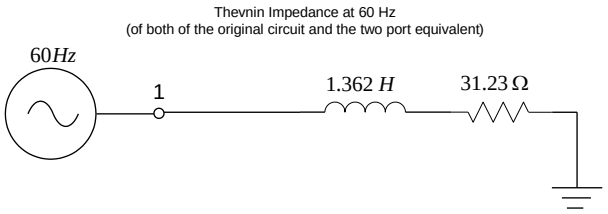

Figure 4-9 Thevenin Impedance at 60Hz
(of the original circuit and the two port equivalent)

If we energize the original circuit and the two-port equivalent circuit with a 50 Hz sinusoidal voltage source from node 1, then the Thevenin impedances of the original circuit and the equivalent circuit are different as shown in Figure 4-10. The resistance of the Thevenin impedance of the original circuit is positive, which means the original circuit absorbs energy when energized by a 50 Hz source. However, the resistance of the Thevenin impedance of the two-port equivalent circuit becomes negative, which means the two-port equivalent circuit will generate energy when energized by a 50 Hz source from node 1, i.e., impassive.

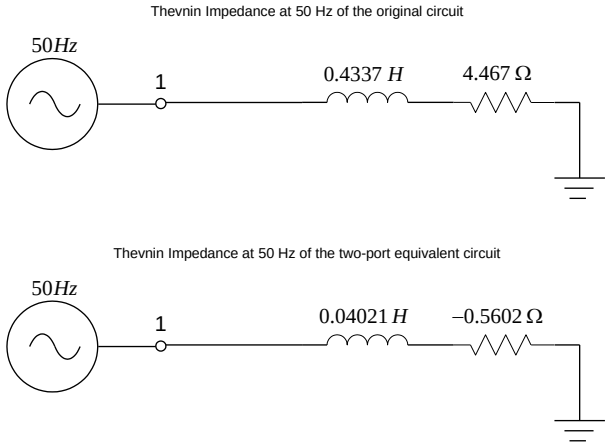

Figure 4-10 Thevenin Impedances at 50Hz
(of the original circuit and the two port equivalent)

Time domain simulations were performed on the two circuits shown in Figure 4-8, using the modeling and simulation methods described in section 2.2 and 4.5.1. In the

simulations, both circuits are energized by a 60 Hz source from node 1. The results are shown in Figure 4-11.

When the two circuits are energized by a 60 Hz source whose internal resistance is 1 Ohm, the two circuits reach the same steady state as shown in Figure 4-11, proving that the two circuits are equivalent to each other at 60 Hz.

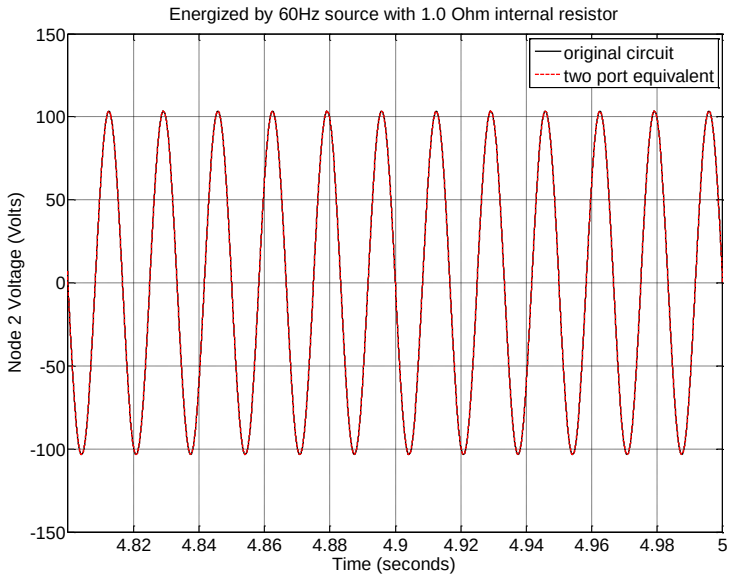

Figure 4-11 Original Circuit and Equivalent Circuit Energized by 60 Hz Source with 1 Ohm Internal Resistor

When the two circuits are energized by a 60 Hz source whose internal resistance is 0.0001 Ohm, the original circuit reaches a normal steady state as shown in Figure 4-12, the voltages and currents contain only 60 Hz component as expected for a linear circuit. However, in the two-port equivalent circuits, the result is different.

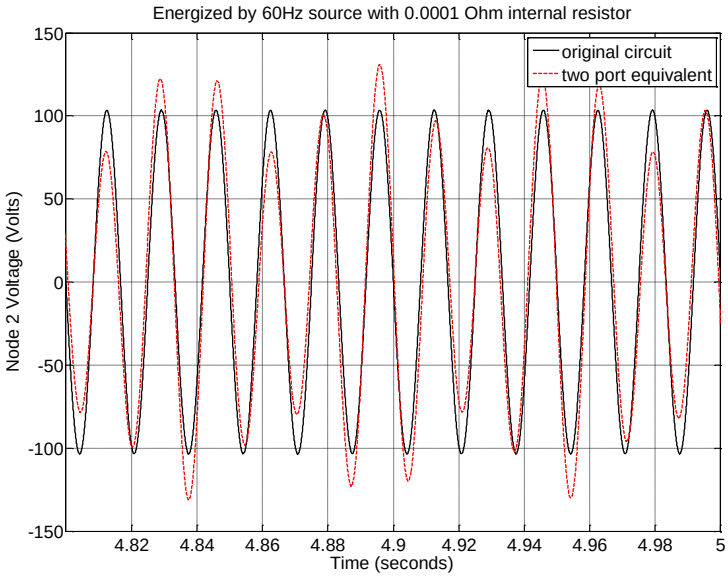

Figure 4-12 Original Circuit and Equivalent Circuit Energized by 60 Hz Source with 0.0001 Ohm Internal Resistor

In this example, the time domain simulation of the two-port equivalent circuit doesn't blow up. However, in many cases numerical stable simulation cannot be performed using network equivalent.

4.7.2 Passivity Criterion and FDNE Example

The FDNE is constructed by connecting frequency dependant admittance branches as shown in Figure 3-2. Each frequency dependant admittance branch is represented by a rational function. In the Vector Fitting algorithm, all the poles (c_k) of a rational function are arbitrarily forced into the left plane. But this doesn't guarantee that the rational function is passive. For example, the transfer function of a negative resistor is a negative gain, which doesn't have right plane pole, but it is not passive. In EMT type simulation, a non-passive component may introduce instability.

But such non-passivity of a branch is necessary, especially for the mutual admittance of multi ports equivalent. For example, a mutual admittance of the two port matrix of a transmission line definitely shows negative resistance at some frequencies. It must be fitted by a rational function which is not passive at these frequencies.

The non-passivity of individual branches doesn't necessarily lead to non-passivity of the whole matrix. A complex admittance matrix is passive when all eigenvalues of the real part of this matrix is positive [36]:

For a admittance matrix Y, the relationship between its inject currents and voltages is:

$$I = Y * V \tag{4.52}$$

For any complex voltage vector $\boldsymbol{V}$, the power absorbed by the admittance matrix Y can be calculated as:

$$P = \mathrm{Re}\{V^* \cdot Y \cdot V\} = \mathrm{Re}\{V^* \cdot (G + jB) \cdot V\} = \mathrm{Re}\{V^* \cdot G \cdot V\} \tag{4.53}$$

Only when the matrix G is positive definite, the absorbed power P is always be positive. The necessary and sufficient condition for the real matrix G to be positive definite is that all the eigenvalues of the matrix G are positive.

For a physical linear network, the passivity condition is always satisfied at any frequency. That is why a physical linear network consisting of real physical components, no matter how complex it is, can always be simulated stably in EMT type simulation. But the frequency dependant matrix obtained from curve fitting may not satisfy this condition. This is illustrated in the following example.

A 6×6 frequency dependant admittance matrix is calculated for a 36 bus system which has two interface buses. The minimum eigenvalues of the real part of the matrix are calculated at various frequency points. They are shown in Figure 4-13.

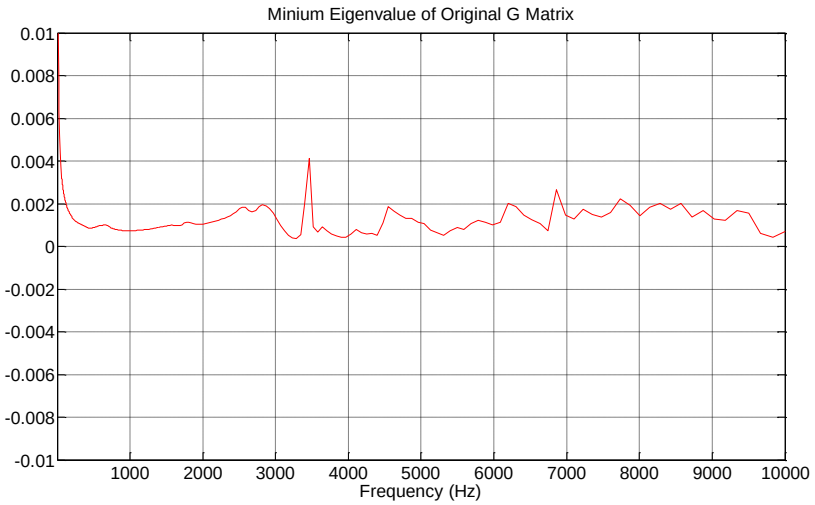

Figure 4-13 Minimum Eigenvalues of Original G Matrices

It can be seen that all the eigenvalues are positive. So the original frequency dependant admittance matrix is passive in the frequency range 0.001Hz~10000Hz. In fact, the matrix is passive at any frequency.

This matrix can be well fitted by Vector Fitting. As an example, one entry of the matrix is plotted in Figure 4-14.

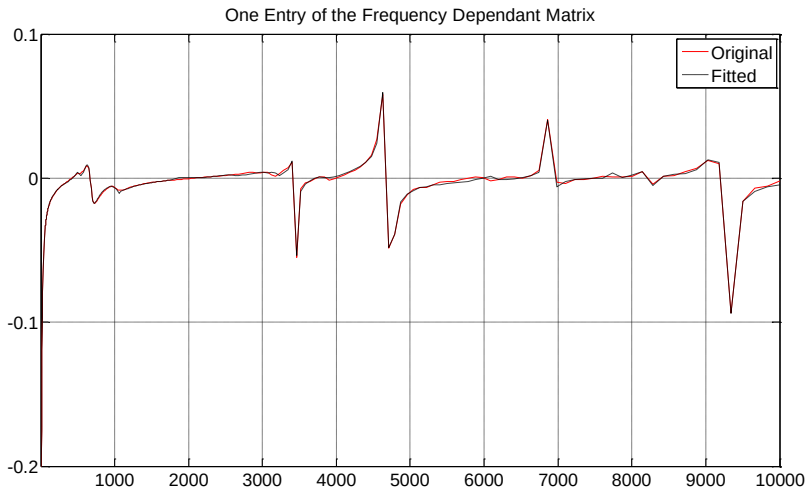

Figure 4-14 Fitting Example

It can be seen that the matrix has been fitted very well by the rational functions. Small errors are inevitable because FDNE is an equivalent meant to reduce the computations by approximations.

The minimum eigenvalues of the fitted matrix G is plotted in Figure 4-15.

It can be seen that the matrix G constructed by rational functions has many negative eigenvalues. Time domain simulation shows the fitted model is not stable.

It is clear that the instability of FDNE is caused by the errors introduced in the curve fitting process. Since the errors are inevitable, what can be done is forcing the fitting errors to move to certain directions which make the matrix constructed by rational functions to be passive at any frequency.

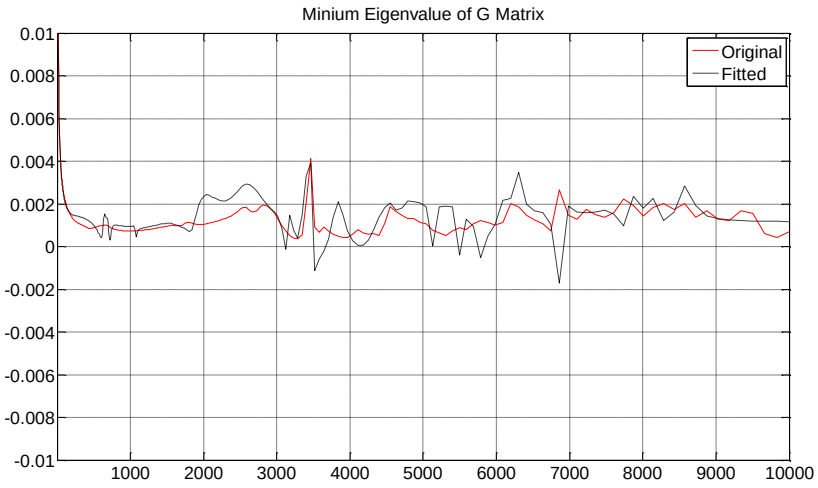

Figure 4-15 Minimum Eigenvalues of the Fitted G Matrices

4.8 A Heuristic Method of Mitigating the Passivity Problem of the FDNE

In this research, a heuristic method was developed to mitigate the passivity problem of the FDNE. This method is based on the fact that in this research, the frequency dependent admittance matrix is obtained in an analytical way (see section 4.2 and 4.3), thus the passivity of it is always guaranteed and the values of its entries at any frequency point can be easily calculated. Other methods of obtaining frequency dependent admittance matrix, i.e. on-site experiment and time domain simulation don't have this advantage.

The method uses recursive fitting to find an accurate and passive fit for the original frequency dependant admittance matrix. This method contains the following steps:

1. Select a series of frequency points for fitting. Calculate the frequency dependant admittance matrix at each point:

   $$Y(\omega_i) = G(\omega_i) + jB(\omega_i) \tag{4.54}$$

   Where i is the index of the frequency point.

2. Use Vector Fitting to get the FDNE, which is a series of s domain rational functions:

   $$f_{fit}(s) = g + sh + \sum_{K=1}^{N} \frac{a_K}{s - c_K} \tag{4.55}$$

3. Check the passivity of the FDNE at a series of frequency points. From experiments, the series of frequency points used for passivity checking should be distributed in a wider frequency range and have more points than the series of points selected for fitting.

   If there is no passivity violation, the process is finished and the passive FDNE is found. Otherwise, continue to the next step to apply recursive fitting.

4. Find the frequency range ($\omega_{Low} \sim \omega_{High}$) where the most significant passivity violation occurs. The significance of the violation can be determined by the value of the negative eigenvalue, i.e. large negative eigenvalue means large violation.
5. Remove all poles in the $\omega_{Low} \sim \omega_{High}$ frequency range of each rational functions ($f_{fit}(s)$) of the FDNE (4.55), so we get a series of reduced fitted functions: $f_{reduced}(s)$.
6. Select a new series of frequency points for fitting. The points should be selected such that in the frequency range ω_{Low} to ω_{High} there is higher density of points (higher resolution). Using more points in that range should enforce a tighter fit; and hence reduce the likelihood of the passivity violation.
7. Calculate the new target frequency response at each frequency point using the following equation:

$$Y_{new}(\omega_i) = G(\omega_i) + jB(\omega_i) - f_{reduced}(j\omega_i) \tag{4.56}$$

Where $G(\omega_i) + jB(\omega_i)$ is the admittance of the original network at the selected frequency point.

8. Use Vector Fitting to fit Y_{new} and get a new series of s domain rational functions:

$$f_{new}(s) = g_{new} + sh_{new} + \sum_{Knew=1}^{Nnew} \frac{a_{Knew}}{s - c_{Knew}} \tag{4.57}$$

9. The new FDNE is:

$$f_{new\_fit}(s) = f_{reduced}(s) + f_{new}(s) \tag{4.58}$$

In this way, $f_{new\_fit}(s)$ is obtained by fitting the series of frequency points which has higher density in the frequency range ω_{Low} to ω_{High}. So normally the fitting accuracy in this frequency range is higher than the original fitting function $f_{fit}(s)$, which means $f_{new\_fit}(s)$ is closer to the actual frequency response. Thus the passivity violation is eliminated or at least mitigated, which means the model will generate less energe in the simulation.

Steps 3 to 9 can be repeated in an iterative way, in each iteration the $f_{new\_fit}(s)$ from last iteration replaces $f_{fit}(s)$, till no passivity violation remains.

Figure 4-16 shows an example of the passivity enforcement using the proposed method. The first fitted FDNE has serious passivity violation. After two more fits with the procedure described above, all passivity violations in the frequency range of 0 to 6 kHz is removed.

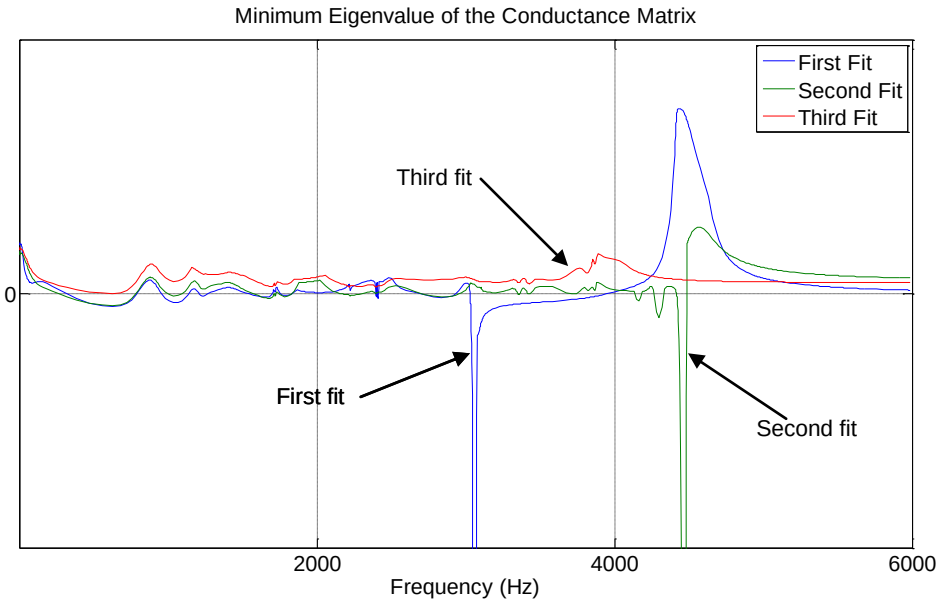

Figure 4-16 Passivity Enforcement Example

In this chapter, the FDNE method has been discussed in detail. A practical method of obtaining frequency response of large power system was introduced, and a heuristic method of mitigating the passivity violation of the FDNE was presented. In the next chapter, another important part of the proposed equivalent, the TSA simulation on the RTDS platform is discussed in detail.

5 Implementation of TSA Type Simulation on RTDS

This chapter discusses the implementation of the TSA part of the proposed equivalent which is used for representing the slow non-linear electromechanical behavior of the external system.

5.1 Difficulties in the Implementation of Conventional TSA Algorithms in Real Time

After decades of development, TSA algorithms are quite mature and there are many powerful TSA programs commercially available. However, it turns out that there are significant difficulties of interfacing a commercial TSA program to RTDS or implementing a conventional TSA algorithm in real time.

Because TSA programs ignore the detailed electromagnetic transients, they can potentially run much faster than full scale EMT programs. Indeed, today a TSA program can even appear to run in real time when simulating a power system with several thousand buses. However, this appearance of "real time" is only in an average sense, which means that some time-steps take much longer to simulate than other time-steps. This is because conventional TSA simulations typically use time-steps ranging from 2ms-10ms. For such relatively large time-steps, a suitable iterative calculation method is usually applied for solving the nonlinear network equations [21]. For a "stiff" transient, i.e., at the time-steps in the neighborhood of the time of application or removal of a fault, more iteration is required for convergence. Consequently, the solution for such time-steps requires a longer CPU time. As the number of iterations in any given time-step is not known a-priori, this results in an unpredictable amount of processing time for each time-step.

In contrast to the above approach which is suitable for off-line simulation, a true real-time simulator is required to keep in absolute synchronism with a real world clock. Hence the system solution in every simulation time-step **Δt** must be completed in an equivalent amount of real world time **Δt**.

There is another difficulty in interfacing a commercial TSA program to RTDS in practice. There is no TSA type simulation program which can run on the RTDS platform yet, so the TSA type program needs to run on an external server, for example, a server which has Microsoft Windows operating system and an Intel processor. A standard operating system like Microsoft Windows is not designed for real time application; it cannot guarantee the necessary amount of computation resource to one application in each time-step. The synchronization between the RTDS and the TSA program is difficult to maintain.

The above discussion reveals the difficulties of interfacing a conventional TSA algorithm to a true real-time simulation platform. An alternate workaround solution is discussed in the following section.

5.2 Structure of the Proposed Scheme

The proposed scheme uses a modified approach to implement the TSA type algorithm for real-time platforms.

The TSA simulation time-step is experimentally reduced so that the iterative calculation approach is no longer needed. This ensures a constant solution time per simulation time-step which is within the real-time requirement. With a sufficiently small time-step, determined in this research by experiments to be 2 ms or smaller, the network voltages in any time-step are close to the voltages in the previous time-step from a TSA

point of view. This permits the network equations to be solved using a linear formulation that does not require predictor-corrector type iteration, permitting the use of a single solution in each time-step. For example, a constant power load ($P + jQ$) at a bus with voltage $\vec{V}(t)$ in the conventional TSA solution can now be modeled as a current source, the value of which is:

$$\vec{I}(t) = \left(P + jQ\right) \Big/ \vec{V}(t - \Delta t)^{*} \tag{5.1}$$

Thus the processing time of each time-step is constant.

A simple conversion method is developed to convert the instantaneous values of the EMT solution into phasor values for the TSA solution.

The general structure of the proposed scheme is shown in Figure 5.1. Block ‘a’ measures the interface currents in the detailed RTDS model (internal system) to be injected into the external system, and converts them from three-phase instantaneous values to fundamental frequency positive sequence phasor values. Block ‘b’ represents the external network using a fundamental frequency phasor formulation. Connected to block ‘b’ are blocks ‘c’ which represent dynamic equipments such as generators, motors etc. These equipments are modeled using differential equations. Block ‘d’ is used to calculate the TSA injected current into the EMT solution.

The phasor signals generated in block ‘a’ are sent to block ‘b’ (TSA network solution) which then calculates the terminal voltages (as phasor values) of the generators and the other equipment components in blocks ‘c’. The TSA type generator models (also, other dynamic equipments models) ‘c’ use the terminal voltages as the inputs to their state equation solvers, and calculate the currents (phasor values) that they inject into the external network. These phasor values are converted back to time domain instantaneous

three-phase values and injected back into the EMT solution using block ‘d’. The details of the TSA-EMT interface are given in section 5.3.

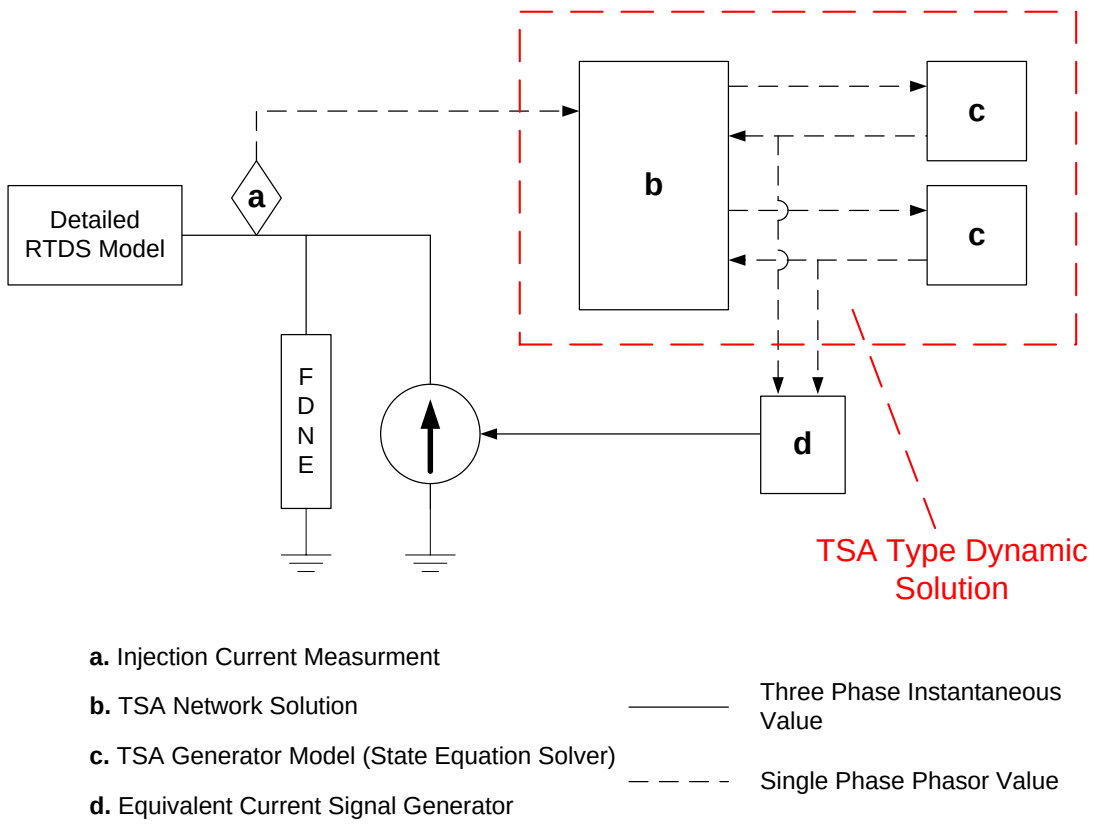

Figure 5-1 General Structure of the Proposed TSA Solution Scheme

The blocks in Figure 5.1 are individually constructed as user defined (UDC) control models in RTDS [37]. They are connected into RTDS as control blocks. Note that the implementation as in Figure 5.1 makes the solution more convenient for real time implementation as the ‘b’ and various ‘c’ blocks can be implemented in parallel on separate processors.

It will be easier to understand the differences between the proposed scheme and a conventional TSA type simulation program by comparing Figure 5-2 and Figure 2-6.

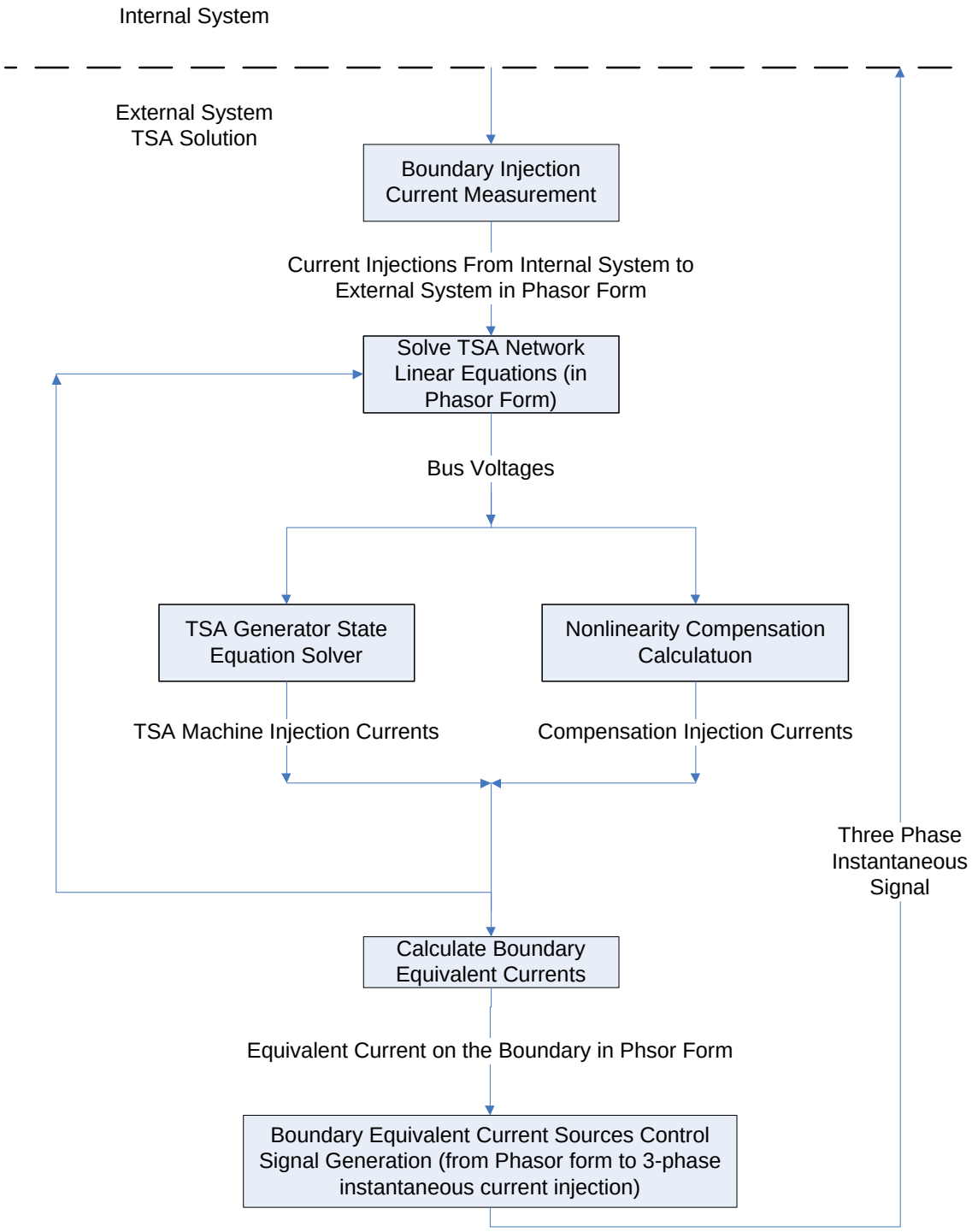

Figure 5-2 Signal Flow of the Proposed Scheme

As mentioned earlier, one of the major difficulties of implementing conventional TSA type algorithms in real time is that the processing time of each time-step is not fixed and predictable. So in the proposed scheme, the predictor-corrector iterative calculation method is not used. The linear equation set of the network is only solved once in each time-step. Thus the processing time of the network solution block is fixed. The disadvantage is that it is necessary to use a small TSA time-step. However, using a small TSA time-step is more numerically stable than the method of predictor-corrector iteration with a large TSA time-step. It is often faster because in the predictor-corrector iteration scheme, the time savings of using a large time-step are offset by the need for a larger number of iterations, which arise during large disturbance. Thus a small TSA time-step is suitable for real time simulation.

As seen in Figure 2-6, in conventional TSA type simulation algorithms, generator model blocks (and other dynamic equipment model blocks) exchange data with the network solution block twice in each time-step if an integration method such as the second order Runge-Kutta method is used; and for the fourth order Runge-Kutta method, such data exchange will be done four times in each time-step. Such a large amount of data exchange is difficult to coordinate when the blocks are distributed on multiple processors of a parallel computation platform. In the proposed scheme, network solution is only done once in each time-step. During the solution of a generator model in each time-step, its terminal voltage is assumed to be constant. This is a reasonable assumption as time-step is small. By doing this, the data exchange between blocks can be greatly reduced, which makes it much easier to coordinate the blocks for parallel computation.

Figure 5.3 shows two possible time sequences which can be employed in the proposed TSA type solution scheme in RTDS. Theoretically speaking the serial sequence has better numerical stability than the parallel sequence, because in the parallel sequence, both the inputs of the generator solution and the network solution are from previous time-step, and in the serial sequence, only the input of the network solution are from previous time-step. However, the serial sequence doesn't take the full advantage of a parallel computation platform. The parallel sequence is like what happens in an analog system; there is no clear and consistent time order in the process, but it is easier to be implemented on the parallel computation platform of RTDS. The shortest time frame of the electromechanical dynamics of AC systems is around 0.02 second. If the TSA time-step is much shorter than this, then the parallel sequence can be employed. In this research, the TSA time-step sizes have been tested ranging from 50μs to 2ms, and no difference have been found between the two sequences.

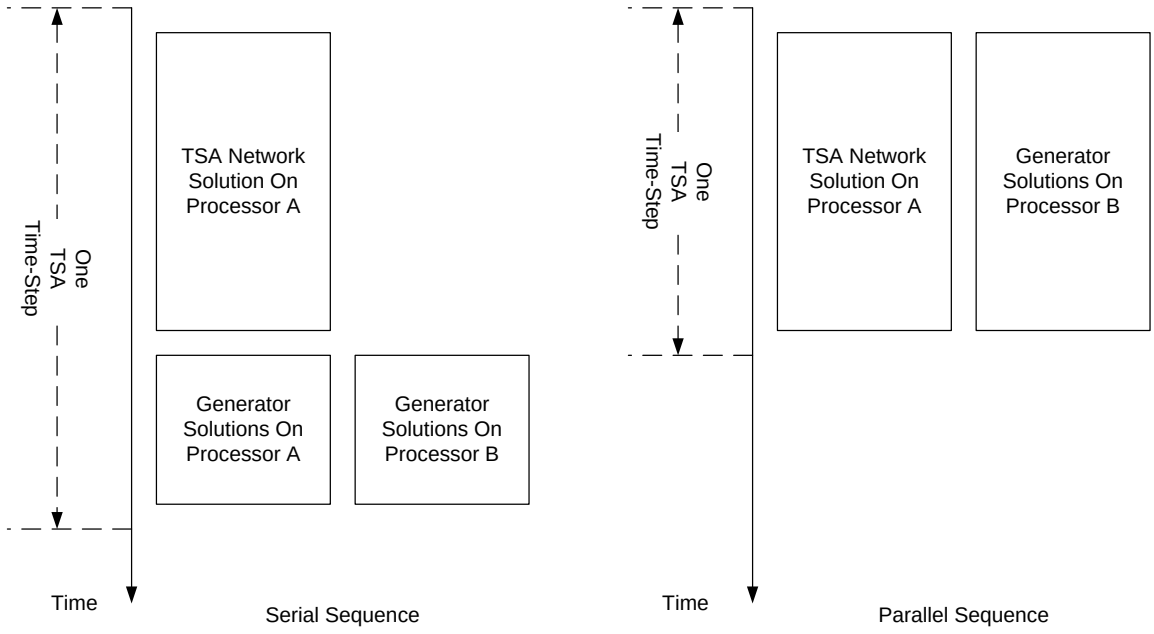

Figure 5-3 Time Sequences in the Proposed Scheme

The following procedure was used to select the TSA simulation time-step Δt. Typical simulation cases were simulated using an approach commonly used in the EMT community, which suggests successively conducting several simulations while reducing Δt by a factor of 2. When the resulting simulation plots show no perceptible differences from the previous simulation, the time-step is deemed to be sufficiently small. This procedure shows that a time-step of 1-2 ms is suitable for the proposed scheme with the parallel sequence. This value is smaller than the commonly used 10ms time-step in TSA simulations, but is much larger than the commonly used 20-50μs time-steps in EMT simulation.

In following sections, the major blocks of the proposed scheme are discussed.

5.3 Interfacing the EMT and TSA solutions

The TSA type solution of the external system is done in the phasor domain. In the EMT type solution of the internal system, all the currents and voltages are represented by instantaneous values. The method of interfacing these two solutions which have very different natures has therefore to be developed.

5.3.1 Interfacing the EMT solution to the TSA program

The interfacing of the EMT solution to the TSA program is done by block ‘a’ in Figure 5-1, which converts the instantaneous values of voltage and current on the boundary bus from the EMT solution to positive sequence phasor values. In other research papers, this has been done by calculating the RMS value of the voltage [14], a Fast Fourier Transformation (FFT) [18] or a consecutive curve fitting technique [15][16][17]. In the FFT and curve fitting method, the fundamental frequency positive

sequence magnitude and phase are extracted from a succession of data points of all three-phases at the boundary.

The method proposed in this research is based on the fact that the generator electromechanical swings represented in the TSA are primarily affected by the real power transferred to the external system at the boundary bus. Note that the electrical network in the external system appears as two distinct model types - once in the EMT solution as an FDNE which represents the wide-band frequency response and again in the TSA solution for calculating the low frequency electromechanical quantities. The solution calculated in the TSA has negligible influence on calculating the higher frequency components of the bus voltage. The quantities calculated within the TSA solution and interfaced as positive sequence fundamental frequency sources into the EMT solution, are primarily affected by the rotor angles which in turn are mainly a function of the real power. Hence a highly accurate interface procedure can be developed which is much simpler to implement than the FFT and curve fitting approaches used by previous researchers as discussed below.

The direct method of representing the effect of the internal system on the external one would have been to extract the fundamental frequency positive sequence components of the boundary current injected by the internal system and to connect it into the TSA formulation as a current source. However, the proposed method uses an energy balance based approach which uses a current source that injects the same amount of power as that calculated by the independent and accurate EMT solution of the internal system. Based on this, a simple conversion method, as demonstrated, in Figure 5-4 is developed.

Figure 5-4 shows the fundamental frequency phasor representation of the proposed two part equivalent of Figure 1-2. The objective is to determine the positive sequence phasor values $\vec{V}_T$ and $\vec{I}_T$ at the boundary bus for use in the TSA solution.

The positive sequence values $G + jB$ of the admittance of the FDNE at fundamental frequency are known. The phasor value ($\vec{I}_E$) of the controlled three-phase current source is calculated in the TSA program with a relatively small time-step (for instance equal to or smaller than 2 ms. Compared to the electromechanical transients which are in the frequency range of 0~5Hz), this is a very small time-step. Hence even though the value of $\vec{I}_E$ was actually calculated in the previous time-step, it can be considered to be the same in the present time-step. The instantaneous values of the corresponding three-phase currents $i_{Ea}(t)$, $i_{Eb}(t)$ and $i_{Ec}(t)$ are thus readily calculated by expressing the above phasor in time domain form.

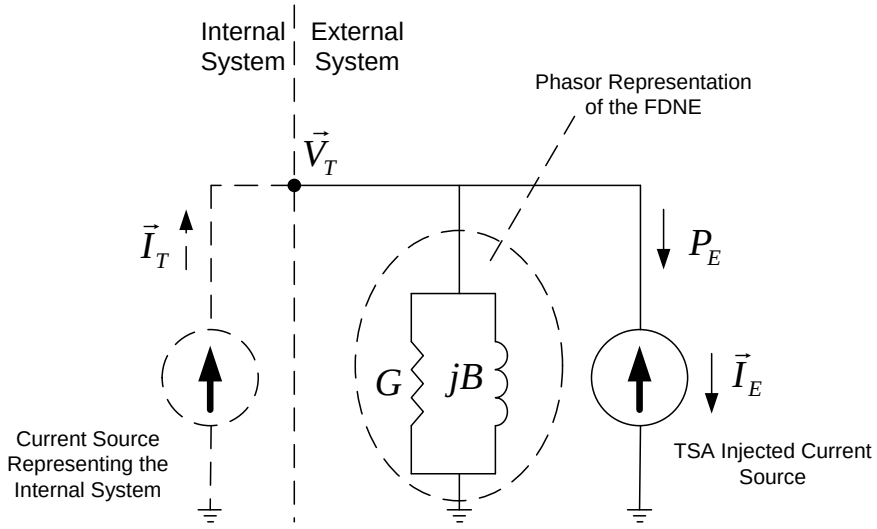

Figure 5-4 Fundamental Frequency Phasor Representation of the Two Part Equivalent

P_E is the instantaneous value of the real power into the controlled current source $\vec{I}_E$ which is used to inject the results of the TSA calculation into the EMT program. Note that using the instantaneous value of $v_{Ta}(t)$, $v_{Tb}(t)$, $v_{Tc}(t)$ calculated in the EMT solution, P_E can be readily evaluated as:

$$P_E(t) = v_{Ta}(t) \cdot i_{Ea}(t) + v_{Tb}(t) \cdot i_{Eb}(t) + v_{Tc}(t) \cdot i_{Ec}(t) \tag{5.2}$$

Consider the current quadrature phasor $\vec{I}_{E1} = j\vec{I}_E$ which has the same magnitude as $\vec{I}_E$, but leads it by 90°. The three-phase time domain currents corresponding to $\vec{I}_{E1}$ are $i_{E1a}(t)$, $i_{E1b}(t)$ and $i_{E1c}(t)$. The product of $Q_E(t)$ defined by (5.3) below represents the reactive power into the TSA part of the external system model by the internal system in the steady state:

$$Q_E(t) = v_{Ta}(t) \cdot i_{E1a}(t) + v_{Tb}(t) \cdot i_{E1b}(t) + v_{Tc}(t) \cdot i_{E1c}(t) \tag{5.3}$$

Once $P_E(t)$ and $Q_E(t)$ are determined, the voltage phasor $\vec{V}_T$ on the boundary bus is calculated so that power balance is satisfied. Using $\vec{V}_T$, the value of the required injection current phasor $\vec{I}_T$ at the interface bus is calculated as shown below.

The phasor $\vec{V}_T$ for use in the TSA can be calculated as:

$$\left|\vec{V}_{TE}\right| = \left|P_E\right| / \left|\vec{I}_E\right| \tag{5.4}$$

$$\left|\vec{V}_{TE1}\right| = \left|Q_E\right| / \left|\vec{I}_{E1}\right| \tag{5.5}$$

$$\left|\vec{V}_T\right| = \sqrt{\left|\vec{V}_{TE}\right|^2 + \left|\vec{V}_{TE1}\right|^2} \tag{5.6}$$

$$\angle\vec{V}_T = \angle\vec{I}_E + \tan^{-1}\left(\frac{Q_E}{P_E}\right) \tag{5.7}$$

The above phasor quantities are shown in Figure 5-5.

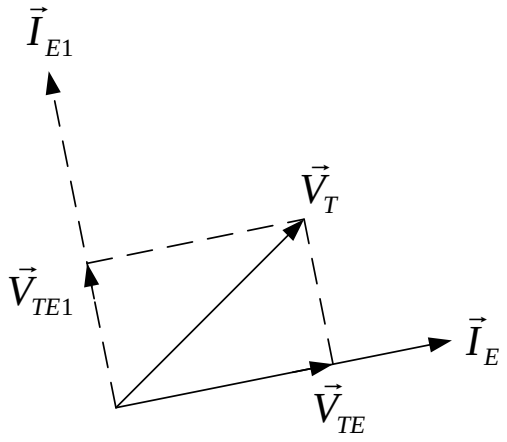

Figure 5-5 Phasor Diagram for Boundary Bus Voltage Determination Fundamental

The injection current $\vec{I}_T$, which is the current that communicates the EMT solution into the TSA, can be calculated as:

$$\vec{I}_T = (G + jB) \cdot \vec{V}_T + \vec{I}_E \tag{5.8}$$

For multi-ports cases, a similar process is used; the only difference is that the matrix form of equation (5.8) is applied. This method is very simple as it does not require curve fitting or Fourier Transformation used in earlier approaches [15][16][17][18]. But it can be seen in the example cases in Chapter 7 that it works well even for unbalanced faults and other distorted waveform conditions.

5.3.2 Interfacing the TSA solution to the EMT program

To make the equivalent for the external AC system, each unit of dynamic equipment such as a generator is simplified to a three-phase Norton Equivalent with a linear shunt impedance in parallel with a balanced three-phase fundamental frequency sinusoidal current source which has dynamically changing magnitude and phase angle. These units

are considered to be connected to the remainder of the external network in which the other non-linearities such as transformer saturation are ignored. The above current injections are calculated from a full TSA solution of the external network, with the connection busses to the internal network being treated as voltage sources (as explained in section 5.3.1). The details of the procedure are explained below.

Consider an external system in which the number of busses is $K1$ connected to the internal system at $K2$ buses. Each bus has three nodes (one per phase). Equation (5.9) represents the frequency dependant relationship between the boundary currents and voltages I_B, V_B and the external network's currents and voltages I_E, V_E. Note that the external network's circuit elements are considered linear.

$$\begin{bmatrix} I_B \\ I_E \end{bmatrix} = Y_E(f) \begin{bmatrix} V_B \\ V_E \end{bmatrix} = \begin{bmatrix} Y_{BB}(f)_{3K2\times 3K2} & Y_{BE}(f)_{3K2\times 3(K1-K2)} \\ Y_{EB}(f)_{3(K1-K2)\times 3K2} & Y_{EE}(f)_{3(K1-K2)\times 3(K1-K2)} \end{bmatrix} \begin{bmatrix} V_B \\ V_E \end{bmatrix} \tag{5.9}$$

The Norton Equivalent as looking into the external network from the boundary can be calculated by eliminating V_E in (5.9).

$$I_B = \left[Y_{Equ}(f)\right] V_B + J_{NE} \tag{5.10}$$

Where

$$\left[Y_{Equ}(f)\right] = \left[Y_{BB}(f)\right] - \left[Y_{BE}(f)\right] \cdot \left[Y_{EE}(f)\right]^{-1} \left[Y_{EB}(f)\right]$$

and

$$J_{NE} = \left[Y_{BE}(f)\right] \cdot \left[Y_{EE}(f)\right]^{-1} I_E$$

In (5.10), $\left[Y_{Equ}(f)\right]$ is the Norton admittance matrix and J_{NE} is the Norton Current source vector.

The admittance matrix $\left[Y_{Equ}(f)\right]$ is inserted as part of the EMT solution as described in Chapter 4. In order to do so, each element is first approximated with a s-domain rational function using vector fitting as in (5.11)

$$\left[Y_{Equ}(s)\right]_{i,j} = g_0 + sh_0 + \sum_{k=1}^{N} \frac{a_k}{s - c_k} \tag{5.11}$$

Using the trapezoidal rule of integration, the multi-node admittance matrix in (5.11) is converted into a circuit representation that uses a constant real conductance matrix in parallel with a history current source vector as described in section 4.5. This conversion completely incorporates the Norton admittance of the external network into the EMT solution.

The following procedure is now used to calculate the Norton current source representing the external network $J_{NE} = \left[Y_{BE}(f)\right] \cdot \left[Y_{EE}(f)\right]^{-1} I_E$ in (5.10) required in the EMT solution.

As described in section 5.3.1 above, the Norton current source is calculated from a positive sequence fundamental frequency TSA solution. The positive sequence fundamental frequency representation for the Norton Current Source calculated in (5.10) is shown in (5.12). The magnitudes and phase angles of the equivalent current sources $\left[I_{E+}(f_0)\right]$ are updated in each TSA time-step. The updating is carried out in block 'c' in Figure 5-1 and equation (5.12) is carried out in block 'd' in Figure 5-1. Noticed that only positive sequence values are used in equation (5.12). Because it is assumed in the TSA part, everything is balance.

$$\left[J_{NE+}\right] = \left[Y_{BE+}(f_0)\right] \cdot \left[Y_{EE+}(f_0)\right]^{-1} \cdot \left[I_{E+}(f_0)\right] \tag{5.12}$$

In obtaining this equivalent, only the positive sequence component impedances of the admittance matrix are used, and so the dimension of $Y_{BE+}(f_0)$ is $K2\times(K1-K2)$; and of $\left[Y_{EE+}(f_0)\right]$ is $(K1-K2)\times(K1-K2)$ respectively (not $3K2\times3(K1-K2)$ and $3(K1-K2)\times3(K1-K2)$ as earlier). Strictly speaking, in (5.12) it is assumed that there is no generator in the external system which is directly connected to the boundary bus. If such generator exist, its contributions can be included in a straightforward manner by adding its current directly to $\left[J_{NE+}\right]$.

The positive sequence Norton current source calculated above is interfaced into the EMT program as three time varying phase displaced currents. Their instantaneous time domain values are updated in each EMT time-step using the following equations:

$$\begin{cases} i_A(t) = \sqrt{2}\cdot\left|J_{NE+}(t)\right|\sin\left(\alpha(t)\right) \\ i_B(t) = \sqrt{2}\cdot\left|J_{NE+}(t)\right|\sin\left(\alpha(t)-\frac{2}{3}\pi\right) \\ i_C(t) = \sqrt{2}\cdot\left|J_{NE+}(t)\right|\sin\left(\alpha(t)+\frac{2}{3}\pi\right) \end{cases} \tag{5.13}$$

Here $\alpha(t)$ is the instantaneous angle of the phasor current and is obtained by adding the instantaneous angle of the rotating reference phasor $1\angle0^o$ in the TSA solution i.e., $2\pi\ f_0\cdot t$ to the phase angle of the current $\angle J_{NE+}(t)$ as in (5.14).

$$\alpha(t) = 2\pi\ f_0\cdot t + \angle J_{NE+}(t) \tag{5.14}$$

Real time digital simulation can run for very long period and works with incremental time-step Δt. Use of an absolute time t can be problematic. This is because in the simulation, absolute time t is reached by adding Δt over and over again which may

create a drift due to truncation errors. The equivalent form of (5.14) which uses only Δt is (5.15), in which $\alpha(t)$ is updated from its previous value.

$$\alpha(t) = \alpha(t-\Delta t) + 2\pi\, f_0 \cdot \Delta t + \angle J_{NE+}(t) - \angle J_{NE+}(t-\Delta t) \tag{5.15}$$

Where

$\alpha(0) = \angle J_{NE+}(0)$

Equations (5.13) and (5.15) are also evaluated in block 'd' of Figure 5-1. Note that as $\angle J_{NE+}(t)$ is updated at each TSA time-step, which can be larger than the EMT time-step Δt. Hence the quantity $\angle J_{NE+}(t) - \angle J_{NE+}(t-\Delta t)$ is zero in between TSA time-steps in equation (5.15).

5.4 TSA Network Solution

Once $\vec{I}_T$ (which is the phasor value of the currents injected from the internal system to the external system) is determined as described in section 5.3.1, it can be used as the input of the TSA network solution block.

The basic work of the TSA network solution block is to solve the network nodal admittance linear equation [21]:

$$[Y] \cdot V = I \tag{5.16}$$

In equation (5.16), $[Y]$ is the admittance matrix of the external system. I is the injection current vector, which is the input to the block. V is the bus voltage vector of the external system, which is to be solved and outputted. Matrix $[Y]$ and vectors V and I are all complex (phasor).

Since the external system is assumed to have no switches, the $[Y]$ matrix is constant. This greatly simplifies the solution process and makes it very fast.

The straight forward way of solving equation (5.16) is to invert matrix $[Y]$:

$$V = [Y]^{-1} \cdot I = [Z] \cdot I \tag{5.17}$$

Where $[Z]$ is the impedance matrix of the external system, and it is also constant. So the inversion can be done off-line and only the $[Z]$ matrix is stored and used in RTDS simulation.

For a power system, $[Y]$ is a very sparse matrix, on the other hand, $[Z]$ is a full matrix. So storing $[Z]$ is not efficient through this is no longer the major concern as the memory size of computers has been increased dramatically. More important, the multiplication is very time consuming, which make equation (5.17) only implementable in very small systems.

Sparse matrix techniques have been widely employed in power system calculations. In this research, a mature and widely used sparse matrix technique is employed [38].

Using LU factorization, the $[Y]$ matrix can be factorized into four matrix: $[L]$, $[U]$, $[P]$ and $[Q]$.

$$[P] \cdot [Y] \cdot [Q] = [L] \cdot [U] \tag{5.18}$$

$[L]$ is a unit lower triangular matrix, $[U]$ is an upper triangular matrix, $[P]$ is a row permutation matrix, $[Q]$ is a column reordering matrix. $[L]$ and $[U]$ can keep the sparse characteristic of matrix $[Y]$.

Equation (5.18) can be rewritten as:

$$[P]^{-1} \cdot [L] \cdot [U] \cdot [Q]^{-1} \cdot V = I \tag{5.19}$$

Equation (5.19) can be solved in four steps:

$$\overset{*}{I} = P \cdot I \tag{5.20}$$

(5.20) only reorders the injection current vector I .

$$[L] \cdot T = \overset{*}{I} \tag{5.21}$$

(5.21) can be solved with a forward substitution process. Notice that only some of the entries of $\overset{*}{I}$ are nonzero (The nonzero entries of $\overset{*}{I}$ are associated with the buses connected to nonlinear loads, generators and other dynamic equipments). And most entries of $[L]$ are zero. So in the forward substitution process, there are many multiplications by zero, which can be ignored. These operations are known beforehand with the knowledge of the sparse structure of $[L]$ and $\overset{*}{I}$. Thus only a small part of $[L]$ must be stored and used. This is called 'Fast Forward Substitution'.

$$[U] \cdot \overset{*}{V} = T \tag{5.22}$$

As (5.21) discussed before, equation (5.22) can be solved with a backward substitution process. Only some 'target' entries of $\overset{*}{V}$ are of interest (those associated with the buses connected to nonlinear loads, generators and other dynamic equipments). Because most entries of $[U]$ are zero, for the calculation of the 'target' entries of $\overset{*}{V}$, it is not necessary to calculate the whole $\overset{*}{V}$ vector, instead, only 'useful' entries of $\overset{*}{V}$ need to be calculated. So only the nonzero entries of $[U]$, which are associated with these 'useful' entries of $\overset{*}{V}$, are used in the calculation. Thus only a small part of $[U]$ must be stored and used. This is called 'Fast Backward Substitution'.

$$V = [Q] \cdot \overset{*}{V} \tag{5.23}$$

As (5.20), (5.23) is just a reordering process.

Since the $[Y]$ matrix is constant, the factorization (5.18) is done off-line using a standard MATLAB [39] function which maintains the sparse structure of the $[Y]$ matrix. The UDC code of the process related to the execution of (5.20) to (5.23) can be optimized and requires minimum memory and computation time since the structures of all the matrices and vectors are known.

5.5 TSA Power System Equipment Models

The modeling procedures for TSA type power system equipment models have been thoroughly explained in reference [21]. They have been followed in this research. Some specific points are outlined below.

5.5.1 Integration Method

It can be easily seen in Figure 2-6 that in conventional TSA type simulation programs, the same integration method is applied to all models in the system. Because during one time-step integration, the models need to exchange data for multiple times with the network and with each others, the integration method determines what data to be exchanged and the exchange procedure. For example, in the fourth order Runge-Kutta method, in each time-step, an exciter model needs to send intermediate excitation voltage signal to the generator model four times and get intermediate terminal voltage signal four times from the network solution. Because the smaller time-step being used, the proposed scheme allows employing different integration methods for different models.

Currently, the second order Runge-Kutta method is applied to the generator models, and the trapezoidal method is applied to exciters and governors.

The numerical stability is a very important issue for the real time simulation. The TSA type dynamic solution shows great stability when running continuously on the RTDS for hours.

5.5.2 Loads

Constant impedance loads are part of the network and are included in the FDNE. Nonlinear loads can be modeled as voltage dependant current injections in the TSA solution. But in this application it might be better to model part of a nonlinear load as a constant impedance load and include it in the FDNE; the remaining can be modeled as a voltage dependant current injection.

5.5.3 Power Electronic Equipment

In the TSA part, a power electronic converter can be modeled using its steady state algebraic equations and the slow dynamics of the controls can be modeled using dynamic equations. For example, a voltage source converter is modeled as a fundamental frequency positive sequence current source, in a manner similar to synchronous generator, with its commutation reactance included as part of the FDNE. The frequency dependent characteristics of power electronic equipments are highly non-linear and hence they have to be ignored in the FDNE part as discussed in section 4.3.

5.5.4 Challenge of the Adoption of the Proposed Scheme

The model libraries of commercial TSA type simulation programs contain hundreds of models. These models have been validated over many years of power system operations.

For a model to be fully commissioned, it requires many details to be handled, corrected, tested and validated. All these have to be done before a fully commissionable model library for the proposed scheme can be constructed.

6 Synthesis of the Entire Equivalent

In this chapter the construction of the whole equivalent model is described and some practical issues are discussed.

6.1 Synthesis of the Entire Equivalent

The proposed wide band two parts equivalent consists of a FDNE and a current source which is controlled by a TSA solution block, as discussed in chapter 4 and 5 respectively. This section describes how the individual components are connected together to form the entire equivalent model which is incorporated in the RTDS simulation.

An example of a one port equivalent is shown in Figure 6-1. Since this is a one port three phase equivalent, the FDNE contains six frequency dependant branches. Instead of modeling six individual branches, it is also possible to model all six branches (circled at right hand side bottom) together as a single frequency dependant matrix; however, this may preclude the running of the model on multiple processors. The components of the TSA solution block are all put into the “Dynamic Hierarchy” (Hierarchy is a graphical component available in the RSCAD, the software of RTDS. Hierarchy is used for schematically separating the user’s circuit diagram into a number of blocks [37]). The developed TSA solution block generates the current reference for the three phase current source.

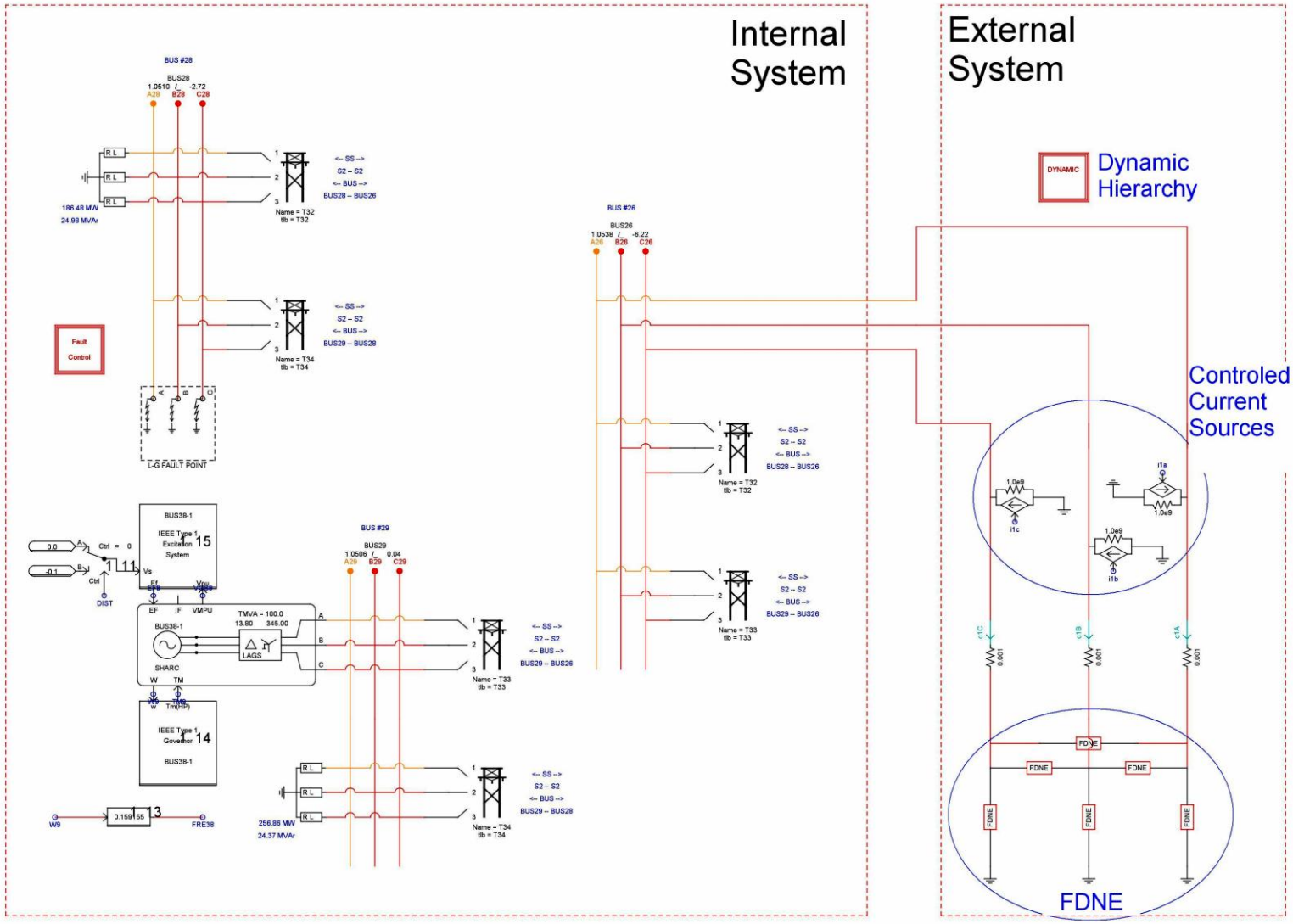

Figure 6-1 Synthesis of a One Port Equivalent

As shown in Figure 6-2, inside the Dynamic Hierarchy there are three parts. The "Injection Current Conversion" part has been described in section 5.3.2. The "Current Control Signal Generation" part is a simple three phase sinusoidal signal generator. The major part is the "TSA Solution", which contains the TSA type network solution model and TSA type generator models (Figure 6-2 only shows 3 generators). Each generator and its exciter and governor is separately modeled. They are set up and connected through RSCAD graphical interface. This procedure is identical to any other models of RTDS. It should be noticed that from the RTDS's point of view, the TSA type generator model is actually a large control system rather than an embedded circuit component.

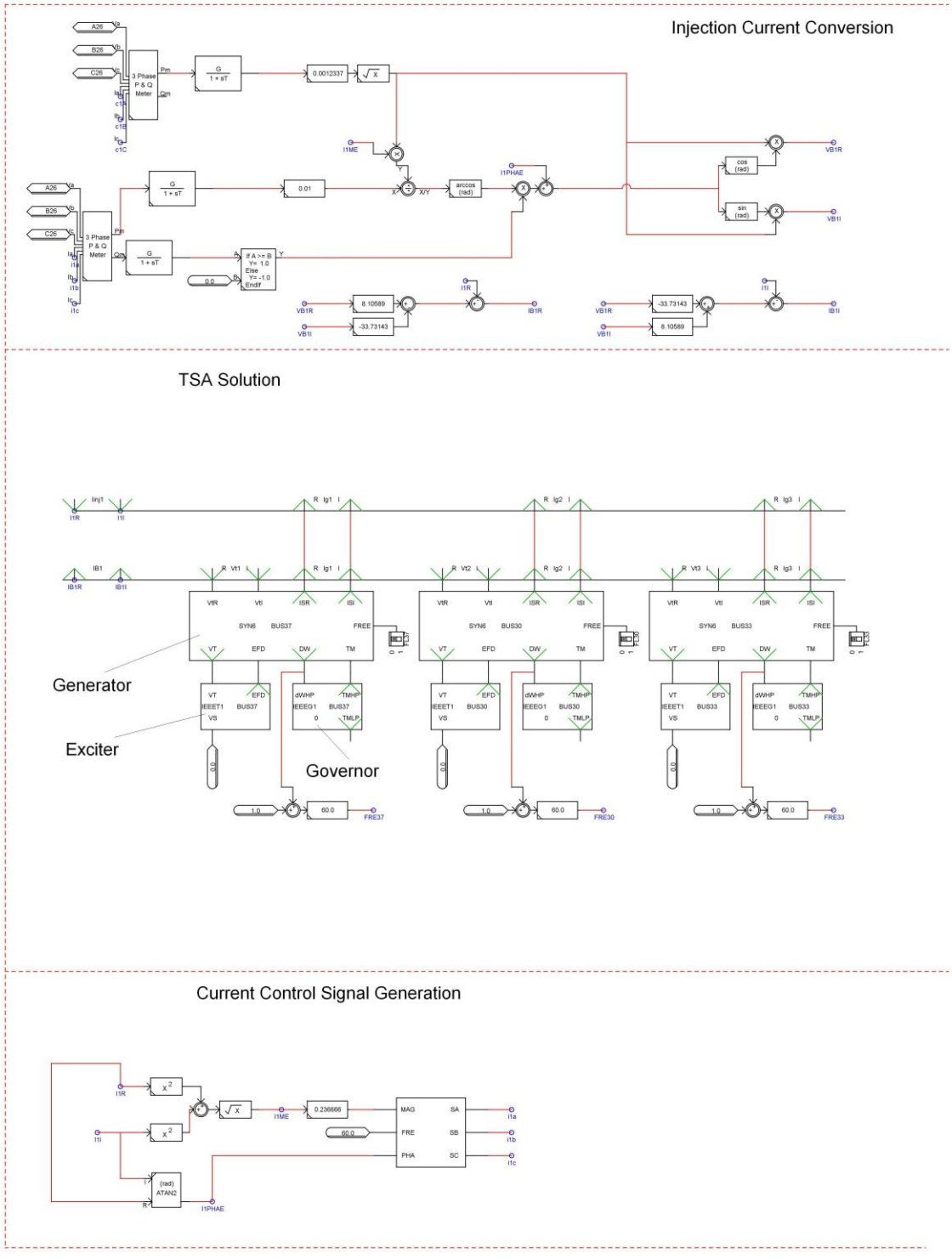

Figure 6-2 TSA Solution Block

6.2 Structures with Multiple External and Internal Systems

Section 6.1 describes a simulation system model in which a one port equivalent system (external system) model is connected to a detailed EMT simulation system (internal system) model. This is the simplest scheme for the simulation model using the equivalent. This scheme is shown as in Figure 6-3(a), and Figure 6-3 also shows two of the other possible schemes.

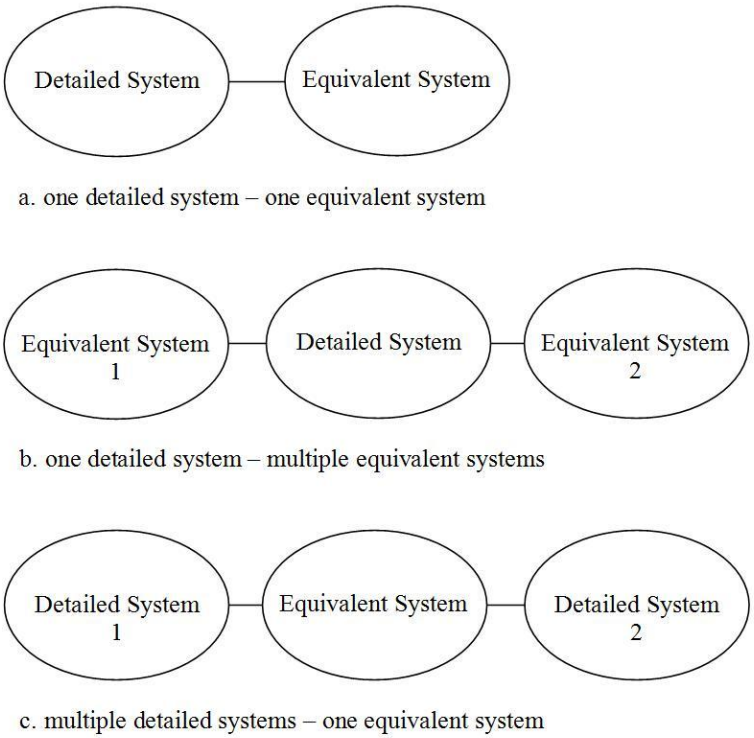

Figure 6-3 Schemes of the Simulation System Model

Figure 6-3(b) shows a detailed system connected to multiple equivalent systems. There is no electrical connection between the equivalent systems except the connections through the detailed system. So the equivalent systems are constructed independently.

During the simulation, each equivalent system is directly affected by the detailed system only. The example case described in section 7.5 utilizes such a scheme.

Figure 6-3(c) shows an equivalent system connected to multiple detailed systems. There is no electrical connection between the two detailed systems except the connection through the equivalent system. During the simulation, each detailed system is directly affected by the equivalent system only. The example cases described in section 7.4 utilize such a scheme.

It should be noticed that in Figure 6-3 each connection between equivalent system and detailed system can be single-port as well as multi-port.

Theoretically saying, the schemes shown in Figure 6-3 can also be extended to more complicated scheme in which multiple equivalent systems are connected to multiple detailed systems in a mesh structure. This was not done in this research.

6.3 Practical Issues

In this research, many different equivalent models have been constructed, and during this process, the following practical issues have been observed.

6.3.1 Size of the Equivalent System

The size of the external system which can be represented by the equivalent model is of major concern of any equivalencing technique. For the two part equivalent proposed in this research, the FDNE and the TSA parts are affected in different way by the system size:

- **The system size limitation for the FDNE part.** Generally, the larger the external system, the more complicated its frequency dependent characteristic is,

which means higher order rational functions need to be used to fit the characteristic. However, it was observed that in most cases, the frequency response characteristic of the external system is dominated by the components which are close to the boundary. Thus the major part of a large system has only minor influence on the frequency dependent characteristic as seen from the boundary and hence the size of external system is not a major concern of the FDNE part, instead, the number of ports of the equivalent is of major concern as will be discussed in section 6.3.2.

- **The system size limitation for the TSA part.** It should be noticed that in this research, no equivalencing has been done from a TSA point of view. The TSA part of the equivalent is a full real time TSA solution of the external system. Since optimal sparse matrix computation technique has been implemented, the number of the linear components in the external system is not of major concern. The size limit is determined by the number and complexity of the dynamic and nonlinear components of the external system, such as generators, generator controls, and nonlinear loads etc. With a TSA time-step of 2 ms utilized (see section 5.2 for details), it is estimated that a typical RTDS rack should be able to perform full TSA solution of a power system of about one thousand buses in real time, which is much larger than a 20 bus system for which a RTDS rack can perform full real time EMT solution. If the real time TSA solution is needed for a really large power system (say, tens of thousands of buses), dynamic reduction techniques as discussed in section 1.3.1 can be implemented. However, this has not been considered and is recommended as future work.

6.3.2 Number of Ports of the Equivalent

In many cases, the number of ports of the equivalent model is the most limiting factor on the application of the proposed equivalent:

- When the number of ports increases, the size of the frequency dependant admittance matrix of the external system as seen from the boundary scales as a square of number of boundary nodes. For example, a one port equivalent (three phase) has 6 frequency dependent branches (see section 3.2) which will be represented by s-domain functions. A two port equivalent has 21 frequency dependent branches; a three port equivalent has 45 frequency dependent branches; and an N port equivalent has $3N(3N+1)/2$ frequency dependent branches. It can be seen that when the number of ports increases, the number of s-domain functions increases rapidly. Though the order of each s-domain function can be reduced by limiting the fitting frequency range, which compromises the accuracy of the FDNE, the computation burden of simulating the FDNE will still increase dramatically.
- When the number of ports increases, it is more difficult to maintain the passivity of the FDNE.

Due to these difficulties, the proposed equivalencing technique is not at present ready for making equivalent for an external system which connects to the internal system at many ports (say, more than 3 ports). For HVDC and FACTS studies, normally the connecting points to the AC system can be chosen as the boundary, thus the number of ports probably can be limited within 2 or 3. For studies of some AC systems which have clearer structure, such as the one described in section 7.5, multiple equivalents can be

used, and it might be possible to limit the number of ports of each equivalent by carefully choosing the boundary. In many cases, the step transformers are good choices for the boundary. For complex meshed AC systems, it might be difficult to find a suitable boundary.

6.3.3 Utilizing the Distributed Computation Platform

In the RTDS, a transmission line form a natural interface between systems modeled on different racks. This is due to the relativistic speed limit of electrical signal propagation on these lines; which essentially decouples the remote ends in any given time-step. As no transmission lines are explicitly modeled in the equivalent, the equivalent must be modeled on one rack.

One way around this is to intentionally partition the external system, by modeling some transmission line cut-sets as additional internal systems. The split parts can then be modeled on different racks, with the transmission line cut-sets serving as natural isolations.

6.3.4 Applying Network Changes in the External System

Simulating network change events is a major task in many time domain simulation studies. Network change events may include short-circuit and breaker switching etc. In this research, it is assumed that there is no networks change to be applied inside the external system.

- If network changes are to be applied in the external system, its frequency dependent characteristic will be changed during the simulation. FDNE is not suitable for simulating the changes of the network, because the network

components are not explicitly modeled and hence the switching transients cannot be simulated.

- As described in section 5.4, assuming topology of the external network to be constant, the admittance matrix in the TSA solution can be factorized in off-line. And the computation needs be done in real-time can be greatly reduced.

A possible way to simulate network change events in the external system is to use compensating currents to approximate the topology change. However, only electromechanical transient caused by the network changes can be simulated using such method. And large topology change, such as short-circuit, might not be able to be simulated due to numerical issues. This topic is therefore left for future researchers.

7 Study Cases

This chapter validates the wide-band multi-port equivalencing method developed in this research. Four examples cases are presented. The simulation results of different simulation tools and different set ups are compared.

7.1 Organization of the Study Cases

The first case is a 39 bus AC system. A one port equivalent is used for this case. The comparison between a standalone TSA type program and the RTDS can be easily conducted on this system.

The second case is a 108 bus AC system; a one port equivalent is used for this case. It shows that the proposed equivalencing method can greatly reduce the RTDS hardware required for simulating large power systems.

The third case is a multi in-feed HVDC system. A two port equivalent is used to represent the AC system. The HVDC systems are modeled in full EMT detail in RTDS. This case shows how the proposed equivalencing method could work in simulations of large power electronic based systems.

The fourth case is a 470 bus AC system. Multiple equivalents are used to represent the external system. Both the internal system(s) and the external system(s) are distributed on multiple RTDS racks. This case shows the scalability of the proposed equivalencing method.

The following terminology is used in the example descriptions to describe the different levels of details included in simulations:

- **RTDS FULL MODEL** --- The candidate test system is first modeled entirely on a real-time EMT algorithm implemented on the RTDS. As the system is represented in full three-phase wide-band detail, its results provide a benchmark for validating the proposed equivalents.
- **TSAT** --- As an additional comparison, some of the cases are compared also with a pure TSA type simulation which completely ignores electromagnetic transients. A stand alone pure TSA type simulation is conducted on a Windows XP based PC, using the TSAT software [40][41].
- **RTDS+FDNE+TSA** --- The internal system is modeled in RTDS in full EMT detail. The external system is represented by the proposed FDNE+TSA equivalent, as shown in Figure 5.1.
- **RTDS+FDNE ---** The internal system is modeled in RTDS in full EMT detail. The external system is represented only by a FDNE. The TSA solution part in Figure 5.1 is ignored. Constant sinusoidal current sources are used to keep the boundary condition at initial steady state.
- **RTDS+TSA ---** The internal system is modeled in RTDS in full EMT detail. The external system is represented only by the TSA solution shown in Figure 5.1. The FDNE part is ignored, and it is substituted with a simplified R-L||R equivalent that has the correct fundamental frequency impedance of the external network as seen from the boundary.
- **RTDS+SIMPLIFIED R-L||R EQUIVALENT ---** The internal system is modeled in RTDS in full EMT detail. The external system is represented by a simplified R-

L||R impedance and a constant sinusoidal voltage source, as shown in Figure 3.1. This is the common practice in most EMT simulations of HVDC systems.

7.2 Simulation of a 39 Bus AC System Using One Port Equivalent

The example considers the well known New England 39 Bus System [42], shown in Figure 7-1.

The system is first modeled in full detail on the RTDS with all transmission lines, generators, exciters and governors included in the EMT model. The distributed parameters of the transmission lines are estimated from the fundamental frequency admittance information using the approach of section 4.3. This full model is simulated in real time with a 50μs time-step on two RTDS racks, consisting of 29 parallel processors. This model provides the basis of validating the equivalents.

The part of the system which is modeled in full detail as the 'internal' system consists of Generator #38 and three transmission lines at the top right of Figure 7-1. Bus #26 forms the boundary bus. The remainder of the network ('external' system, containing 9 generators) is modeled as a one port (3 phase) equivalent. The internal and external systems together can now be run in real time with a 50μs time-step using only a single RTDS rack. For additional comparison, a stand alone pure TSA type simulation is conducted on a Windows XP based PC, using the TSAT software.

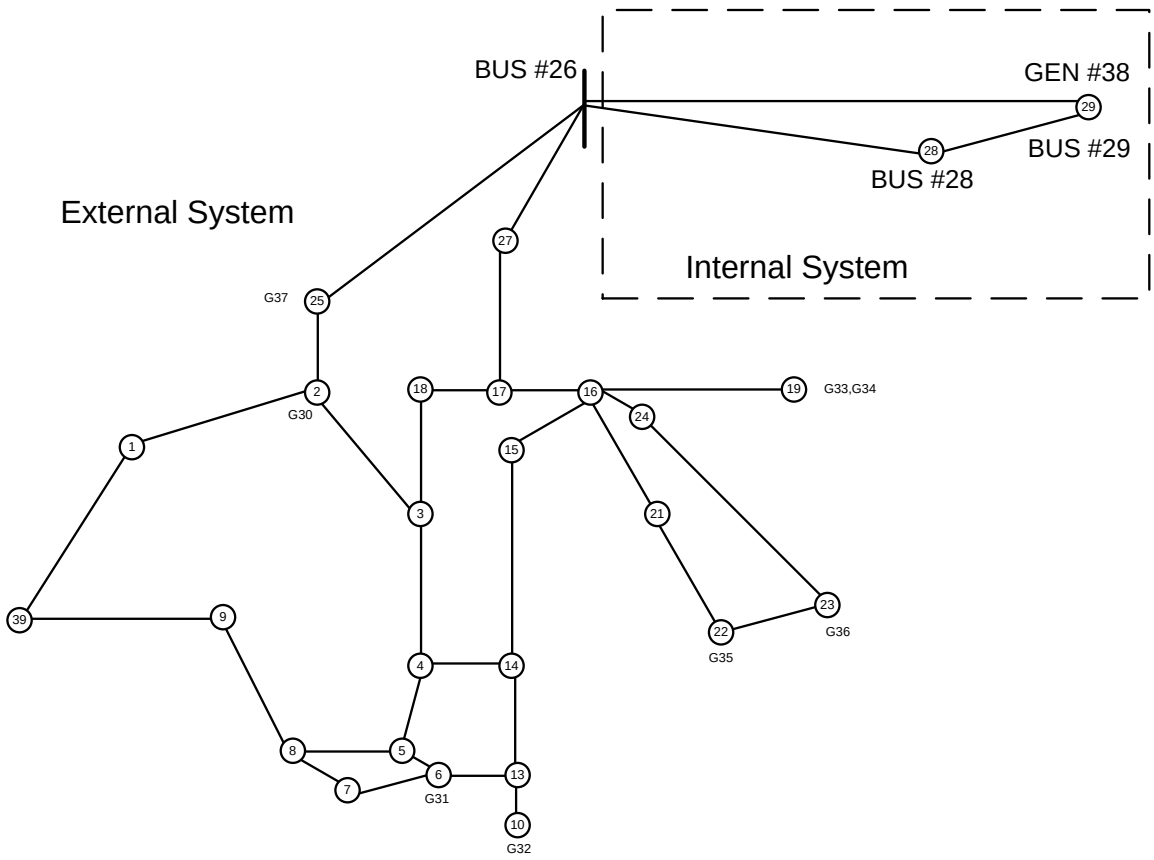

Figure 7-1 The 39 Bus Test System

A single phase to ground fault lasting 100 ms is applied at Bus #28. The generator rotor speed curves are shown in Figure 7-2 for the lone generator #38 in the internal network. Four curves are shown. The first is for a detailed EMT-only implementation (benchmark), the next for the proposed FDNE+TSA equivalent representation of the external system, the third for an equivalent that ignores the FDNE and only considers the TSA solution and the fourth for the pure TSA solution.

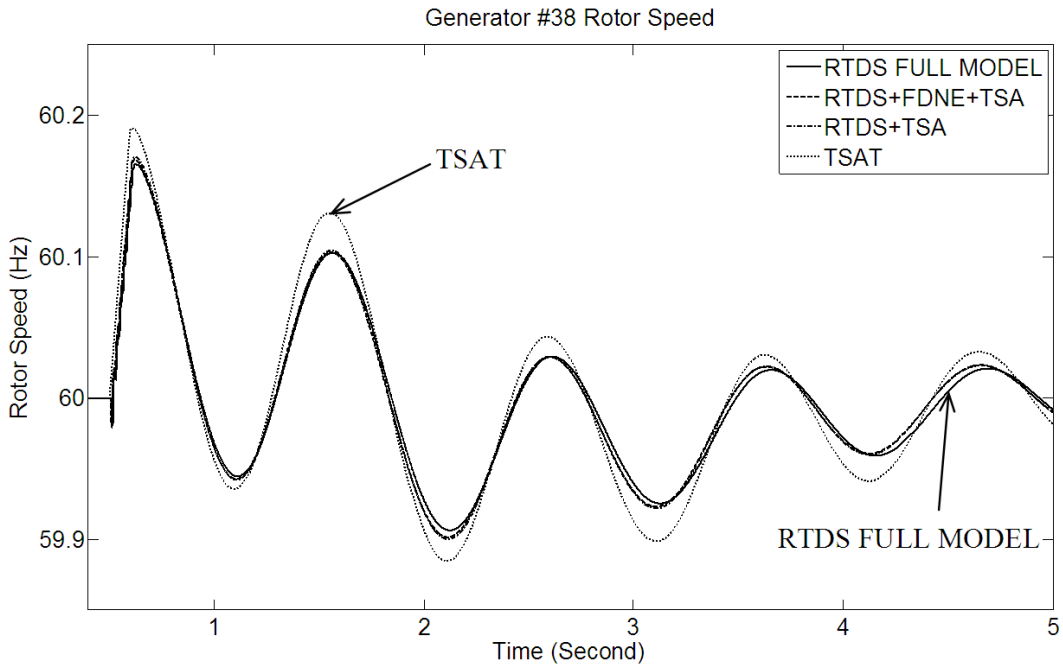

Figure 7-2 Generator #38 Rotor Speed Curves

(i. Full EMT model in RTDS, ii. with proposed FDNE+TSA equivalent, iii. The equivalent with only TSA representation, iv. A pure TSA solution)

Figure 7-2 shows that the benchmark result is closely matched by all the other approaches. However it is evident that the 'RTDS+FDNE+TSA' and the 'RTDS+TSA' curves are much closer to the 'RTDS FULL MODEL' curve in comparison with the swing curve obtained from the standalone TSAT simulation. This is to be expected, since the simulation using the proposed equivalent is a combination of EMT simulation and TSA simulation, and hence is more accurate than TSA simulation alone.

There is a very small difference between the 'RTDS+TSA' curve and the 'RTDS+FDNE+TSA' curve, which means the higher frequency network transients have no significant effect on the electromechanical dynamics of the AC system for this particular case and the benefit from using the FDNE might not be significant.

In the next test, a 100ms three-phase to ground fault is applied at Bus #28. The resultant transient waveform for the b-phase ac voltage of Bus #29 is shown in Figure 7-3, for three of the four different levels of modeling detail of the previous example. The TSA-only model is omitted as it only allows a fundamental frequency positive sequence phasor solution that cannot consider single phase instantaneous fault transients.

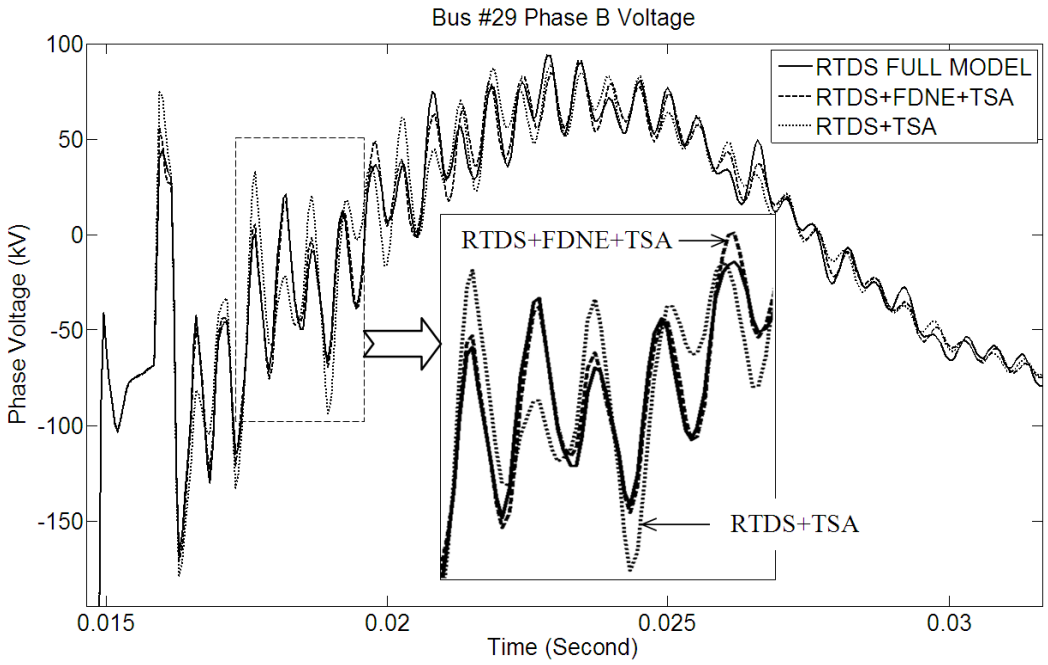

Figure 7-3 Bus #29 Phase B Voltage during a Three-Phase Fault at Bus #28

In Figure 7-3, the result with the proposed 'RTDS+FDNE+TSA' equivalent is seen to perform better than with the 'RTDS+TSA' equivalent.

7.3 Simulation of a 108 Bus AC System Using One Port Equivalent

A 108 bus system is used for testing the capability of the proposed equivalencing method of handling large AC system with reduced RTDS hardware. The system is

divided into two parts. A small part (2 generators, 4 transformers and 2 transmission lines) is modeled in full detail and connected to a one port equivalent which contains 19 generators. RTDS full model simulation is run on five RTDS racks, using a 50μs time-step. The RTDS simulation using the equivalent is run on one RTDS rack, with the detailed model using a 50μs time-step and the TSA part of the equivalent using a 1ms time-step. The standalone TSAT simulation uses a 10ms time-step. A single phase to ground fault is applied inside the small internal network for 100 ms, the rotor speed curve of Gen #241, which is in the internal system, is shown in Figure 7-4.

In this case, there is a difference between the results of RTDS and the standalone TSAT. However, the 'RTDS+FDNE+TSA' curve matches the benchmark 'RTDS FULL MODEL' curve far more closely than the 'TSAT' curve.

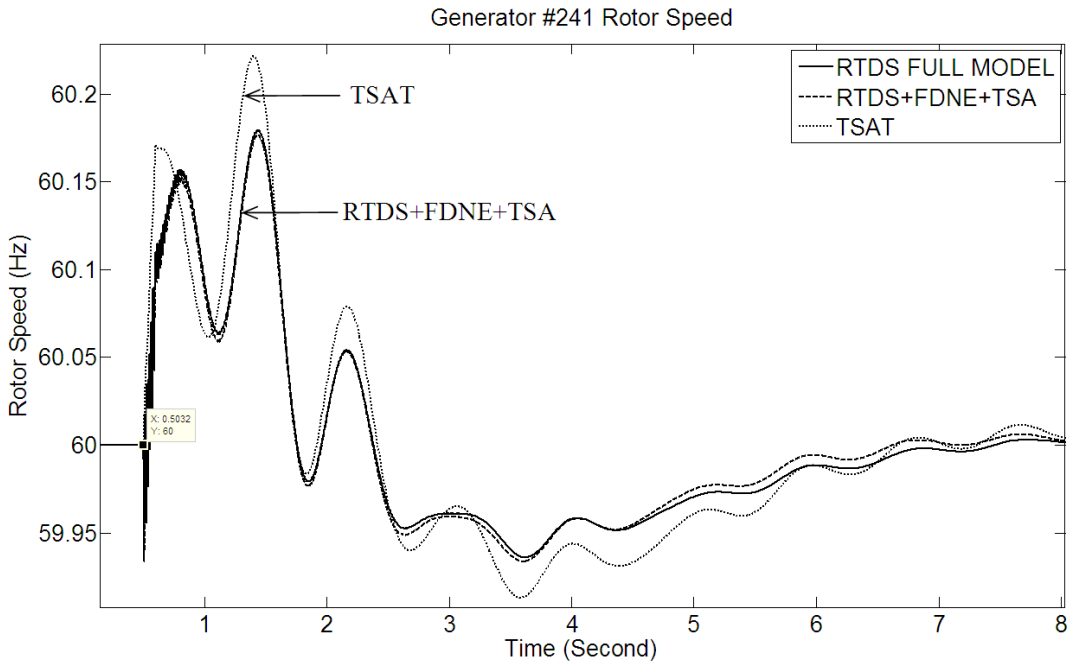

Figure 7-4 Generator #241 Rotor Speed

7.4 Simulation of a Multi In-Feed HVDC-AC System Using Two Port Equivalent

As seen in Figure 7-2, for the pure AC system simulation case, the 'RTDS+FDNE+TSA' solution is not significantly better than the 'RTDS+TSA' solution. This is because the higher frequency electromagnetic transients are quickly damped within about one cycle by the internal network. Hence the contribution made by the FDNE which represents the high frequency behaviour of the external network, is only marginal.

On the other hand, when power electronic devices such as HVDC or FACTS are connected in the internal network, the switching operations are repeated several times in a cycle and continuously generate higher frequency transients which propagate into the external network. Hence such systems are expected to require the FDNE for accurate results. As an example, consider the multi in-feed HVDC system configuration shown in Figure 7-5. The ac system has two HVDC inverters as terminating ends of the two HVDC links at boundary buses #3 and #8. The HVDC links form the 'internal' network and are modelled in full EMT detail. The 'external' ac network to the right of the boundary buses contains 33 buses and 9 generators. When modelled as an equivalent, it interfaces as a two port (2×3 phases) network at the two boundary buses.

As a representative example, the admittance between BUS #3 a-phase and BUS #8 b-phase (i.e. $-Y_{1,5}(f)$) is shown in Figure 7-6 as a function of frequency. This admittance is calculated from the power-flow data, and it is overlaid with the FDNE characteristic fitted up to an upper frequency of 3 kHz which is considered to be sufficiently accurate for an RTDS running with a 50μs time-step.

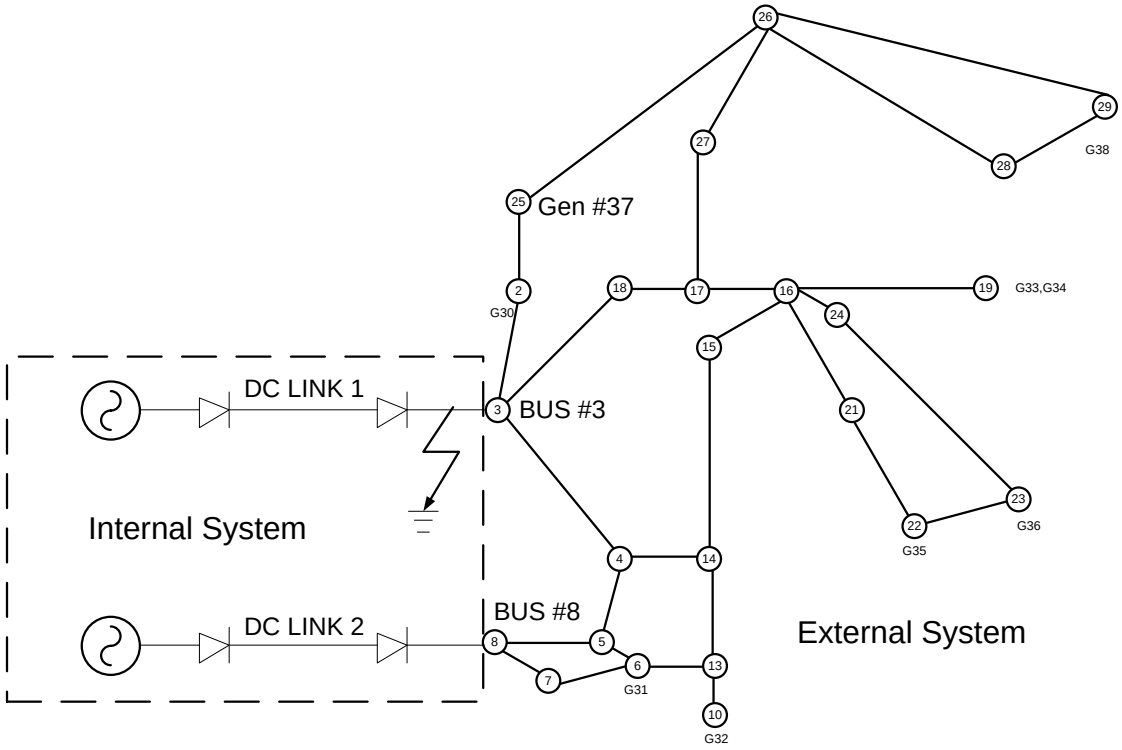

Figure 7-5 Multi In-Feed HVDC Test System

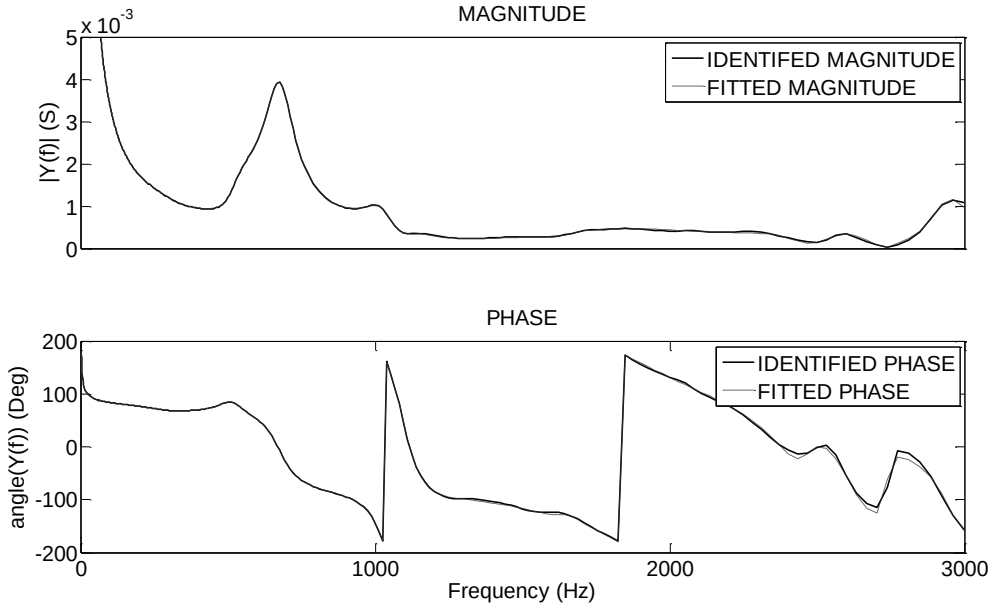

Figure 7-6 Multi-port FDNE Example

The RTDS full model simulation is run on two RTDS racks, using a 50μs time-step. The RTDS simulation using the equivalent is run on one RTDS rack, with both the detailed 'internal' system and the equivalent 'external' system running with the same 50μs time-step.

A single phase to ground fault is applied at Bus #3 for 100 ms, the bus voltage waveforms of Bus #3 and Bus #8 are shown in Figure 7-7 and Figure 7-8 respectively.

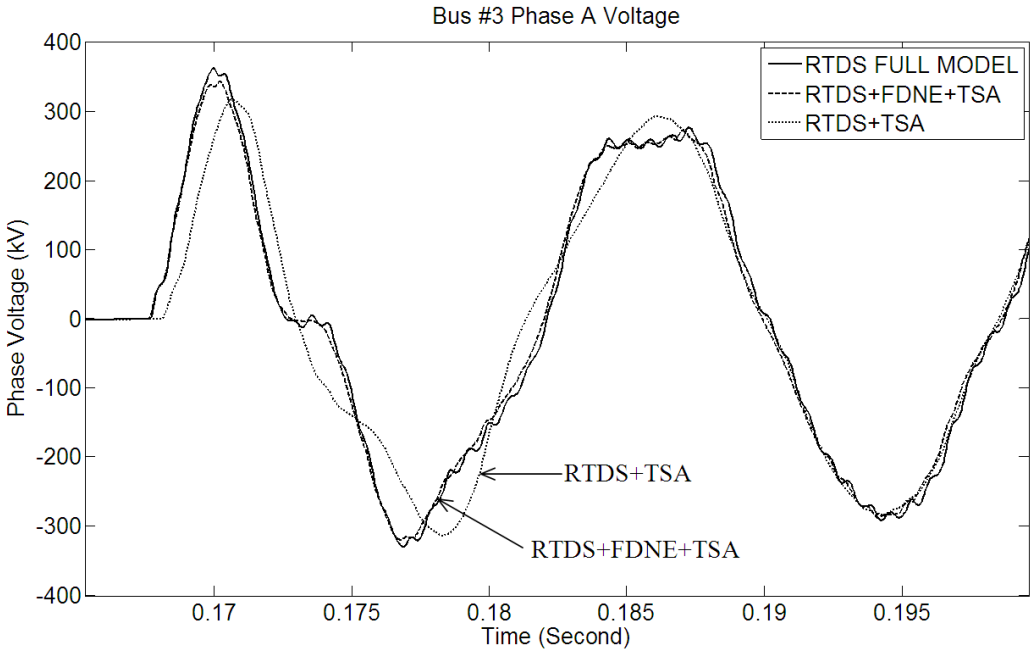

Figure 7-7 Bus #3 Phase A Voltage after Fault Clearing

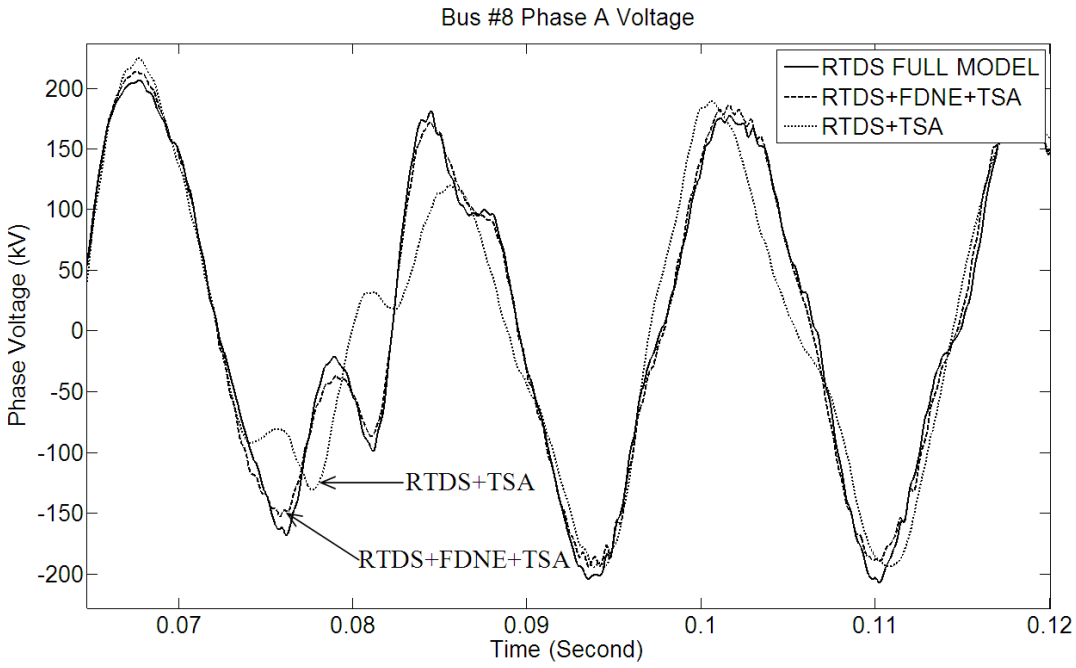

Figure 7-8 Bus #8 Phase A Voltage during Bus#3 Fault

In comparison with the benchmark (full EMT) solution, it is evident that the RTDS+FDNE+TSA model accurately simulates the transient voltages of both interface buses. This is considered a particularly challenging case to simulate because the boundary buses are the critical HVDC converter buses themselves, without an intermediate buffer network to separate the internal system and the external system. Earlier approaches [15] suggested inclusion of a detailed modeled portion of the ac network between the converter and the remote external system as a buffer. This was deemed necessary to obtain an accurate frequency dependent equivalent representation at the HVDC converter bus. Note that the HVDC converter produces harmonics and has a fast transient response, and hence requires an accurate representation over a wide range of frequencies. The approach presented in the report does not require the presence of the buffer network because it accurately models the high frequency behavior of the external network in the

developed FDNE Norton Equivalent. The inverter side DC voltage of DC Link 2 is shown in Figure 7-9.

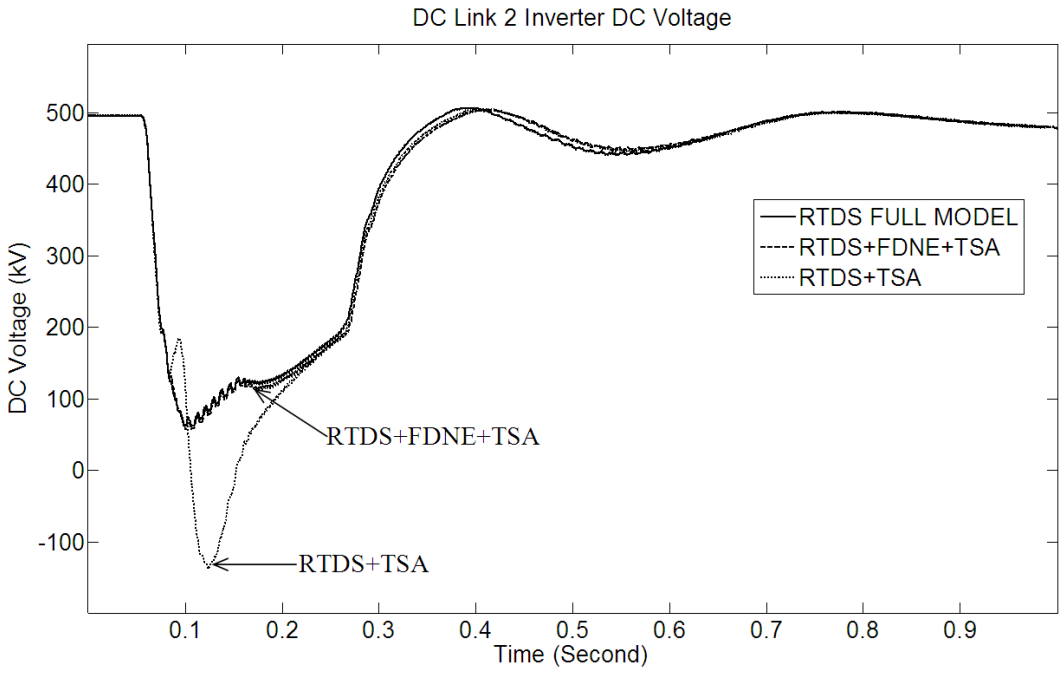

Figure 7-9 DC Link 2 Inverter Side DC Voltage

From Figure 7-7, Figure 7-8 and Figure 7-9, the effects of using the FDNE are clearly visible. The FDNE improves the electromagnetic transient simulation significantly, and since commutation failures are sensitive to the AC bus voltage transients, using a FDNE is advisable.

The TSA solution can be disabled by converting the TSA injection current source in Figure 5-1 to a constant magnitude and phase sinusoidal source. Doing so brings into focus the effect of neglecting the electromechanical dynamics on the HVDC system's simulation. Figure 7-10 plots the inverter dc voltage for the above fault on Bus #3 calculated using the three approaches that include the full benchmark solution, the solution using the proposed FDNE+TSA equivalent and the solution obtained by omitting

the TSA solution. As can be seen, the proposed approach gives a highly accurate solution which is close to the RTDS full model benchmark, whereas the solution with the TSA disabled is less accurate, with the recovery of dc voltage occurring approximately 40 ms too early.

The graphs in Figure 7-9 and Figure 7-10 clearly demonstrate the effectiveness of the equivalent that accurately models both the AC system electromechanical dynamics as well as the higher frequency electromagnetic transients.

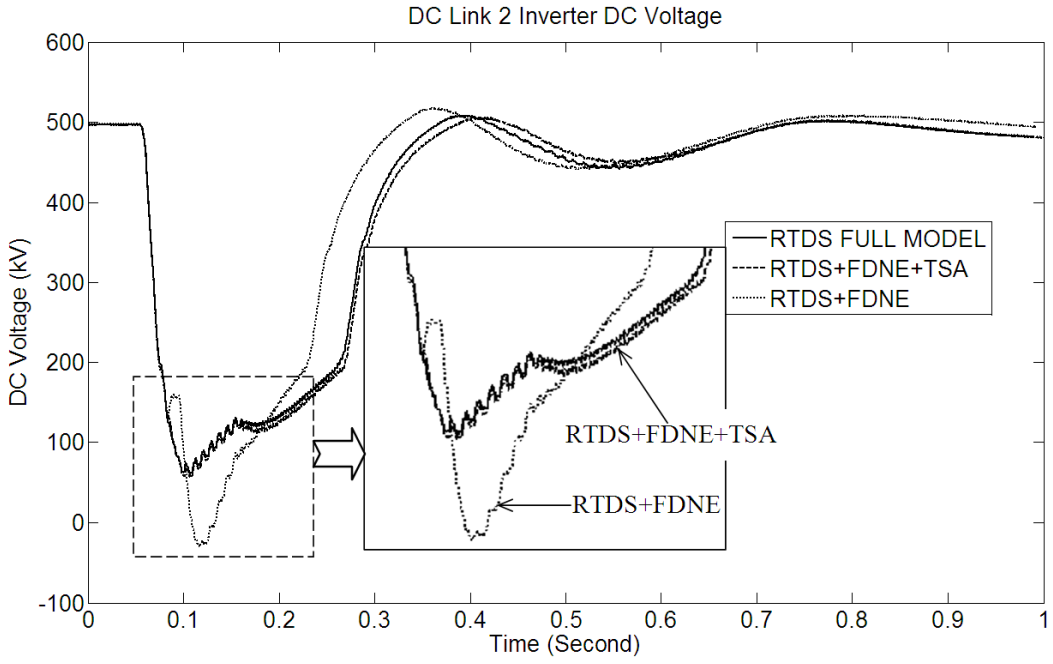

Figure 7-10 DC Link 2 Inverter Side DC Voltage: the Effect of TSA Solution

In another study, the resistance of the fault at Bus #3 is varied to assess the dependence fault severity on commutation failure (CF) which is the failure to transfer current from a conducting valve to the next valve in the conduction cycle. The fault resistance is initially set at infinity (no fault) for the first simulation run. It is then progressively decreased (i.e. fault severity is increased) until CF occurs at one or both of

the two dc inverters in the multi in-feed system. It is observed that as the resistance is reduced, CF is first observed in the inverter connected at Bus #3 (local inverter). As the fault severity is increased further, the remote inverter also fails commutation. Table 7.1 tabulates the critical fault resistance values obtained with the fully detailed benchmark solution as well as with various other equivalents. $R1$ represents the borderline value that just causes CF at both the local (DC Link 1) and remote (DC Link 2) converters, whereas $R2$ is the borderline resistance which just causes CF at DC Link 1 but not at DC Link 2. It can be clearly seen that the only equivalents whose results accurately match the benchmark model results are those that include the FDNE representation. When FDNE is ignored, highly inaccurate values of $R1$ are obtained (shaded in Table 7.1).

It is clear that the frequency dependent characteristic of the AC system plays a critical role in the DC system commutation failure behaviors; hence the conventional fundamental frequency network equivalent is not suitable for commutation failure studies. This case shows that a FDNE can greatly improve the accuracy of the simulation.

Table 7.1 Commutation Failure Simulation Results

Simulation Setup	$R1\ (\Omega)$	$R2\ (\Omega)$
RTDS FULL MODEL (benchmark)	**40**	**72**
RTDS+FDNE+TSA	41	77
RTDS+FDNE	40	78
RTDS+TSA	84	83
RTDS+SIMPLIFIED R-L||R EQUIVALENT	83	82

$R1$ --- Minimum Fault Resistance below which Commutation Failure occurs on DC Link 2

$R2$ --- Maximum Fault Resistance above which Commutation Failure does not occur on DC Link 1

This can be further demonstrated by simulating an intermediate 100 ms single phase to ground fault at Bus #3. The fault resistance is set to be 60 Ohms. The inverter side DC voltage of DC Link 2 is shown in Figure 7-11. The generator rotor speed of generator #37 is shown in Figure 7-12.

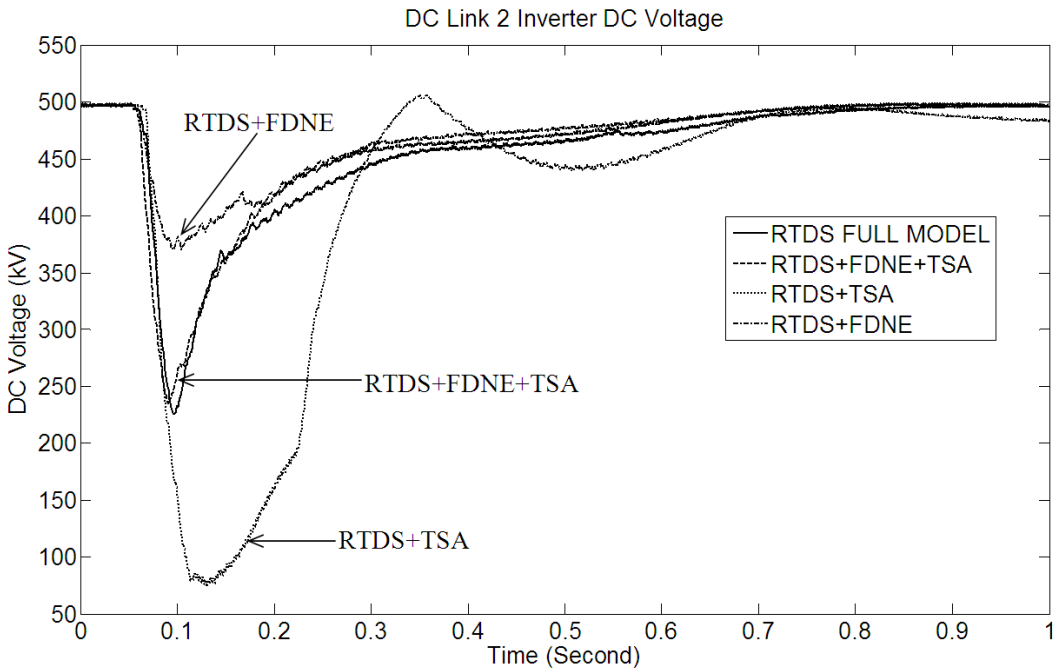

Figure 7-11 DC Link 2 Inverter Side DC Voltage, Intermediate Fault

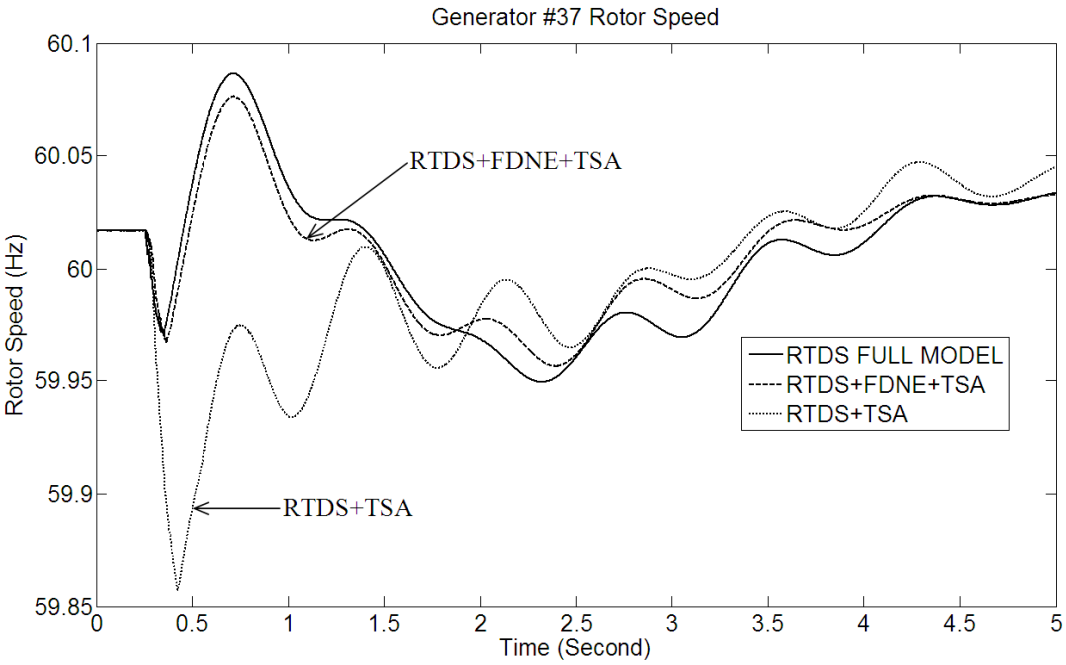

Figure 7-12 Generator #37 Rotor Speed, Intermediate Fault

In this case, it is only when both the FDNE and the TSA of the equivalent are included in the simulation that good simulation results are obtained. The example clearly shows the advantage of the proposed multi-port equivalent which was connected directly at the converter buses on which the faults were applied. Previous approaches with simpler equivalents would have required the equivalent to be more remotely located with additional intermediate buses included in the detailed EMT model. From Figure 7-5 it is clear that this would have required the detailed EMT simulation of at least five additional transmission lines and local bus components, and the equivalent would become a 5 port equivalent, which is very difficult to implement as discussed in section 6.3.2.

7.5 Simulation of a 470 Bus AC System Using Multiple Multi-port Equivalents

A 470 bus system is used for further demonstrating the capability of the proposed equivalencing method of handling large AC system with reduced RTDS hardware. The system has a 345kV network, which is considered as the 'internal' system and is modeled in full EMT detail (62 buses, 17 generators). It feeds lower voltage sub-networks of 161kV, which are considered as the external system and modeled using 11 equivalents, totaling the remaining 408 buses and 28 generators. The 11 equivalents include 1 three-port, 4 two-port and 6 one-port equivalents. The RTDS simulation using equivalents is run on six RTDS racks. A full EMT model on the RTDS would need more than twenty racks to run, and currently there are only two real time digital power system simulation systems in the world which have the capability of simulating such a large system in full EMT detail. The structures of the 470 bus system and its simulation model are shown in Figure 7-13 and Figure 7-14 respectively.

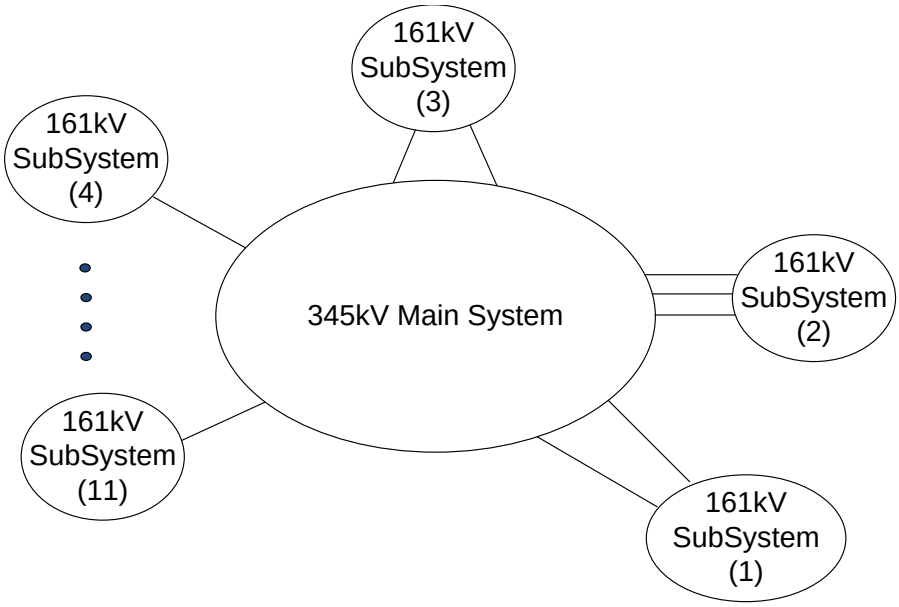

Figure 7-13 Structure of the 470 Bus System

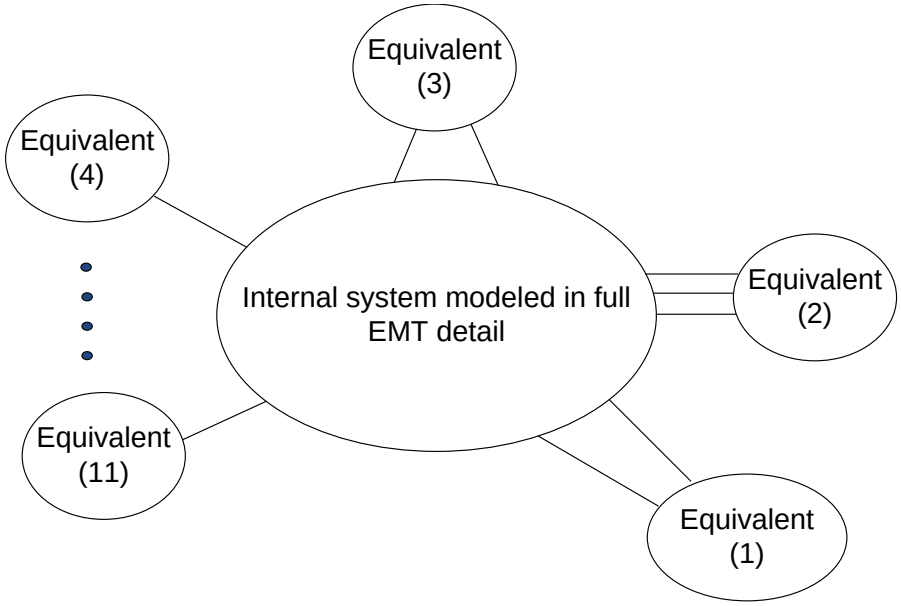

Figure 7-14 Structure of Simulation Model of the 470 Bus System

Both the detailed model and the equivalents use a 50μs time-step. For comparison, a stand alone pure TSA type simulation is also conducted using the TSAT software and a time-step of 0.01s. Due to the large size of the system, the hardware available to the author was not adequate for conducting a full EMT solution for comparison (which has been done for the 108 bus system as described in section 7.3).

Figure 7-15 and Figure 7-16 show the oscillations in rotor speed following a bus to ground fault in the internal system for two generators - Gen #3212 (which is in the 'internal' system and modeled in full detail) and Gen #230 (which is represented in the equivalent).

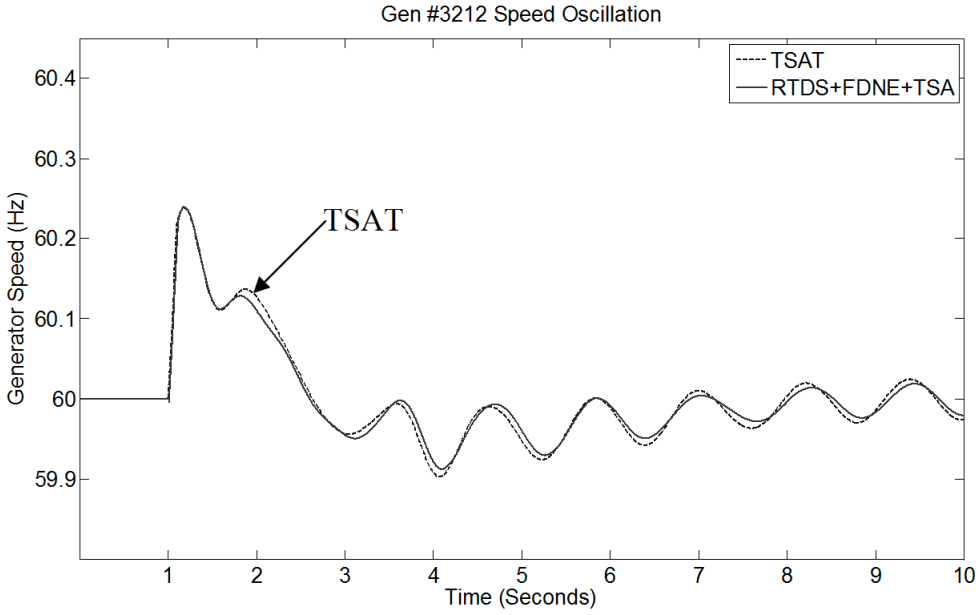

Figure 7-15 Generator #3212 Rotor Speed

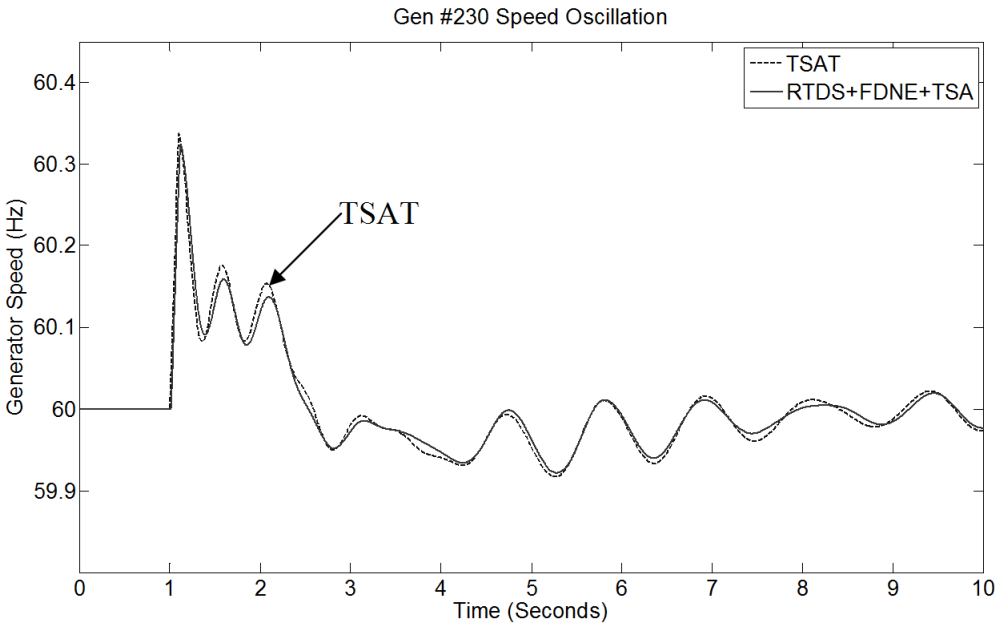

Figure 7-16 Generator #230 Rotor Speed

It can be seen that with the equivalents, the electromechanical transients of the system are accurately simulated in real time and agree with the TSA only simulation.

This case also demonstrates some features of the proposed equivalencing method:

- Three-port and two-port equivalents have been deployed in this case.
- Eleven equivalents have been deployed in the same simulation, they have been distributed on different racks and run in real-time in parallel. The proposed equivalent is scalable: when really large system needed to be modeled, normally it is possible to divide the external system into sub external systems, and distribute the computation on multiple racks.

8 Summary and Future Work

This chapter summarizes the report, and future research works are proposed.

8.1 Summary

This thesis deals with the equivalencing method for real time digital power system simulators. Since the introduction of digital time domain simulation methods for power system analysis, the equivalencing method has been an important topic. This is due to the extremely large scale of power networks, the complexity of power system components, and relatively limited computation resources.

RTDS is a real-time implementation of the EMT type simulation algorithm. With custom high performance computation hardware, the EMT simulation is performed in a speed that is synchronized with the real world clock. The tool makes it possible to connect real controllers to digital simulation models in closed loops, and has been widely used by manufacturers, utilities and research institutes etc. By utilizing the travelling wave characteristic of transmission lines, the RTDS simulator is scalable, i.e. large power system can be simulated in real-time by using more computation hardware. However, real power systems are so large that practically it is only possible to model a small portion of the power system, which is of main interest, in full detail (internal system), and the rest of the system needs to be modeled as an equivalent (external system).

The thesis proposed an accurate wide-band two part multi-port equivalent for real time digital simulators. The equivalent was developed based on such assumptions that most high frequency electromagnetic characteristics of the external system can be represented by a linear L-C-R network; and on the other hand, low frequency electromechanical

behaviours of a large power system can be represented by a TSA type, nonlinear, positive sequence, phasor domain model.

The high frequency part (FDNE) of the proposed two part equivalent was constructed in three steps:

(1) The frequency domain characteristics of the large L-C-R external network were identified. A practical method was proposed to obtain such characteristics from powerflow data, which is widely available in the industry.

(2) The identified frequency domain characteristics were fitted with a multi-port rational function. The Vector Fitting method was used in this step. The fitting errors introduced in this step may cause instabilities during the time-domain simulation, mainly due to a loss of passivity of the fitted rational function form. A heuristic method was proposed to mitigate the problem.

(3) The multi-port rational function was modeled in the RTDS simulation.

In the low frequency electromechanical part of the proposed two part equivalent. The number of power system components represented in the simulation was not reduced. Instead all the components in the external system were represented by a full TSA type, nonlinear, positive sequence, phasor domain model. The TSA algorithm was implemented on the RTDS platform to simulate the external system model in parallel with the detailed EMT simulation of the internal system. To make the TSA simulation in synchronization with the hard real-time RTDS simulation, a modified TSA algorithm was implemented. In this algorithm, a relatively smaller (compared to conventional TSA algorithms) time-step was used to eliminate the necessity of using an iterative TSA network solution. By doing this, the computation time of each time-step was fixed and

the TSA simulation could always remain synchronous with the RTDS (EMT) simulation, i.e., with the real world clock. This thesis also presented a new method of interfacing the TSA solution (positive sequence, phasor domain) and the EMT solution (three-phase, instantaneous). Recognizing that it is the real power that is responsible for rotor accelerations, the method is based on the energy balance concept. It is simple and produces satisfying results, as it can take account of not only fundamental frequency real power, but also real power resulting from waveform distortions in the internal system.

Other implementation issues of the proposed method were discussed in this thesis, such as the structures of the simulation model, the limiting factors of the external system model, the TSA network solution, the modelling of power system components in the TSA part, and utilization of the distributed computation platform of RTDS etc.

A few examples with different system sizes and complexities were presented in this thesis. For each example, various different equivalent types were tried out and the results were compared with a 'benchmark' solution based on a pure EMT solution method whereas possible. The equivalents constructed with the proposed method worked uniformly well in these examples.

The multi-infeed HVDC example showed that the proposed equivalent is capable of reproducing the essential electromagnetic response as well as the essential electromechanical response of the external system. It was clearly shown that both of these aspects were important for studies of such systems. Additionally, the accuracy of the FDNE permits the boundary to be conveniently located at the converter buses and prevents the need for including more components in full EMT detail.

The 470 bus AC system simulation example showed multiple equivalents being used in one simulation. The 345kV main system was modeled in full EMT detail and the model was distributed on six RTDS racks by utilizing the travelling wave characteristic of transmission lines. The 161kV subsystems were modelled as eleven equivalents (from one port to three ports). They are also distributed on the six RTDS racks and connected to different interconnection points of the 345kV main system. The results showed that the electromechanical transients in both the internal system and the external system were well represented. In this example, the computation hardware requirement is reduced by about 75% by using the proposed equivalent.

The approach in the thesis results in a fast algorithm that was implemented on a real time simulator with considerably reduced hardware requirements than would be required for a fully detailed model.

8.2 Future Work

In order to expand the capability of the proposed equivalencing method, the following research works are proposed:

1. In this thesis, equivalents with up to three 3-phase ports were presented. Equivalents with more ports may be needed for simulation of complex mesh power network. As discussed in subsection 6.3.2, there are two challenges in making equivalents with higher number of ports. The first one is to maintain the passivity of the FDNE. The current available passivity enforcement methods can only mitigate small passivity violations. With additional ports, a more robust method may be necessary. The other challenge is that the computation resources needed for the FDNE increase as quadratic functions of the number of ports. It should be

noticed that since the transmission lines of the external system were not explicitly modeled in the EMT simulation, the travelling wave characteristic was not utilized, and thus the FDNE can only be processed on one RTDS rack. Hence the number of ports of the FDNE is limited by the computation power of one RTDS rack. Additional research may be done in this area to make the FDNE model distributable or simplified.

2. The TSA part of the proposed equivalent is not distributable either. It was estimated that with the current RTDS hardware, a single equivalent could represent a power system of up to about one thousand buses and one hundred generators. One RTDS rack would not be able to handle the TSA simulation of a system larger than this. For simulating really large power system with tens of thousands buses and generators on one rack, the size of the external system may need to be reduced first. The possibility of incorporating traditional TSA type dynamic reduction techniques with the proposed equivalencing method should be investigated. Another possibility is to make the TSA part of the equivalent also distributable.
3. In this research, network disturbance (short circuit fault, topology change etc.) could only be applied in the internal system during the simulation, only control disturbances (step change of the AVR reference, loss of PSS etc.) could be applied in the external system. The capability of simulating network disturbances in the external system is desirable, especially disturbances far away from the internal system. This could be an area for future research.

References

[1] P. Forsyth, R. Kuffel, R. Wierckx, Jin-Boo Choo, Yong-Beum Yoon, and Tae-Kyun Kim, "Comparison of Transient Stability Analysis and Large-Scale Real Time Digital Simulation", *Power Tech Proceedings, 2001 IEEE Porto.*

[2] P. G. McLaren, R. Kuffel, R. Wierckx, J. Giesbrecht, and L. Arendt, "A Real Time Digital Simulator For Testing Relays", *IEEE Trans on Power Delivery, vol.7, No.1, pp.207-213, Jan. 1992.*

[3] IEEE/CIGRE Joint Task Force on Stability Terms and Definitions, "Definition and Classification of Power System Stability", *IEEE Trans on Power Systems, vol.19, No.2, pp.1387-1401, May 2004.*

[4] J. Arrillaga and N. Watson, *Power Systems Electromagnetic Transients Simulation*, The Institution of Engineering and Technology, London, 2002.

[5] L. Wang, M. Klein, S. Yirga and P. Kundur, "Dynamic Reduction of Large Power System for Stability Studies", *IEEE Trans. Power Systems, vol.12, No.2,pp.889-895, May 1997.*

[6] R. J. Galarza, J. H. Chow, W. W. Price, A. W. Hargrave, and P. M. Hirsch, "Aggregation of Exciter Models for Constructing Power System Dynamic Equivalents", *IEEE Trans. Power Systems, vol.13, No.3,pp.782-788, Aug. 1998.*

[7] R. Nath, S. S. Lamba, K. S. Prakasa Rao, "Coherency Based System Decomposition into Study and External Areas Using Weak Coupling", *IEEE Trans on Power Apparatus and systems, vol. PAS-104, No.6, pp.1443-1449, Jun. 1985.*

[8] J. R. Winkelman, J. H. Chow, B. C. Bowler, B. Avramovic, and P. V. Kokotovic, "An Analysis of Interarea Dynamics of Multi-Machine Systems", *IEEE Trans on Power Apparatus and systems, vol. PAS-100, No.2, pp.754-763, Feb. 1981.*

[9] R. Podmore, "Identification of Coherent Generators for Dynamic Equivalents", *IEEE Trans on Power Apparatus and systems, vol. PAS-97, No.4, pp.1344-1354, Jul. 1978.*

[10] A. S. Morched, J. H. Ottevangers, L. Marti, "Multi-Port Frequency Dependent Network Equivalents for the EMTP", *IEEE Trans on Power Delivery, vol.8, No.3, pp.1402-1412, Oct. 1993.*

[11] N. R. Watson and J. Arrillaga, "Frequency-Dependent A.C. System Equivalents for Harmonic Studies and Transient Convertor Simulation", *IEEE Trans on Power Delivery, vol.3, No.3,pp.1196-1203, Jul. 1988.*

[12] A. Abur and H. Singh, "Time Domain Modeling of External System for Electromagnetic Transients Programs", *IEEE Trans on Power Systems, vol.8, No.2, pp.671-679, May 1993.*

[13] B. Gustavsen and A. Semlyen, "Rational Approximation of Frequency Domain Responses by Vector Fitting", *IEEE Trans on Power Delivery, vol.14, No.3,pp.1052-1061, Jul. 1999.*

[14] M. D. Heffernan, K. S. Turner, J. Arrillaga and C. P. Arnold, "Computation of AC-DC System Disturbances, Parts I, II and III", *IEEE Trans on Power Apparatus and systems, vol. PAS-100, No.11, pp. 4341-4363, Nov. 1981.*

[15] J. Reeve and R. Adapa, “A New Approach to Dynamic Analysis of AC Network Incorporating Detailed Modeling of DC Systems, Part I and II”, *IEEE Trans on Power Delivery, vol.3, No.4, pp.2005-2018, Oct. 1988.*

[16] G. W. J. Anderson, N. R. Watson, C. P. Arnold and J. Arrillaga, “A New Hybrid Algorithm for Analysis of HVDC and FACTS Systems”, *Energy Management and Power Delivery, 1995. Proceedings of EMPD '95., 1995 International Conference on.*

[17] H. Su, K. W. Chan, L. A. Snider and J-C. Soumagne, “Advancements on the Integration of Electromagnetic Transients Simulator and Transient Stability Simulator”, *International Conference on Power Systems Transients Montreal, Jun. 19-23, 2005.*

[18] X. Wang, P. Wilson, D. Woodford, “Interfacing Transient Stability Program to EMTDC Program”, *Power System Technology, 2002. Proceedings. PowerCon 2002. International Conference on.*

[19] A. O. Soysal and A. Semlyen, “Practical Transfer Function Estimation and its Application to Wide Frequency Range Representation of Transformers”, *IEEE Trans on Power Delivery, vol.8, No.3, pp.1627-1637, Jul. 1993.*

[20] A. M. Gole, A. Keri, C. Kwankpa, E. W. Gunther, H. W. Dommel, I. Hassan, J. R. Marti, J. A. Martinez, K. G. Fehrle, L. Tang, M. F. McGranaghan, O. B. Nayak, P. F. Ribeiro, R. Iravani, and R. Lasseter, “Guidelines for modeling power electronics in electric power engineering applications”, *IEEE Trans on Power Delivery, vol.12, No.1, pp.505-514, Jan. 1997.*

[21] P. Kundur, *Power System Stability and Control*, McGraw-Hill, New York, 1994.

[22] H.W. Dommel, *Electromagnetic Transients Program Reference Manual (EMTP Theory Book)*. Portland, OR, U.S.A.: BPA, 1986.

[23] H. W. Dommel, "Digital Computer Solution of Electromagnetic Transients in Single and Multi-phase Networks", *IEEE Trans on Power Apparatus and systems, vol. PAS-88, No.4, pp.388-399, Apr. 1969.*

[24] A.M. Gole, *Power Systems Transient Simulation*, Course Notes, University of Manitoba, 2005.

[25] N. Balbanian and T. Bickert, *Linear Network Theory, Analysis, Properties, Design and Synthesis*, Matrix Publishers, Boston, 1981.

[26] L. M. Wedepohl, "Application of Matrix Methods to the Solution of Travelling-Wave Phenomena in Polyphase Systems", *Proc. IEE, vol. 110, No.12, Dec. 1963.*

[27] A. M. Gole, R. W. Menzies, H. M. Turanli, and D. A. Woodford, "Improved Interfacing of Electrical Machine Models to Electromagnetic Transients Programs", *IEEE Trans on Power Apparatus and systems, vol. PAS-103, No.9, pp.2446-2451, Sep. 1984.*

[28] W. H. Press, S. A. Teukolsky, W. T. Vetterling and B. P. Flannery, *Numerical Recipes, the Art of Scientific Computing*, Cambridge University Press, Cambridge, 1986.

[29] M. Meisingset and A.M. Gole, "Control of capacitor commutated converters in long cable HVDC-transmission", *IEEE PES Winter Meeting, Jan. 28-31, 2001, Columbus, Ohio, USA, Vol. 2, pp 962-967.*

[30] CIGRE WG 13-05 III, "Transmission Line Representation for Energization and Re-energization Studies with Complex Feeding Networks", *Electra, vol.62, pp.45-78, Jan. 1979.*

[31] Åke Björck, *Numerical Methods for Least Squares Problems*, SIAM, Philadelphia, 1996.

[32] C. D. Meyer, *Matrix analysis and applied linear algebra*, Society for Industrial and Applied Mathematics, Philadelphia, 2000.

[33] L. M. Wedepohl, *The Theory of Natural Modes in Multiconductor Transmission Systems*, Course Notes, University of Manitoba, 2002.

[34] H. Saadat, *Power System Analysis*, 2nd Edition, McGraw-Hill, New York, 2002.

[35] *PSS/E 30 Program Operation Manual Volume I*, Power Technologies Inc., Schenectady, 2004.

[36] B. Gustavsen and A. Semlyen, "Enforcing Passivity for Admittance Matrices Approximated by Rational Functions", *IEEE Trans on Power Systems, vol.16, No.1,pp.97-104, Feb. 2001.*

[37] *RTDS Manual Set*, RTDS Technologies Inc., Winnipeg, 2006.

[38] W. F. Tinney, V. Brandwajn, S. M. Chan, "Sparse Vector Methods", *IEEE Trans on Power Apparatus and systems, vol. PAS-104, No.2, pp.295-301, Feb. 1985.*

[39] MATLAB® *the Language of Technical Computing*, 5th Printing, *The* MathWorks Inc., Natick, 2002.

[40] L. Wang and K. Morison, "Implementation of online security assessment - tools for reducing the risk of blackouts", *IEEE Power & Energy Magazine, vol.4, No.5, pp.46-59, Sep. 2006.*

[41] *TSAT* User *& Model Manual*, Powertech Labs Inc., Surrey, 2006.

[42] M. A. Pai, *Energy Function Analysis for Power System Stability,* KluwerAcademic Publishers, 1989.

Appendix 1

The Frequency Dependant Characteristics of a Transmission Line and its Simplified Model

Considering an ideally transposed three phase transmission line which has the following parameters:

- Line length: $l = 100km$
- Conductor DC resistance: $r_c = 0.03\Omega / km$
- Ground resistance: $\rho_e = 100\Omega \cdot m$
- Number of conductors per phase: $n = 1$
- Line space: $D = 10m$
- Conductor radius: $r = 0.03m$
- Line to ground height: $h = 30m$
- Nominal frequency: $f_0 = 60Hz,\ \omega_0 = 314.16\ rads/s$

In the power flow data, it will be described in the following parameters.

- Positive sequence resistance: $R_+ = 3.045\,\Omega$
- Positive sequence reactance: $X_+ = 40.669\,\Omega$
- Positive sequence shunt Susceptance: $B_+ = 3.618 \times 10^{-4}\ Si$
- Zero sequence resistance: $R_0 = 19.649\,\Omega$
- Zero sequence reactance: $X_0 = 143.431\,\Omega$
- Zero sequence shunt Susceptance: $B_0 = 1.872 \times 10^{-4}\ Si$

Using the parameters in the power flow data, a simplified model of the transmission line can be constructed, which is a combination of distributed lossless transmission lines and lumped resistors. It has exactly the same parameters as the original transmission line at 60 Hz. In the following figures, the frequency dependant characteristics of the original transmission line and the simplified model are compared. The frequency dependant characteristics of the original transmission line are derived by using the accurate two ports equations.

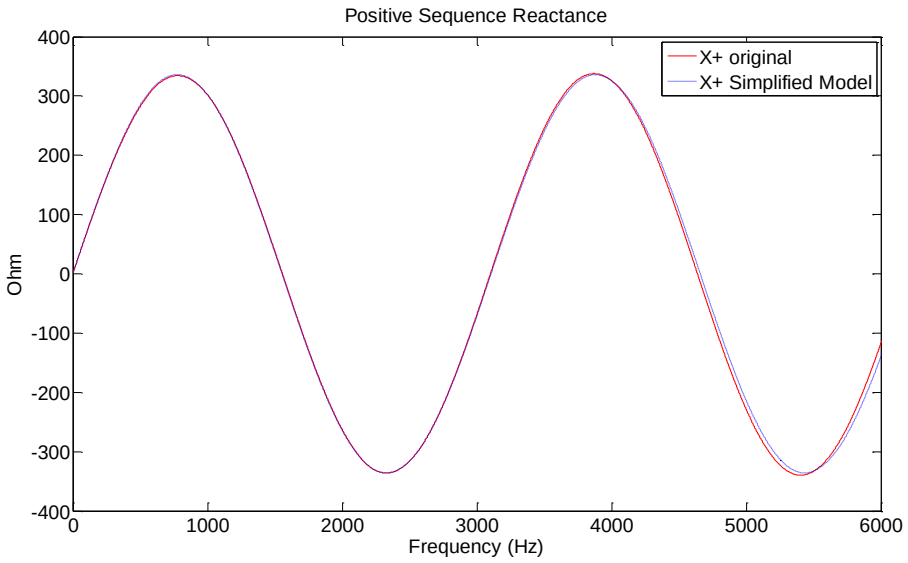

Figure A1.1 Positive Sequence Reactance

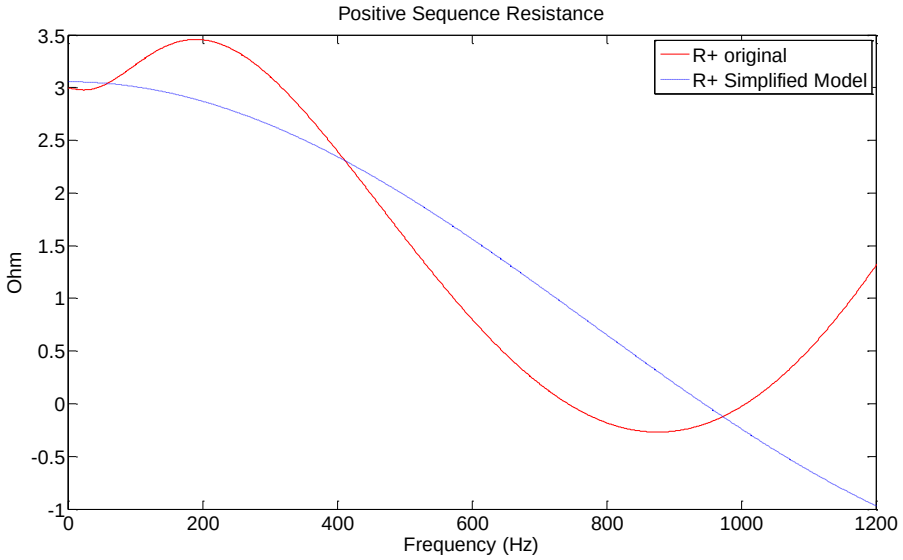

Figure A1.2 Positive Sequence Resistance

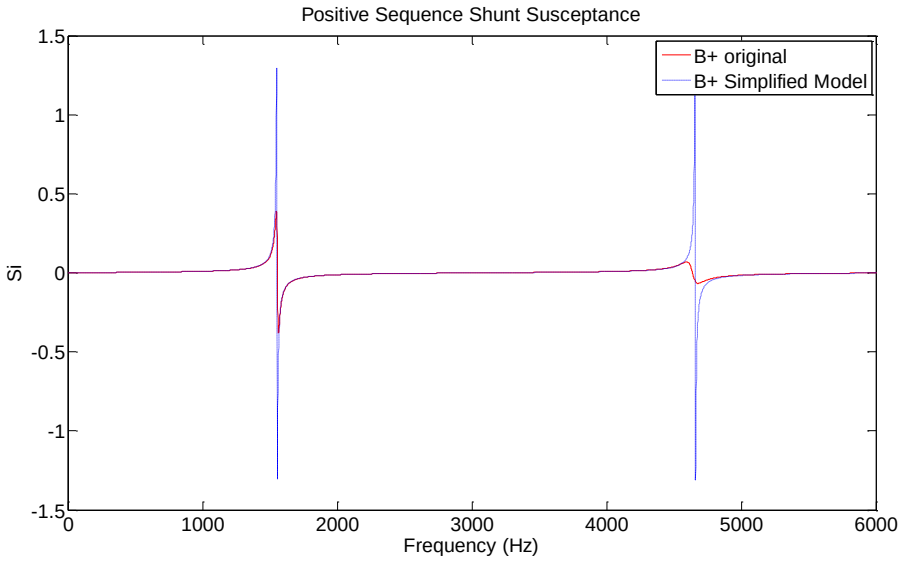

Figure A1.3 Positive Sequence Shunt Susceptance

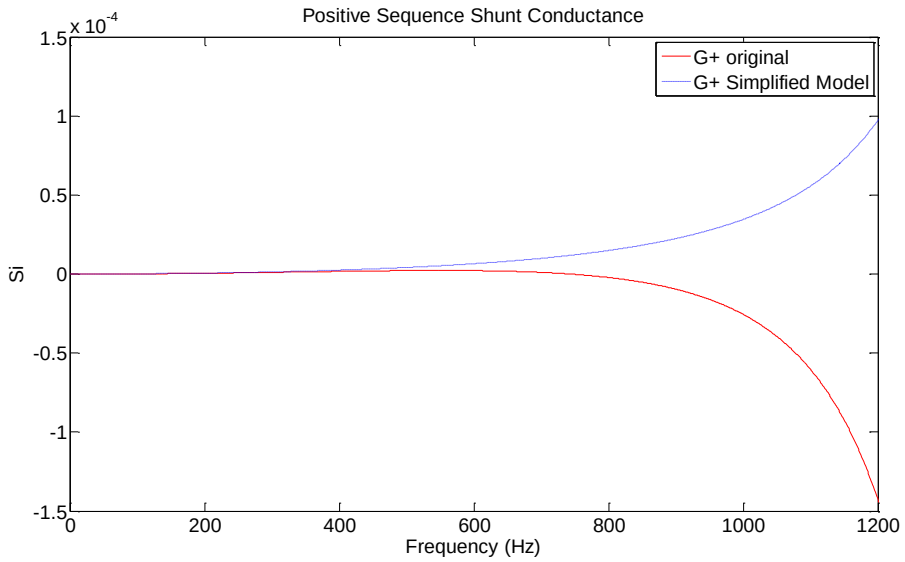

Figure A1.4 Positive Sequence Shunt Conductance

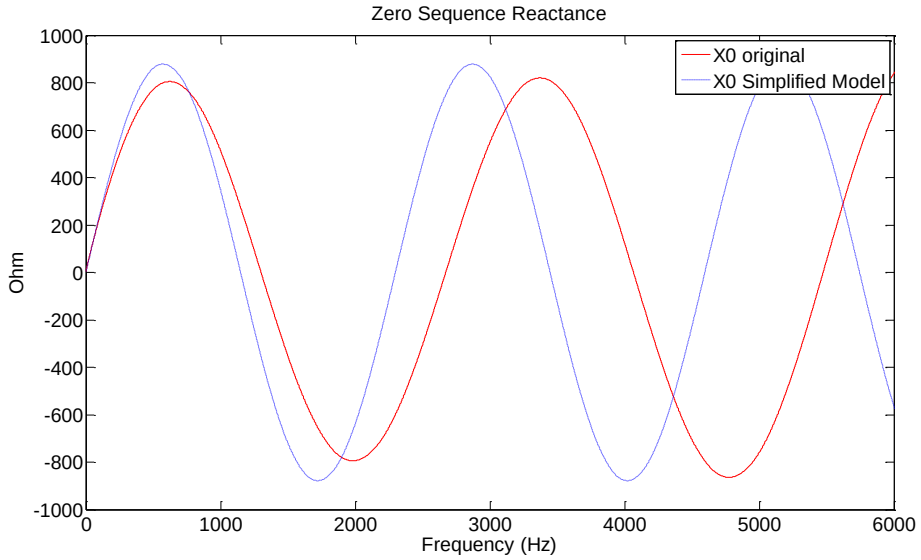

Figure A1.5 Zero Sequence Reactance

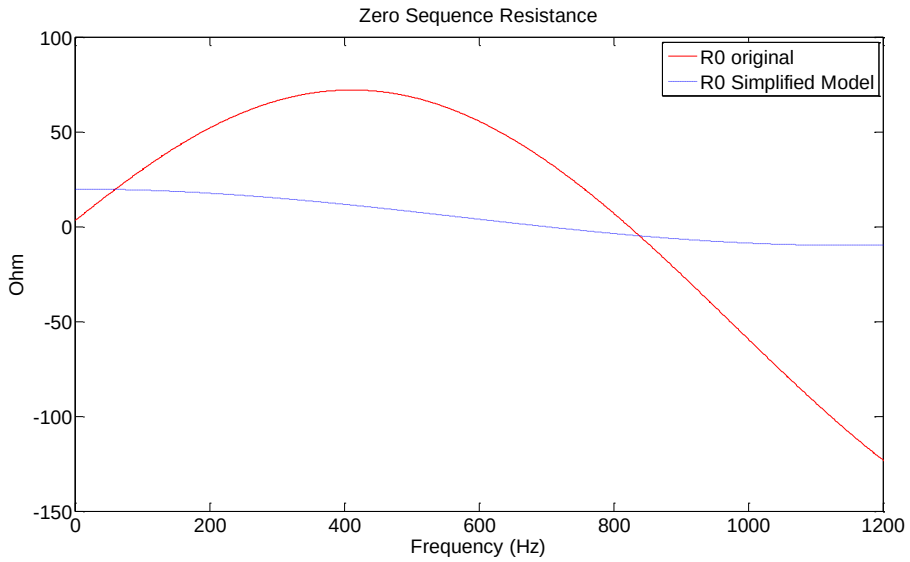

Figure A1.6 Zero Sequence Resistance

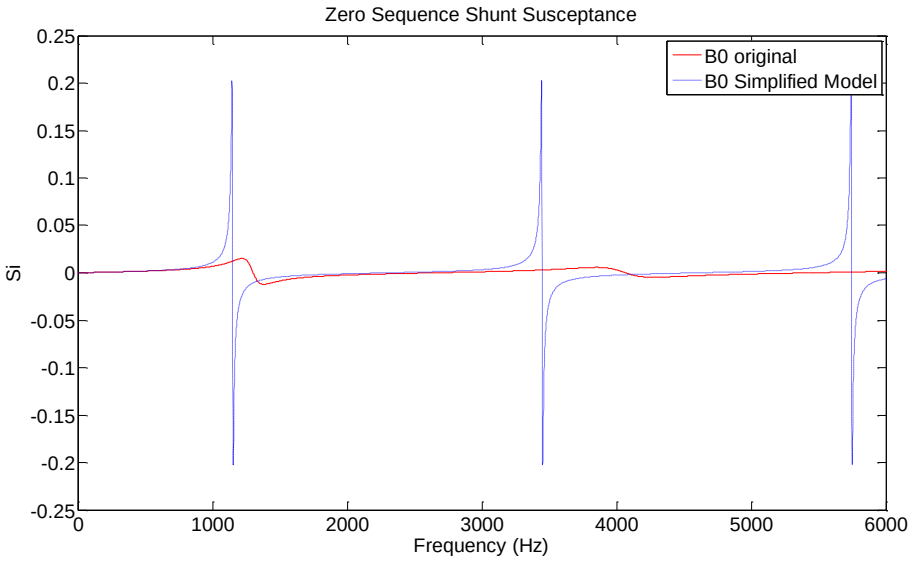

Figure A1.7 Zero Sequence Shunt Susceptance

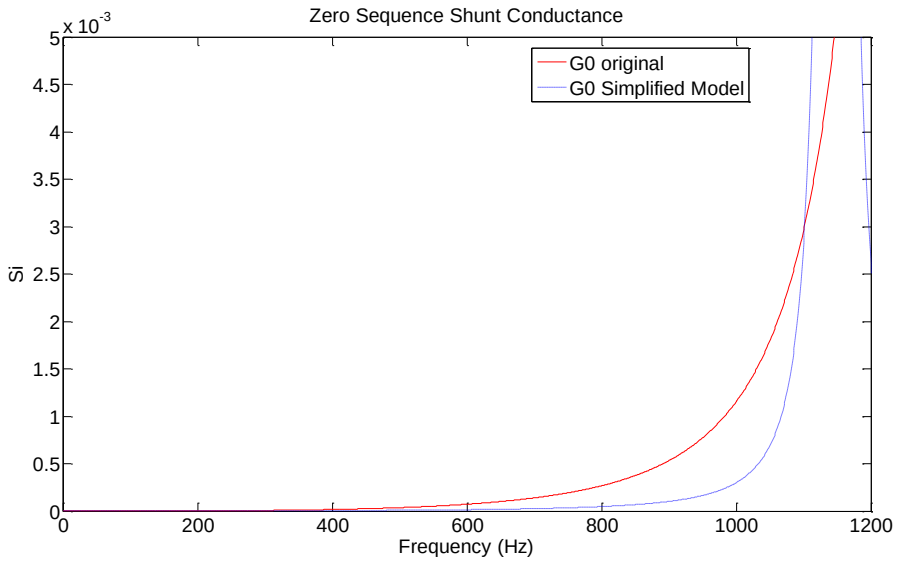

Figure A1.8 Zero Sequence Shunt Conductance

It can be seen that the most important positive sequence reactance of the simplified model can flow the reactance of the original transmission line pretty well up to 6000 Hz. So does the positive sequence shunt susceptance except it has some big errors at resonance frequencies. Positive sequence resistance and positive sequence shunt conductance of the simplified model are only accurate at 60 Hz.

Compared to positive sequence parameters, zero sequence parameters of the simplified model show much more errors.